UNIVERSITÉ DE MONTRÉAL

DESIGN OF A MECHATRONIC SYSTEM FOR THE CHARACTERIZATION OF
POLYMER COMPOSITE MATERIAL PROPERTIES DURING MOLDING PROCESSES

ALVARO GEOVANY RAMIREZ URIBE

DÉPARTEMENT DE GÉNIE MÉCANIQUE

ÉCOLE POLYTECHNIQUE DE MONTRÉAL

THÈSE PRÉSENTÉE EN VUE DE L'OBTENTION

DU DIPLÔME DE PHILOSOPHIAE DOCTOR (Ph. D.)

(GÉNIE MÉCANIQUE)

DÉCEMBRE 2018

UNIVERSITÉ DE MONTRÉAL

ÉCOLE POLYTECHNIQUE DE MONTRÉAL

Cette thèse intitulée :

DESIGN OF A MECHATRONIC SYSTEM FOR THE CHARACTERIZATION OF
POLYMER COMPOSITE MATERIAL PROPERTIES DURING MOLDING PROCESSES

présentée par : RAMIREZ URIBE Alvaro Geovany

en vue de l'obtention du diplôme de : Philosophiae Doctor

a été dûment acceptée par le jury d'examen constitué de :

M. LABERGE LEBEL Louis, Ph. D., président

M. ACHICHE Sofiane, Ph. D., membre et directeur de recherche

M. RUIZ Eduardo-Antonio-Julian, Ph. D., membre et codirecteur de recherche

M. SAUSSIÉ David, Ph. D., membre

M. SANTOS Ilmar Ferreira, Doctorat, membre externe

DEDICATION

To my beloved wife and daughter

"I have no special talent. I am only passionately curious."

"Once we accept our limits, we go beyond them."

Albert Einstein

ACKNOWLEDGEMENTS

RÉSUMÉ

La fabrication de matériaux composites à la base de polymères est de plus en plus importante dans les industries aérospatiale, automobile et du sport. La principale raison de l'utilisation de ces types de matériaux est la proportion poids / résistance, mais ils peuvent également être conçus pour répondre à des exigences spécifiques en choisissant la résine polymère et le renforcement appropriés.

Mais le choix des bons matériaux ne constitue que la première étape de la conception de structures composites, car le processus de fabrication est un défi technique majeur. Les paramètres de traitement optimal génèrent une structure composite dotée d'excellentes propriétés mécaniques et d'une bonne tolérance dimensionnelle. En même temps, le processus doit utiliser un minimum d'énergie et de temps de traitement. D'autre part, un ensemble inadéquat de paramètres du processus peut entraîner une pièce présentant un mauvais état de surface, des distorsions géométriques, des propriétés mécaniques insuffisantes et un temps de production prolongé.

Pour améliorer la pièce fabriquée, l'ingénieur a besoin des données détaillées sur l'évolution du matériau dans le moule. La caractérisation nécessite plusieurs dispositifs dans un laboratoire standard. La méthodologie de caractérisation traditionnelle prend du temps et la configuration des expériences est difficile à reproduire. De plus, la taille de l'échantillon change d'un appareil à l'autre. En général, les équipements de laboratoire traditionnels ne peuvent pas caractériser les matériaux composites. Un échantillon représentatif de ce type de matériaux est simplement trop grand et dépasse les capacités de ces dispositifs. Les chercheurs ont tenté à plusieurs reprises de produire une meilleure stratégie de caractérisation. Cependant, pour obtenir un appareil entièrement fonctionnel, plusieurs défis technologiques doivent être résolus. L'objectif principal de ce projet de thèse est de relever ces défis et de trouver des stratégies qui permettront l'intégration de plusieurs équipements de laboratoire de caractérisation dans un seul appareil.

Pour atteindre cet objectif, nous étudions les dispositifs de caractérisation proposés dans la littérature et nous en résumons les limites. Pour étayer nos conclusions, nous utilisons une machine de laboratoire capable de reproduire les conditions des cycles de fabrication standards. Nous faisons nous-mêmes l'expérience des défis liés à la fabrication d'un matériau composite. Toutes les informations collectées nous ont permis de trouver les exigences de périphérique souhaitées.

Dans cette thèse, une méthodologie de conception mécatronique intégrée pour identifier et résumer les défis de fabrication dans les exigences des produits a été développée. La méthodologie proposée nous a permis de comprendre la relation entre les différentes exigences de conception. De plus, les stratégies intégrées permettent de décrire les exigences fonctionnelles de l'appareil à l'aide de schémas fonctionnels simplifiés. Les interactions trouvées dans les schémas permettent de regrouper les blocs fonctionnels en modules. La méthodologie mécatronique intégrée fournit les outils nécessaires pour réaliser une stratégie de conception proactive. Au fur et à mesure que le projet évolue, les multiples itérations de conception améliorent le produit final.

La mise en œuvre de la méthodologie proposée ici nous a permis de trouver les défis technologiques nécessaires pour caractériser les propriétés d'un matériau composite polymère à l'aide d'une seule expérience. À cet égard, nous discutons des éléments critiques du dispositif mécatronique souhaité, des limites du produit et des innovations requises pour atteindre cet objectif.

Le dispositif de caractérisation mécatronique proposée ici peut changer la manière dont les composites sont produits. Le fait de disposer d'une machine capable d'obtenir plusieurs matériaux composites en une seule expérience donnera aux chercheurs les informations nécessaires pour produire de meilleurs modèles de matériaux, améliorer les moules, simuler les processus et d'optimiser les paramètres de fabrication.

ABSTRACT

The manufacturing of polymeric composite materials is nowadays more and more common in the aerospace, automotive and sports industries. The main reason for the use of these materials is its strength to weight ratio advantages, but beyond that, is that they can be engineered to meet specific requirements by choosing the proper polymer resin and reinforcement.

But choosing the right materials is just the initial step in the design of composite structures since the manufacturing process is a major engineering challenge. Optimum processing parameters generate a composite structure with excellent mechanical properties and good dimensional tolerance. At the same time, the process must use a minimum of energy and processing time. On the other hand, an inadequate set of process parameters may result in a part with bad surface finish, geometric distortions, lower mechanical properties and long production time.

To improve the manufactured part, the process engineer requires detailed data about the evolution of the material inside the mold. This characterization requires of multiple laboratory characterization devices. Also, the traditional characterization methodology is time consuming and the experiments setup are difficult to reproduce. Moreover, the sample size changes from one device to the other. In general, traditional laboratory equipment cannot characterize composite materials, a representative sample of this material type is just too big and surpasses the capabilities of the traditional characterization devices. Researchers have made several attempts to produce a better characterization strategy. However, to achieve a fully functional device, several technological challenges need to be resolved. The main objective of this PhD project is to find those challenges and find strategies that will allow the integration of multiple characterization laboratory equipment into a single device.

To achieve this objective, we study the proposed characterization devices in the literature and abstract those devices limitations. To support our findings, we use a laboratory scale machine capable of reproducing the conditions of regular manufacture cycles. We experience by ourselves the challenges in the manufacturing of polymer matrix composite material. All the collected information allowed us to find the desired device requirements.

This thesis developed an integrated mechatronic design methodology to abstract the manufacture challenges into product requirements. The proposed methodology allowed us to understand the relationship between the different design requirements. Additionally, the integrated strategies

permit to describe the device functional requirements with simplified functional diagrams. The interactions found in the diagrams make possible to group the functional blocks into modules. The integrated mechatronic methodology provides the tools to achieve a proactive design strategy. As the project evolves, the multiple design iterations refine the final product.

The implementation of the proposed methodology allowed us to find the technological challenges required to characterize the properties of a polymer composite material using a single experiment. In this respect, we discuss the critical parts of the desired mechatronic device, the product limitations and the innovations required to achieve this objective.

The mechatronic characterization device proposed in this work can change the way the composites are produced. Having a machine capable of obtaining multiple composite material's characteristics in a single experiment will give researchers the information to produce better material models, improving molds, process simulations and optimal manufacturing parameters.

TABLE OF CONTENTS

LIST OF TABLES

LIST OF FIGURES

LIST OF SYMBOLS AND ABBREVIATIONS

Abbreviations

AC   Analog current

ARM   Advanced RISC Machine

ASTM   American Society for Testing and Materials

CCHP   Chaire sur les Composites à Haute Performance

CTE   Coefficient of Thermal Expansion

DC   Direct current

DEA   Dielectric Analysis

DGEBA   Bisphenol A diglycidyl ether

DMTA   Dynamic Mechanical Thermal analyzer

DSC   Differential Scanning Calorimeter

ERFT   Engineering Research & Flow Technology

FWO   Research Foundation Flanders

HAL   Hardware Abstraction Layer

HMI   Human Machine Interface

IMDM   Integrated Mechatronic Design Methodology

LCM   Liquid composite molding

LVDT   Linear Variable Differential Transformer

MTHPA   Methyl Tetrahydrophthalic Anhydride

MOSFET   Metal Oxide Semiconductor Field Effect Transistor

OB   Thesis objective

PCB   Printed Circuit Boards

PID   Proportional, Integral and derivative controller

PMCM   Polymer Matrix Composite Materials

PREPEG   Pre-impregnated resin fabric

PVT   Pressure Volume Temperature

PWM   Pulse Width Modulation

QFD   Quality function deployment

RFIM   Resin film infusion

RTM   Resin transfer molding

RTOS   Real Time Operating Systems

SCRIMP   Seaman composite resin infusion molding process

SMPS   Switching Mode Power Supply

SysML   Systems Modeling Language

TGA   Thermogravimetric analysis

TMA   Thermo-Mechanical Analyzer

TTS   Time Temperature Superposition principle

UML   Unified Modeling Language

UTM   Universal testing machine

VAC   Volts alternating current

VARTM Vacuum-assisted resin transfer molding

VDI   The association of German engineers (Verein Deutscher Ingenieure)

Symbols

α Cure degree

α_{gel} Cure degree at gelation point

α_{diff} Full degree of cure

T_g Glass transition temperature

T Temperature

E Elastic modulus

μ Viscosity

$\mathbf{K}$ Permeability tensor

P Pressure

v Velocity

γ Fluid surface tension or shear strain

θ Angle

H Heat

ε	Strain
σ	Stress
δ	Phase lag
E^*	Complex modulus
E'	Storage modulus
E''	Loss modulus
G^*	Complex shear modulus
G'	Complex storage modulus
G''	Complex loss modulus
τ	Shear stress
λ	Wavelength
η^*	Complex viscosity
ω	Angular frequency
ν	Poisson's ratio or specific volume
ρ	Density
c	Ultrasonic velocity
a	Ultrasonic attenuation coefficient
f	Frequency
L'	Ultrasonic elastic modulus

L"   Ultrasonic loss modulus

t   Time

V   Volume

LIST OF APPENDICES

CHAPTER 1   INTRODUCTION

Mechatronic systems are intrinsically multidisciplinary. They evolved from simple mechanical devices controlled by electronics, to complex machines with the ability to perform data acquisition, record information over time, communications, interact with the user, error checking, etc. These capabilities make them attractive to disciplines outside the typical scope of the mechanic or electronic science.

The inclusion of new disciplines like material science requires that the mechatronic designer gain a deep understanding of the underlying phenomena, the mutual relationship between the system parameters and their impact into the device functionality.

The challenges on the design of mechatronics have been summarized from an extensive literature review by Torry-Smith *et al.* [1-3]. Authors found that they are not only inherent by the device complexity or the synergy between the multiple disciplines, but they also reside in the human interactions. People behaviour influence the project evolution, social ordeals result from the engineer mindset, their training, and the organization hierarchy structure. Communication problems come from insufficient understanding about the phenomena involved in the system and the incapability to transfer the information between the groups experts [1, 2]. A holistic view and functional modelling techniques solve these difficulties and allows a concurrent design process [4-6].

This global view of the system allows to identify modules within the product architecture. Modularity reduces the development time and the costs [7-9]. Although it shows many advantages, in heavily constrained applications (e.g., by power or weight) a non-modular architecture produces better results [10]. Seamlessly, Whitney [11] argue that parts specifically made to do multiple jobs will increase their complexity, costs, space and power consumption if they are divided into subsystems. The teams that recognize this paradox will choose the best architecture for their designs.

In this research, mechatronic modelling techniques are implemented to derive a functional system design of the composite materials characterization device. Afterwards, modules and components within the architecture can be tested and prototyped.

1.1 Research methodology

An increase trend in the implementation of evolutionary algorithms into the mechatronics design is being seeing in recent studies. They exploit the iterative nature that resides in the mechatronic design. Authors report that they give good results even at early stages of the project. Also, they select the best combination of components and reduce the design iterations [12-14]. Despite the possible advantages, their implementation requires an extensive database, custom developed software and a framework platform that will impose an additional load and delay for this study. Instead, this research chose an adaptive design methodology. It is flexible to allow artificial intelligence optimization in future iterations of the design progress.

Figure 1.1 shows the v-shaped mechatronic design methodology from the Association of German Engineers named VDI 2206 [15]. It begins with the system requirements. They are of great significance because the describe the product functionality and serve for the final validation. Group meetings, human interaction and hands-on of the company manufacturing processes provide the information to define and classify the incoming design tasks.
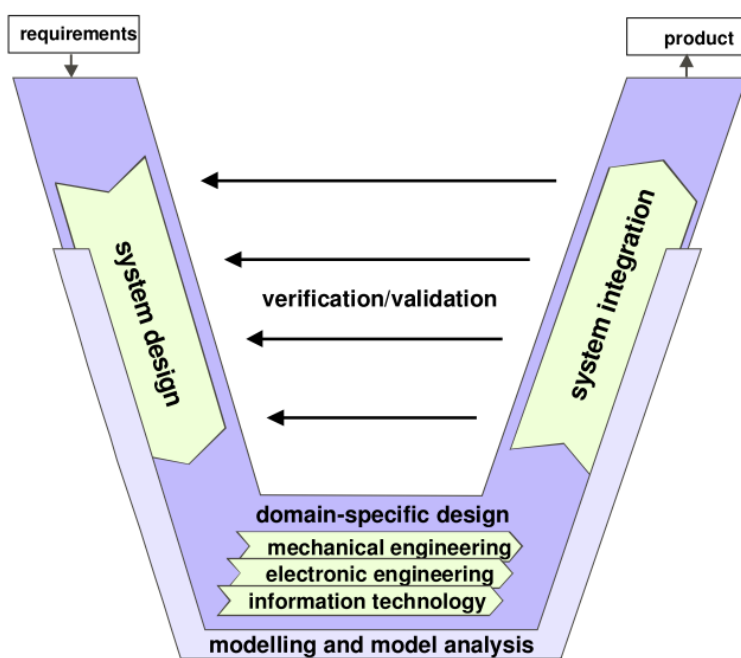
Figure 1.1: VDI 2206 V-shaped generic mechatronic design model [15]

Afterwards, the main objective of the system design is to find a cross-domain answer in response to the requirements. The goal is to describe, in simple words or sketches the architecture behaviour.

Engineers tend to choose components and solutions during this phase. Functional model techniques prevent this tendency by using flow diagrams that represent concepts, relationships and constraints in the system [4]. Figure 1.2 shows the difference between a concept and a solution, an electrical engineer will understand that a Linear Variable Differential Transformer (LVDT) measures displacement, meanwhile a computer science engineer or a project manager could be confused or not interested in that term.
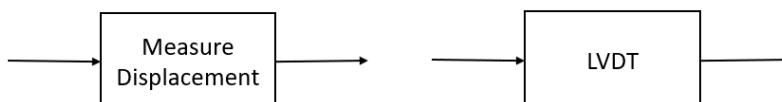
Figure 1.2: Concepts vs Solutions

Specific terms lead to communication problems. Also, premature solutions bias the design towards their implementation. In the displacement example, it is pointless to have a sensor type without knowing the impact over the system. It is likely that the engineer used that component before and will feel comfortable used it again, even if it is nor beneficial or nor optimal to the design. These questions require a deeper analysis and are domain specific.

When the multidisciplinary team agrees about the chosen system design, each domain develops specific engineering models and simulations. By using their calculations and the imposed constraints, they search for possible device components. In this scenery, parallel work is achieved due to the total comprehension of the architecture by all the people involved.

As the project evolves, the teams meet to present their progress. It does not require that everyone finish their goals. During the system integration, individuals present their results and limitations. Consensus on the needed changes refine the functional model or redefine the constraints. These multiple validation loops benefit the project and bond the multidisciplinary teams.

During the process loops, computer aid modelling software supports the mechatronic design methodology. These tools produce graphs, simulations and computational models that helps to understand, visualize and solve engineering problems instead of complex differential equations.

The final product results from multiple iterations. Figure 1.3 shows the project growing in a V-shape macro structure. A working device could be launched once it reaches a good degree of

maturity. Later, the functional model continues to evolve through newer versions or system upgrades of the same device.
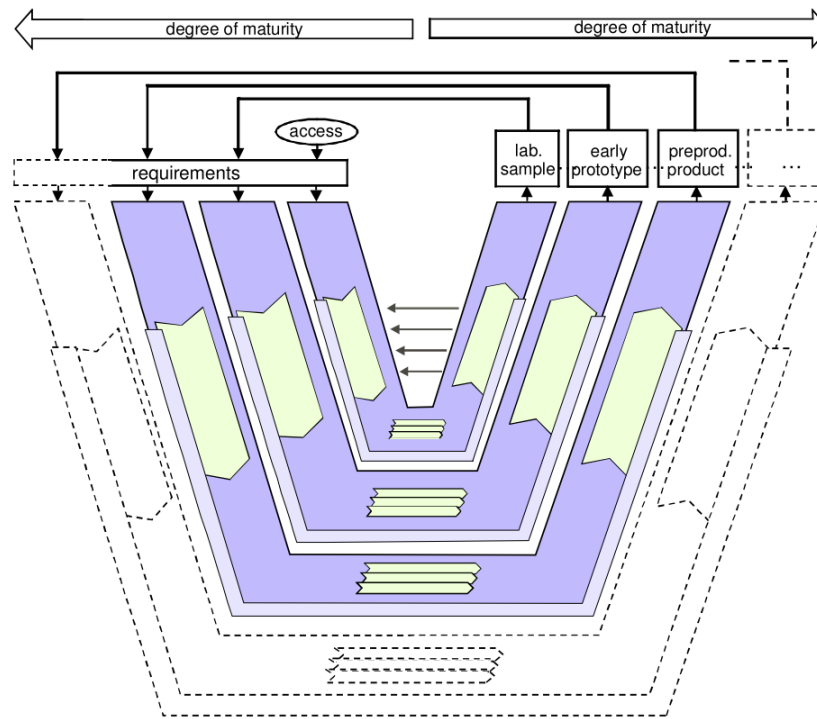
Figure 1.3: V-Shape extended macro model[15]

1.2 Problem statement and research motivation

New products require the development of advanced materials. They obtain special characteristics through complex modifications on their internal structure. For example, lightweight components reduce the fuel consumption and increase the load and flight capacity in an aircraft. Boeing and Bombardier have been in the race to design more efficient machines. State of the art airplanes use more than 50% of polymer matrix composite materials (PMCM) in their structure [16, 17] and by doing so, a 20% on fuel reduction was achieved [18].

The Boeing 787 faced several manufacturing problems, all related to the PMCM structural pieces. Company leaks reported that the final-assembly presented gaps [19, 20]; a common and recurrent challenge on the PMCM moulding. Non-optimal manufacturing parameters induce shape distortions and imperfections. Researchers are generally interested in the process optimization and part defects reduction, subjects broadly covered in the literature of the last decades.

The manufacturing process and the material properties connect each other in order to understand how, the basics on material science need to be explained. Materials science involves the study of the internal structure and its effect in the material properties and performance. Models and theories explain how the constituent elements of the materials interact. Engineers utilize those representations to modify the material structure through mechanical and chemical transformations. This is called the material science paradigm [21-24].

Figure 1.4 presents the complex interaction between processing, structure, properties and performance. The materials science tetrahedron shows the complex relationships required to produce new materials like the PMCM. Each corner influences the other three sides of the tetrahedron, but the characterization is in the core of these interactions. Material models and theories are explained through the collected data. The process history requires a meticulous characterization through the whole process, in such a way, that all the collected data relates to the resulting properties, no matter the size or shape of the material. The performance can be inferred using mathematical models, that save development time and costs but requires at the end an experimental validation.
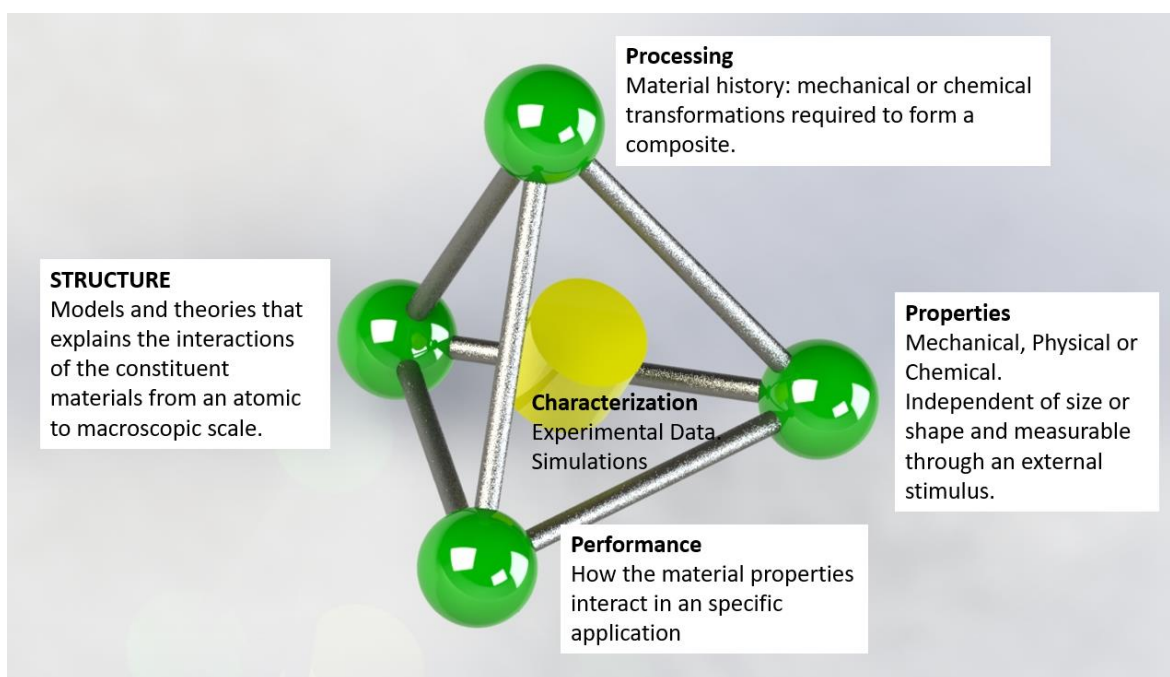
Figure 1.4: Composite materials tetrahedron. Adopted from [21-24]

This research thesis situates in the processing, properties side of the tetrahedron. The design of the mechatronic device requires that the manufacture parameters vary in a safe range of operations.

Meanwhile, the material history is recorded to reproduce the evolution of the PMCM properties during the molding process.

Researchers have been improving the strategies to record the developing of the PMCM properties during the molding process for decades. Their characterization methodology relies on several laboratory equipment [25-28]. The most used are: The Differential Scanning Calorimeter (DSC), the Rheometer, the Thermo-Mechanical Analyzer (TMA) and the Dynamic Mechanical Thermal analyzer (DMTA). This results in labor intense methodology with tests hard to reproduce [29, 30]. Equally important, the sample dimensions change from one device to the other, which in turn, generate ambiguous data [31, 32]. Although material properties do not rely on the size and shape, during the measurements, the sample must be a representative part of the internal structure. In thick PMCMs with fiber reinforcements layers lay on different directions, the composite arrangement is just too big for the existing characterization devices. Therefore, the main objective of this research thesis is to design a mechatronic device in response to these characterization challenge.

The advances in the characterization of PMCM can be divided in two: attachments to traditional characterization devices and custom-made. The attachments take advantage of the existing platform, they add new sensors and fixtures that allow the old device the characterization of new properties in a single experiment. Their drawback is that they carry the original machine limitations. As expected, researchers study only the polymer part of the composite. Next, a generalized law of mixtures or empirical phenomenological models estimates the mechanical properties of the composite structure. This approach makes possible to reduce the number of experiments, but the properties of the composite are still inferred.

In contrast to the attachments, custom-made devices shown the most promising results in the characterization of PMCMs properties using a single experiment. The Pressure - Volume - Temperature (PVT) technique is the most reliable, popular and used in traditional and custom-made characterization equipment. Figure 1.5.a. displays the PVT simplified diagram. First, a plunger or piston applies a constant force to the sample. Next, the material heats or cools following a controlled thermal profile. At the same time, the piston displacement measures the volumetric changes. The collected data during the test relates the thermo-mechanical properties of the material.

Boyard *et al.* [33] placed a mold inside a press. The piston closes at constant pressure and the molding begins. Displacement, temperature and heat sensors register the volume evolution, the

applied temperature and the exothermic chemical reaction in a polymer resin. They proved that custom-made setups give comparable results to those obtained with laboratory equipment, and besides, that a single experiment could measure thermal expansion, chemical shrinkage and polymerization degree of thermosets polymers materials.
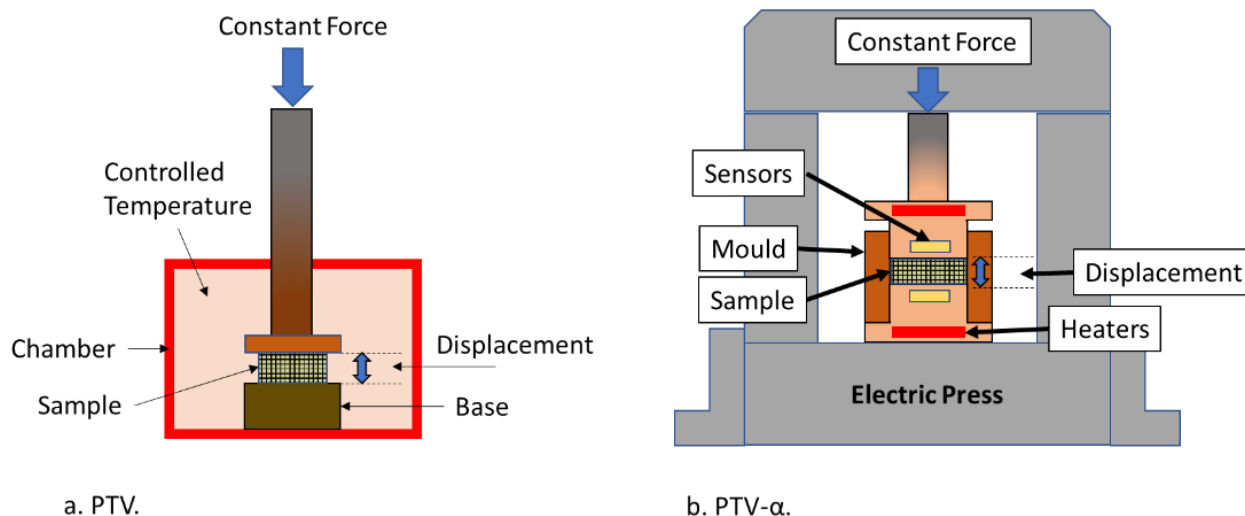
Figure 1.5: PTV devices

Nawab *et al.* [34] developed a newer version of the PTV mold, the PVT-α, as in Figure 1.5.b. A commercial press and a LabVIEW data acquisition system upgrade the device. The improved device shows that it is possible to obtain the development of the material properties on a PMCM using a single experiment. Later in [35], the same device attempted to measure the properties of a thermoset resin under a dynamic force. But limitations imposed by the electric press made not possible to apply a pure sinusoidal stress to the sample. Rather than the optimal 10Hz stress frequency [36], the load applied was a sinusoidal cycle with one minute period, followed by another minute of constant pressure for stabilization. Thus, this new setup could not characterize the viscoelastic properties apart from the bulk modulus. On the other hand, the variations on pressure during the experiment did not affect the volumetric and chemical properties obtained with static tests, which indicates the feasibility of dynamic tests with such equipment.

Last of all, Peron *et al.* [37] in 2017 published the most recent upgrade on the custom PVT like device. The PVT-HADDOC in the Figure 1.6, the device has the capability to measure the multi-axial strain of a composite material. Pressurized silicone oil and a Instron specialized press test machine, maintain a constant pressure inside the mold. Meanwhile, external and internal sensors

record the polymerization and the changes in the sample volume in all directions. Despite the dynamic capabilities of the specialized Instron press, authors did not attempt to obtain the viscoelastic behavior of the composite. This was disclosed as a future work in their final remarks. Until now, the dynamic characterization of thick PMCM using one single experiment remains elusive to researchers.
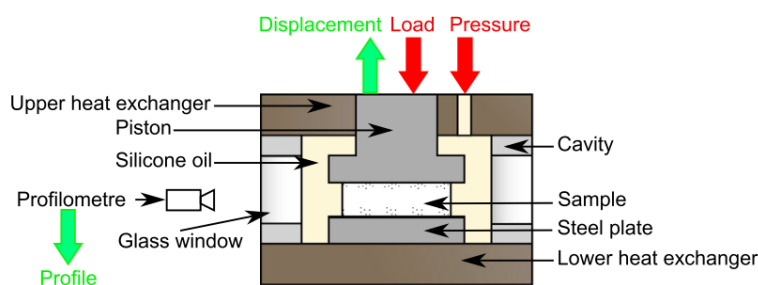
Figure 1.6: Multi-axial composite testing machine [37]

During the design of the mechatronic device we explored the possibility to implement a commercial press, but despite the capabilities of those machines we found their platform not to be flexible enough to coordinate with the other parts of the system. The actuator that applies the force is an important component of the mechatronic device and is often covered by a patent.

Unlike the PVT devices presented, the mechatronic system requires to obtain the development of the material properties, the viscoelastic behavior of the composite and to provide the means to analyze how the voids develop during a typical manufacturing cycle. Voids compromise the structural integrity of the material and cause many part defects due to the residual stresses that they generate [38-40]. Great part of the voids results from the fiber impregnation. For this reason, the injection of the resin becomes a part of the system design. We follow a mechatronic design technique to answer the following research question:

What are the technological challenges in the characterization of PMCMs, and how the solutions could be integrated into a single device?

The investigation will be developed progressively resolving in detail each of the following questions:

- What are the most relevant material properties and which techniques are readily available to characterize them?

- What are the challenges and limitations encountered in characterizing multiple properties at the same time?

- How the multidisciplinary team could approach the mechatronic device development in a proactive and efficient way to focus on the critical parts of the product?

- What are the innovations required to obtain a working prototype?

1.3 Project Main Objective (Goal)

The objective of this research is to integrate multiple characterization laboratory equipment into a single device for PMCMs. To this end, we will need to better understand the characterization challenges on PMCMs.

The development of this device could reduce the characterization time and its complexity to an only one experiment. This will help composite material researchers produce better phenomenological models, and to give manufacturing companies the capability to test their manufacturing processes and raw materials in house.

To reach this goal we need to fulfill the objectives described in the next section.

1.4 Project objectives

- OB1: To identify the laboratory equipment limitations and manufacturing challenges in the characterization of PMCMs properties.

To reach this objective, this research will examine the literature about the characterization methodologies and techniques that are typically used to obtain the PMCM properties. Then, we will look for the main publications and teams working in obtaining multiple properties with a single experiment. In general, we will be looking for the limitations found in those research works and translate them into design challenges. To support those findings, we will carry out tests in a resin transfer molding machine at laboratory scale. In this respect, we expect to experience the manufacture process. Gaining a deeper understanding on the manufacture of PMCM and their challenges will allow us to clearly define the equipment limitations to obtain multiple properties in a single experiment.

- OB2: To develop an integrated mechatronic design methodology

The characterization of composite materials is per se a difficult task. If we add the challenges embedded in the mechatronic design, we found ourselves in a situation where a typical design methodology is not enough to lead the path of the design team. In this context and to reach the main objective, we found necessary to develop a proactive design methodology. It must be capable of abstracting the device requirements and weight the team decisions. Essentially, we will be looking for a way to structure and minimize the effort to design the device.

- OB3: To identify the most critical machine components for design embodiment.

All systems contain critical components that require to be developed before others. They are the core of the device, without them, the system will not reach the required functionality. This final objective will describe the technological challenges required to obtain a fully working product. Usually those are related to the innovations or non-existent technology required to complete the machine.

1.5 Scope and limitations of the research

This research aims to design a device that does not rely on existing of-the-shelf commercial solutions. The main reason is that these types of solutions tend to considerably increase the device costs and functioning constraints by imposing annual licensing and additional system requirements. Consequently, the number of proprietary parts to develop increase considerably. This self-imposed requirement increases the control over the device and decreases significantly the final product price, conversely, increases the development time.

Despite these limitations, commercial tools can serve for rapid prototyping or concept testing. Even so, it is impossible to complete, during the length of this PhD project, a fully functional finalized characterization device. Hence, the present work is the first stepping stone for future researchers and projects in the field. Achieving a functional prototype will require complementary masters and doctoral projects to develop domain-specific components. The functional model and the results from this research will make it easier for them to understand the cross-domain requirements and the importance of their contributions to the composite materials characterization science.

1.6 Thesis structure

This thesis is organized into six chapters. After the introduction of the thesis, the literature review of chapter 2 introduces the subject of characterization of composite materials using a single device. The chapter begins with a general overview of the manufacture process. Them, the traditional characterization techniques are presented. To contribute to reaching the first objective (OB1) and identify the laboratory equipment limitations, the chapter presents the devices made by the researches and organized then into two categories, attachments to typical characterization devices and custom-made devices. At the end of the chapter, a summary of the review devices with their limitations and challenges are presented in the conclusion. To support the findings of the literature review, chapter 3 presents the laboratory test that supports the challenges reviewed. The industrial experience using a laboratory scale manufacturing device, contribute to find the specific challenges and limitations in the manufacturing and characterization of PMCMs (OB1).

To integrate multiple characterization laboratory equipment using a single device, it is required to design a strategy capable to deal with the complexity of this PhD project. Chapter 4 achieves the second objective (OB2) by proposing an integrated mechatronic design methodology. After describing in detail, the design steps, the challenges found during the first objective (OB1) are translated in a form of "wishes and demands". The list of requirements is abstracted one more time into the quality function deployment (QFD) to understand the correlations between the design parameters. Then, the system design is made through the functional model and the product architecture.

At this point of the thesis, the product requirements and the device functions are well defined. Moreover, in chapter 5 the device layouts and solutions to the critical machine components made possible to achieve the final project objective (OB3).

Finally, chapter 6 present a general overview of the work presented, the achievements and how the objectives were progressively solved. Additionally, this final chapter presents the three main scientific contributions of this thesis and discusses the future work.

CHAPTER 2   LITERATURE REVIEW

To answer the main objective, integrate multiple characterization laboratory equipment into a single device. This chapter presents a literature review on the attempts made by researchers to reach this goal. To understand this subject, the literature was organized as follows: First, we present a general overview on the manufacturing process and known manufacture challenges found in the molding process. Second, a review of the characterization techniques and traditional laboratory equipment shows the regular characterization methodology. Finally, we review the state of the art in the developed of laboratory equipment to characterize multiple material properties using a single experiment.

2.1 Manufacturing of PMCM – General Overview

A polymer matrix and a fiber reinforcement blends, forming a tougher material. This new composite material possesses better properties than the constituent ones. The fiber reinforcement bears the load applied to the composite. Meanwhile, the polymer matrix conveys that load to the reinforcement, hold the fibers together and give shape to the composite structure. Appendix A have all the basic information required to understand the chemical transformation that undergoes during the manufacturing of PMCMs. The morphological changes that allow the polymer matrix to transform from liquid to solid is called polymerization. Researchers represent this chemical reaction with a normalized scaled defined as cure degree (α).

Appendix B summarizes the manufacturing process. Figure 2.1 condense the molding process into three phases. First, a liquid thermoset resin soaks the dry reinforcement placed inside the mold. The action of the injection pressure ensures that the liquid flows and wets the fibers. At the same time, the resin displaces the air that is inside the reinforcement. Second, the resin undergoes into the morphological change of polymerization from liquid to solid. The consolidation pressure inside the mold gives shape to the part and reduce the number of voids. Moreover, the heat increases the rate of the chemical reaction reducing the molding time. Finally, the part is cooled to temperature ambient and removed from the mold.
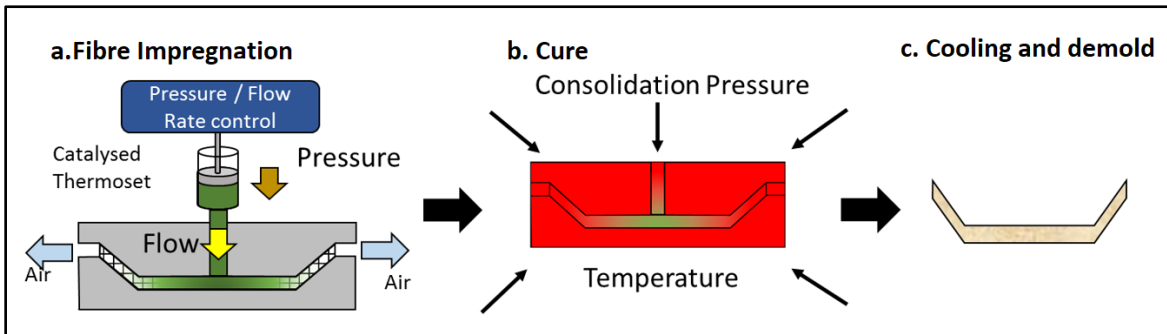
Figure 2.1: Generalized manufacturing cycle

PMCMs molds in an irreversible process, the materials undergo molecular changes while the part takes shape. Curing a thermoset PMCM is like boiling an egg, the resin begins as a low viscous liquid. The chemical reaction links the chains of monomers, as the liquid solidifies, the material changes into a solid macromolecule with infinite molecular weight. In between, the polymer resin turns into a rubber like substance. This transformation represents the gel point. It is important to obtain this change in the matter because from that point, it is not possible to mold the composite. In other words, the molecular links prevent the flow of the polymer resin and any change on the shape could destroy the part. This permanent transformation marks the starting point on the development of the mechanical properties. A fully cured composite cannot be reshaped or melted again.

2.1.1 Fiber impregnation

In the liquid state, the process designer needs to know the point of minimal viscosity and its duration to begin the impregnation. That is the exact time when the resin melts and the cross-links begin. Figure 2.2 shows the two coupled phenomena that drive the evolution of the viscosity. At the beginning of the process the resin is heated, this increases the movement of molecules causing an abrupt decrease in the viscosity. At the same time the chemical reaction makes cross-links which increases the viscosity until the resin cannot flow anymore.
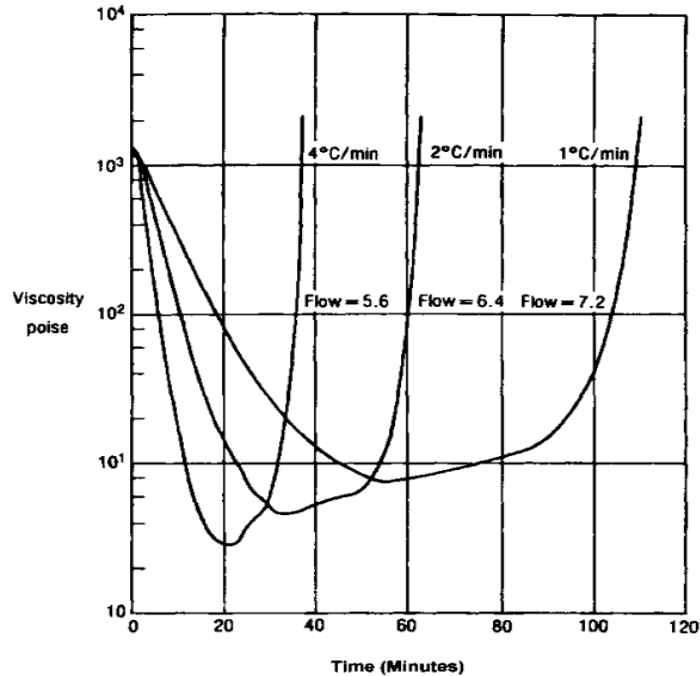
Figure 2.2: Viscosity evolution to heat rate of a thermoset [41]

Once the viscosity of the resin is modeled, the process designer needs to find the reinforcement wettability. In other words, the resistance of the compacted fiber to be wet. One analogy regularly used is the water flowing through a pipe filled with sand. Higher the sand compression, higher the pressure needed to push the water through the pipe. By knowing the viscosity of the resin and the permeability of the fibers, the engineer can calculate the amount of pressure needed to allow the resin to flow and wet the fibers. Darcy's law [42] describes the ability of a liquid to flow though a porous media like the fibers reinforcement presented in the PMCMs.

However, composite materials have more and more complex fiber tow arrangement that requires more effort to impregnate. Researchers have identified two porosity scales that distorts the resin flow. They are the macro porosities or the space between tows and the micro pores or the microscopic spaces in the tow itself[43]. Figure 2.3 shows the effect of the dual scale porosity in the fiber impregnation. Naturally, the liquid flows faster in the macro pores which causes a partially saturated region with a characteristic length. As the flow advance, the liquid penetrates inside the tow fully saturating the textile. In order to understand this phenomenon, a deeper analysis is next presented.
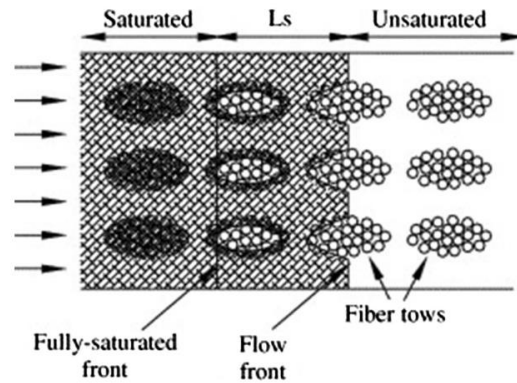
Figure 2.3: Fiber impregnation, flow front and dual scale porosity [43]

Figure 2.4 describes the effect of the two competing forces involved during the impregnation. At low flow velocity the capillarity force dominates. The fluid goes faster inside the tows which causes macro voids as the fluid front joint in the macro pores. On the contrary, with a high flow velocity, the viscous forces allow the fluid to pass through the big channels of the textile. Because the fluid requires more time to pass through, micro voids forms in the small spaces inside tow [38].

In conclusion, the fiber impregnation depends on the textile physical characteristics, the flow velocity and the resin viscosity.
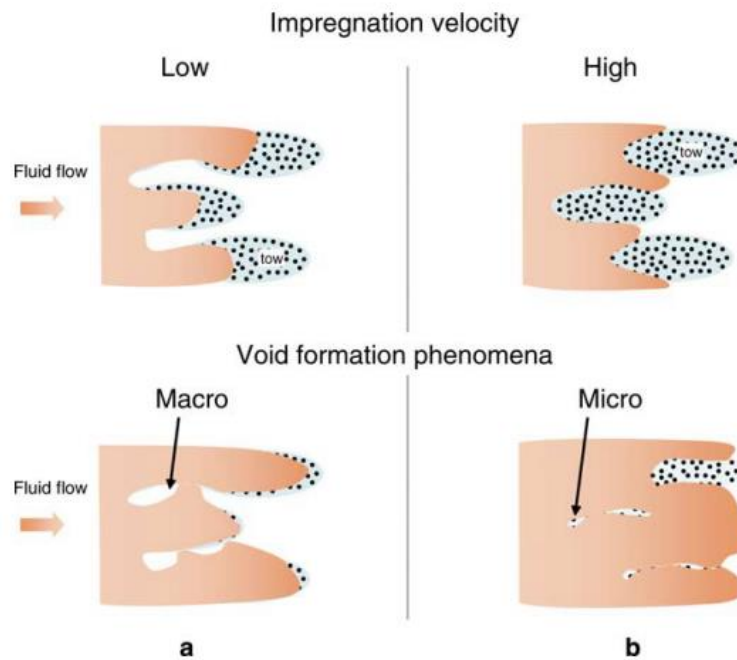
Figure 2.4: Void formation during fiber impregnation [38]

2.1.2 Volumetric changes and mechanical properties

Volumetric changes result from the chemical and thermal phenomena. The material expands or contracts during heating and cooling. Simultaneously, the polymer resin cures leading to a chemical shrinkage. Researchers found that small molecules known as monomers change during the reaction from weak Van Deer Waals bonds to shorter covalent cross-links [27]. Therefore, the new polymer structure undergoes in a volume reduction. During the polymerization the liquid resin increases its viscosity with the number of cross-links, until it solidifies into a rigid material. Thus, the mechanical properties and the volume reduction relate to the cross-link density [44]. From an industrial perspective, the desired part shape requires of specific mold dimensions. Proper characterization of the combined phenomena leads to optimal mold design. But this task is so challenging that manufacturers often prefer doing it by trial and error, with small adjust in the mold geometry until the part has the desired result, this process leads to material waste and sometimes requires redoing the whole mold.

ASTM D6289 – 13 [45] standard describes the experiment to measure the shrinkage in a PMCM. The test consists in a mold with known dimensions. Then, the final part dimensions are subtracted from the mold size. Given the complexity of the phenomena, this number does not represent the whole history of the material during the manufacturing process. ASTM describes a series of standard tests to obtain the material properties but in the case of PMCM they restrain to the available commercial characterization devices. In general, they share similarities to the existing laboratory equipment manuals. In this context researchers use them as a mere guideline on how to use an equipment to perform a test.

Generally, the composite cures using temperatures near the 200 °C, this reduces the manufacturing cycle. In addition, the chemical reaction releases heat which makes difficult to decouple the phenomena of shrinkage from the thermal expansion. Figure 2.5 shows an isothermal cure. α_{gel} denotes the cure degree of the onset gelation and α_{diff} the full degree of cure. The gel state marks the mechanical properties development and the material shrinkage history of the material. After the gelation point, the modulus of the composite begins to grow. This is the result of the fibers and polymer bonding during this phase. Also, the mechanical module is developed following the typical "S" shape of the cure degree. At the end of the cycle, the cure completes, and the modulus remains constant in the solid state.
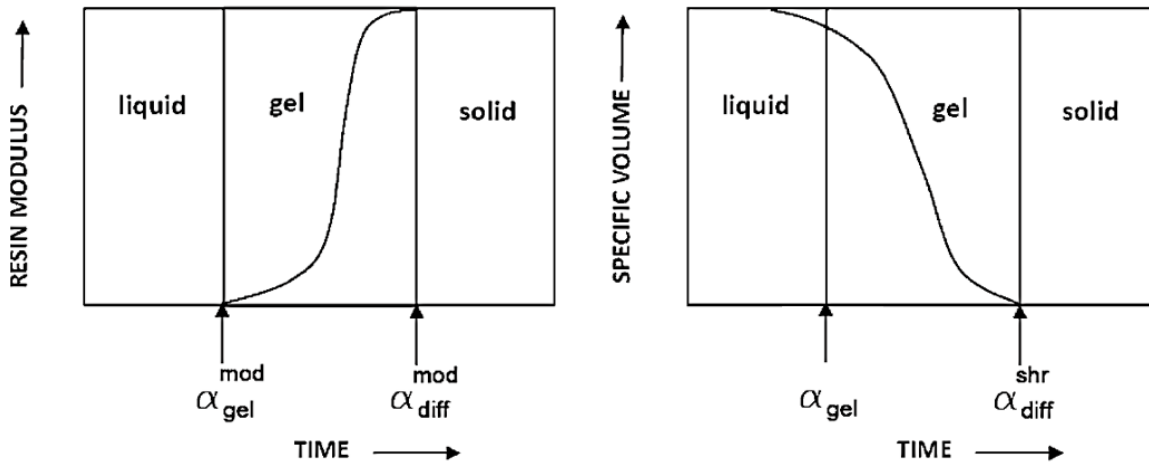
Figure 2.5: Shrinkage and modulus development [44]

Figure 2.6 shows the volumetric changes during a manufacturing cycle. The thermal profile has a heating ramp, a dwell temperature and a final cooling slope. From a - b, the resin remains in the liquid form, as it heats, the volume increases following a linear expansion proportional to the heating ramp and the coefficient of thermal expansion (CTE) of the liquid resin. A moment before the gelation point α_{gel}, from b - c, the CTE and the chemical shrinkage expands and contracts the material at the same time. At constant temperature, from c - d, the thermal expansion stops, and the chemical reaction continues. As a result, the cure shrinks the material until the reaction ends. Finally, from d-e, the solid composite contracts while the part cools down. The CTE from the liquid form is higher than the solid one [46], this results from the polymer - fiber interaction on the consolidate part.
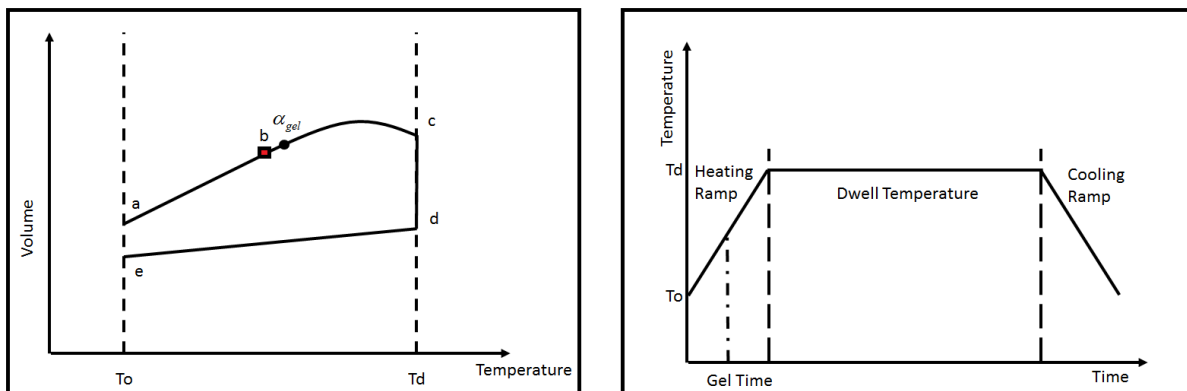
Figure 2.6: Composite shrinkage during a manufacturing process adapted from [46]

In the manufacturing of thicker PMCM parts, the cure evolution through the thickness plays a key role in the molding process. The cure evolution begins from outside or the sides close to the mold. A skin like layer forms due to the proximity to the heat sources. Due to the poor thermal conductivity of the polymers, these layers cannot remove efficiently the heat generated in the core of the material by the exothermic chemical reaction. The temperature gradient through the thickness results in residual stress [47]. Figure 2.7 shows the geometric distortion due to the release of those stresses at de-mold. Figure 2.8 sums up the steps required to the optimization of the industrial molding process. Researchers aims to reduce the process induce defects, they gather all the data necessary to explain the composite formation. Models and computer simulations estimate the part properties. Finally, engineers optimize the process parameters increasing the part quality and productivity.
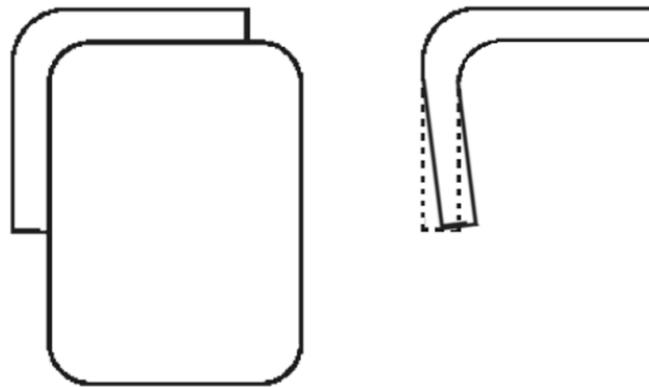
Figure 2.7: Geometric defects [44]

Process Induced Defects	Characterization Methodology	Models and Optimization	Industrial Implementation
•Surface Finish •Geometric Distortions •Matrix Degradation •Delamination •Voids, porosities •Filling Problems •Residual Stresses	•Process Parameters. •Cure kinetics. •Permeability •Viscosity •Chemorheology •Thermo-mechanics •Volumetric changes	•Phenomena Understanding •Mechanistic, semi-empirical models •Numerical Prediction •Optimization methods	•Simulation Software •Process Optimization •Process Control •Productivity •Part Quality

Figure 2.8: Composite materials science knowledge transfer to the industry

2.2 Characterization Methodologies

In this section the methodologies for the characterization of the material properties are presented. It is important to structure the analysis of the multiple phenomena. With a well-defined methodology, the various components of the manufacturing can be combined in a coherent form. Loos *et al.* [48] in 1983 divide the characterization methodology into an integrated sub-model approach. Later, Bogetti *et al.* [49] and Johnston *et al.* [50] introduces a structure chart that describes the methodology. Figure 2.9 divides the manufacturing process into three well-defined steps. The thermo-chemical model explains the cure kinetics evolution to temperature, the flow model describes the fiber impregnation and finally, the stress model contains the mechanical properties development.
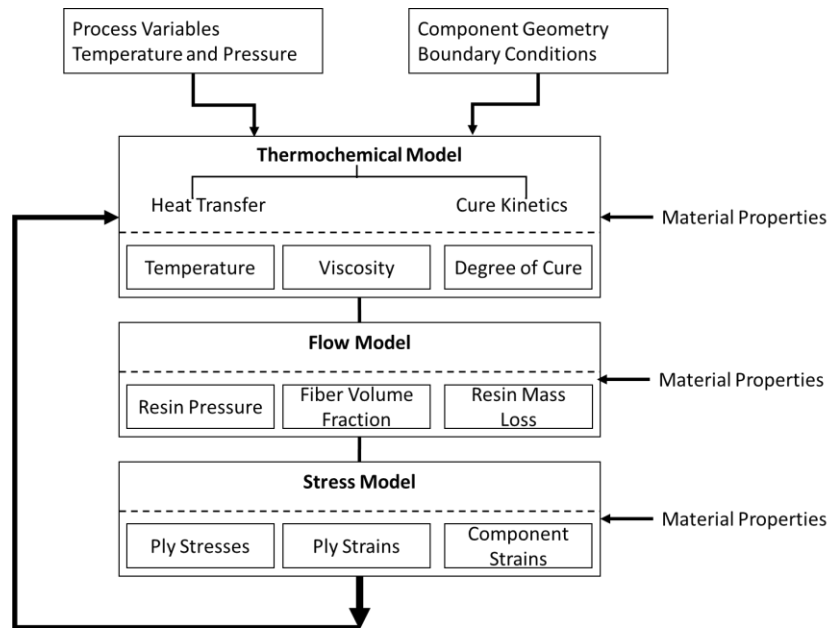
Figure 2.9: Integrated sub-model approach flow chart [50]

Figure 2.10 shows the improved characterization methodology from Khoun *et al.* [30] and Abou Msallem *et al.* [29]. Step 1 determine the process window. A thermogravimetric analysis (TGA) test machine measures the mass of the sample as it heats. The temperature at which the sample start to decompose indicates the thermal degradation or the maximum process temperature. Step 2, a DSC measures the cure degree of the resin as a function of time and temperature. Step 3a, a Rheometer measures the viscosity as function of temperature. Then, phenome-logical models relate the collected data to the degree of cure obtained in the step 2. Step 3b, a thermo-mechanical

analysis (TMA) characterizes the glass transition temperature (T_g), this temperature marks the phase change in the polymer from glassy to rubbery. This change affects in a big way the mechanical properties. Dynamic tests measure the changes on the mechanical properties to temperature, which in turn are related to cure degree. Step 4a, b measures the volumetric changes with a TMA machine or the PVT method, both relies in the same principle. A piston applies a normal force and the gap variation or sample thickness measure the shrinkage or thermal expansion of the material. Step 4c requires a meticulous setup in a DMA machine. Solid enough pre-cured samples heats in the test machine while a dynamic force measures the elastic modulus. Step 5, relates the constitutive models developed during the characterization methodology through numerical solvers. Simulation software allows to predict the part properties, the mold requirements and the optimal process parameters.
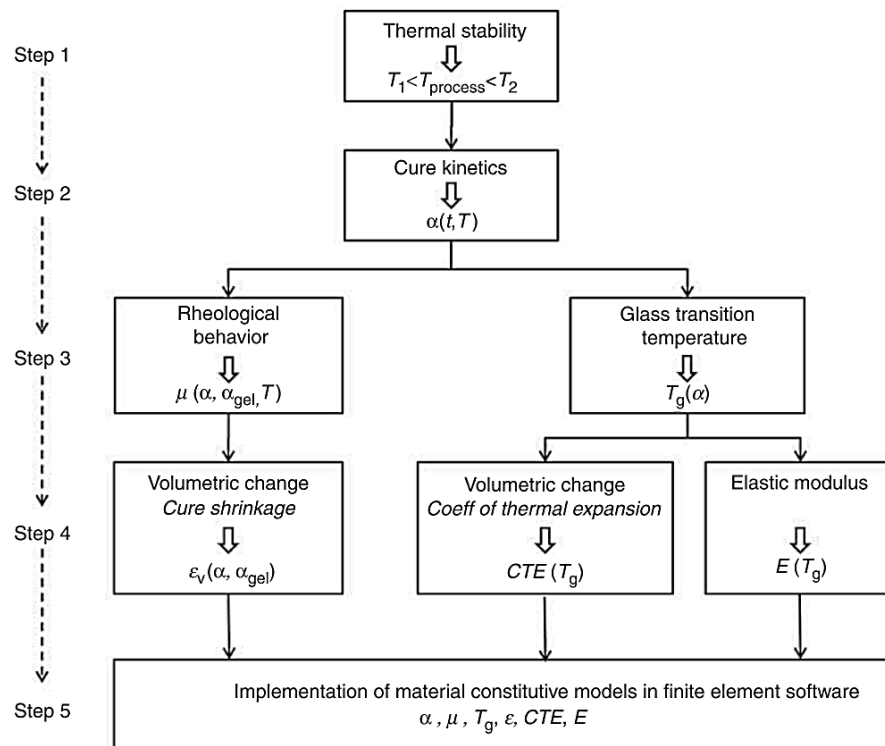
Figure 2.10: Characterization Methodology [30]

Surprisingly, no methodology relates the void content to the final composite properties. Even that researchers have found that a 3% of void content decreases in 14% the mechanical properties [39]. This is because the traditional characterization devices use small samples with little to no fiber content. So, it is not possible to include the void formation in the analysis.

The voids form during the fiber impregnation and the polymer cure. Polymer resin and fiber reinforcement absorb water from the air. During the cure, the molding temperature turns the constituent materials humidity into vapor. Furthermore, gas and water molecules develop as sub-products of the chemical reaction of polymerization [51]. Olivier *et al.* [40] showed that the content, shape and size of the voids have a direct impact in the mechanical properties. Traditionally, the voids formation methodology relates the flow rate of the injection and the consolidation pressure to the final mechanical properties[38, 39, 52]. Typically, researchers measure the final properties through destructive methods, techniques non-suitable for online monitoring of the voids grow in composite structures.

Next, the techniques for the characterization of the properties described in the characterization methodology are reviewed.

2.3 Traditional characterization techniques

This section describes the techniques and equipment used for the characterization of the material properties. Also, delineate the procedure to derive the mathematical models and phenomenological equations.

2.3.1 Fiber impregnation

Despite the similarity of the methods used to find the fiber impregnation, there is no standard methodology for the characterization. The impregnation phenomenon is explained through the Darcy's law and the capillarity number [53, 54]. Equation (2-1) is the empirical mathematical expression that describes the flow of a liquid through a porous media. $\mathbf{v}$ represents the average Darcy's flow velocity vector, $\mathbf{K}$ is the permeability tensor, μ is the viscosity of the fluid and ∇P is the pressure gradient measured from the input to output of the test experiment.

$$\mathbf{v} = \frac{\mathbf{K}}{\mu} \nabla P \tag{2-1}$$

Equation (2-2) calculates the dimensionless number for the capillarity force. μ is the viscosity of the fluid, $\mathbf{v}_f$ is the fluid velocity, γ is the fluid surface tension and $\cos\theta$ is the angle between the fibers and the fluid direction. This number must be greater than 1.0E-3 [53] so that the impregnation is dominated by the viscosity forces (negligible capillary forces).

$$Ca = \frac{\mu.v_f}{\gamma.\cos\theta} \tag{2-2}$$

Figure 2.11 shows the typical test setup. A mold with an open window lets the camera to record video or take pictures of the fluid flow. Image recognition software or manual eye inspection measures the shape of the wet fibers and the fluid velocity. Researchers pumps a fluid with known properties through the mold while sensors measure the pressure gradient.
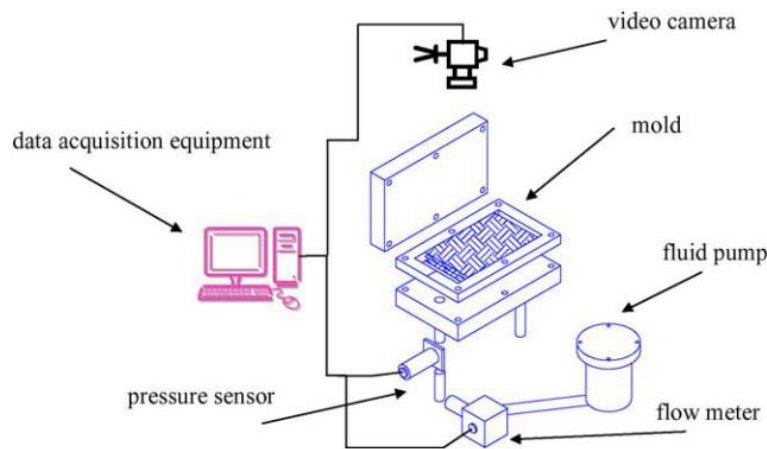
Figure 2.11: Permeability characterization setup [55]

2.3.2 Void formation

Monitor the voids grow during the molding process is a major manufacturing challenge. The industry requires non-destructive techniques to monitor the voids in the final part. Due to the size and cost of composites material parts like a plane cockpit, an on-line monitoring system could assist the engineers during the molding process. Engineers adjust the temperature and consolidation pressure based in their experience, which could lead to non-conformed products. The most promising technique lies in embedding an optical fiber in the composite structure. This type of sensor could measure the void formation, the degree of cure, find the gelation point, the volumetric changes and residual stress [56, 57]. Unfortunately, it is an expensive solution hard to calibrate and is difficult to obtain repeatable experiments. Their major advantage it is also their biggest challenge. Embedding a fiber with a diameter in the scale of micrometres does not influence the final part [58]. However, the sensors hardly survive the cure process or are barely functional due to micro-bending and micro-constriction from the molding process [59]. To compensate the

structural damage of the sensor, researchers require high-end electronics and software capable to do the wavelength corrections. Despite the advantage to obtain several online properties with the same sensor including voids grow, this technology is too expensive and not mature enough to be implemented in this PhD project.

Traditional research on void formation share the same methodology. Cure a composite sample at different impregnation flow rates, consolidation pressures and/or heating ramps [38-40, 52]. Then, researchers divide the sample into pieces to be tested with several tests methods. Some pieces are sized to be tested in a universal stress - strain laboratory equipment. The machine measures the fully cured mechanical properties. Next, a microscope measures the void shape and size though image processing techniques. Finally, the techniques in the ASTM D3171 [60] describes how to measure the void content. The standard requires to dissolve the matrix from a sample with known size and weight. Then, the researcher calculates the void content with the undamaged fiber weight and the materials density. Regardless the fact that the sample preparation is labor-intense, the results from this methodology accurately measure the effect of the void on the resulting mechanical properties.

Non-destructive techniques rely on image processing. X-ray, fluoroscopy, tomography and ultrasonic scans map a fully cured composite. Figure 2.12 shows an ultrasonic C-scan of a composite material cured at three different pressures. As in traditional destructive techniques, image processing monitoring could only characterize fully cured parts.
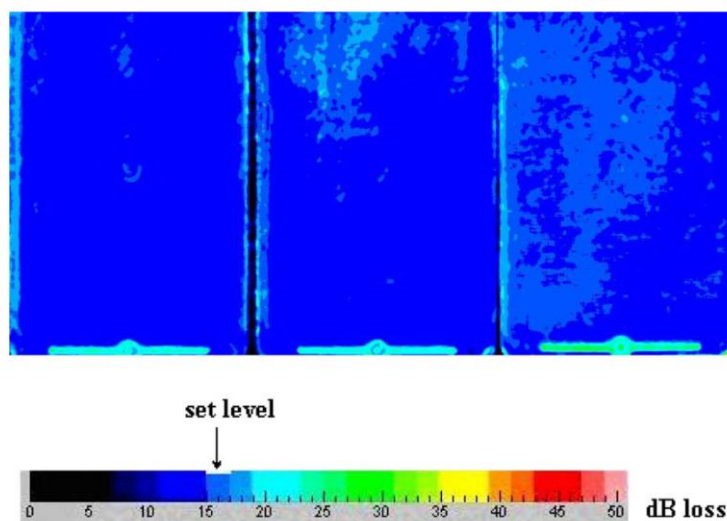
Figure 2.12: C-scan images of the voids on three fully cure composite plates [61]

To the best of our knowledge, researchers still have not developed an online monitoring characterization technique for the void formation different to the fiber optics.

2.3.3 Cure Kinetics

Microscopic and macroscopic measurements allow the cure kinetics characterization or measure the degree of cure evolution in a thermoset polymer [62]. Microscopic measurements implement expensive techniques and sensors. The method consists of dispersing radiation from a transmitting source through the material. Then, a receptor sensor collects the spectrum from the other side. Because each functional group of the thermoset resin have a characteristic spectrum, dedicated software compares it to the measured data. In PMCMs, fiber Bragg optical fiber sensors represent the most recently published microscopic techniques [56-58, 63-65]. However, their implementation represents a major challenge. Section 2.3.2 Void formation described the fiber optic sensors and their problems.

The most widely spread method is the macroscopic technique. Heat flow sensors or an array of thermocouples measure the heat released during the cure. Equation (2-3) shows the mathematical expression. Is it assumed that the heat flow is proportional to the rate of the reaction [66].

$$\frac{d\alpha}{dt} = \frac{1}{H_T}\frac{dH}{dt} \tag{2-3}$$

Isothermal or heat ramps test measure the cure kinetics, an integration of the collected data calculates the overall heat of reaction (H_T), while the partial integration calculates the rate of the reaction. Figure 2.13 represents the collected data from (a) a dynamic test and (b) an isothermal.
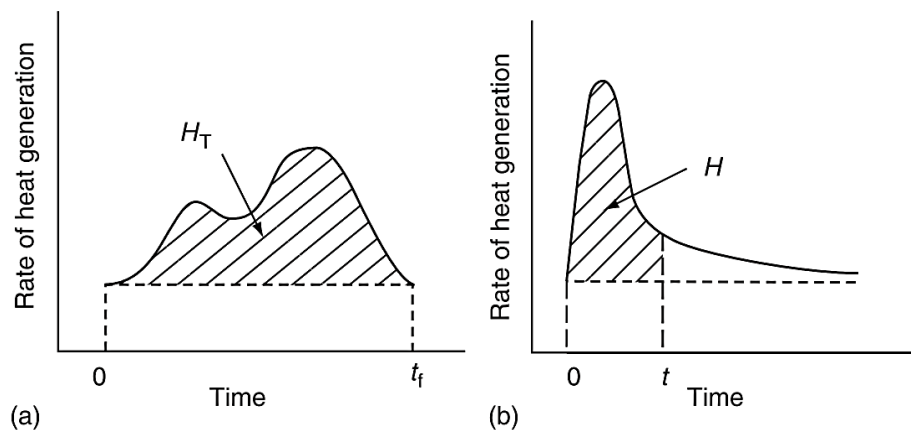
Figure 2.13: Schematic representation of the rate of heat [67]

Commercial DSCs performs experiments at heating rates between 0.1 °C/min and 100 °C/min and temperature ranges between -196°C and 700 °C[68]. Figure 2.14 shows a typical "S" shape result on the cure degree of a thermoset resin.
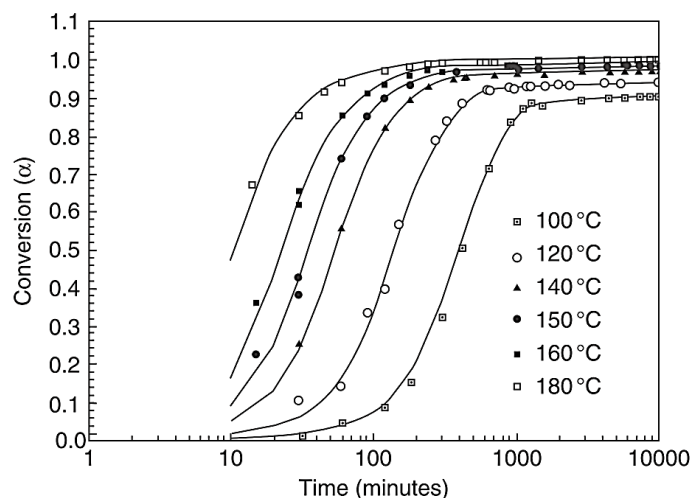
Figure 2.14: Degree of cure vs time for an epoxy-amine in different isothermal experiments[68]

2.3.4 Rheological behavior

The rheological behavior of a material requires a dynamic mechanical analysis. The machine applies a sinusoidal strain (ε). Then, a sensor measures the material response in terms of stress (σ). Figure 2.15 shows the possible results for a dynamic mechanical test.
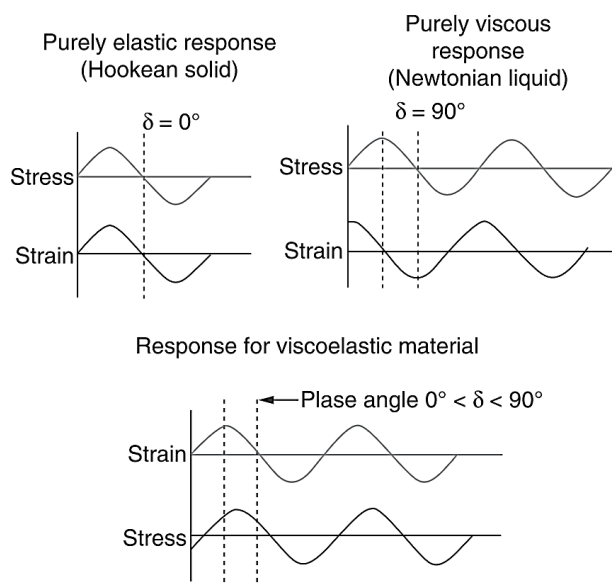
Figure 2.15: DMA material responses [68]

If not phase lag (δ) is presented in the two measurements, the material is purely elastic, and the Hooke's law modulus represents the amplitude ratio between the stress and strain. On the other hand, if the phase lag is 90° the behavior is purely viscous. The response of polymers is in the middle and corresponds to a viscoelastic material. The complex modulus E* represents the material behavior. Equation (2-4) shows the viscoelastic mathematical representations. The complex modulus can be divided into two expressions. The storage modulus E' describes the elastic nature of the material, whereas the loss modulus E" represents the liquid behavior.

$$E^* = E' + iE''$$

$$E' = \frac{\sigma}{\varepsilon}\cos(\delta) \qquad (2\text{-}4) \qquad\qquad \frac{E''}{E'} = \frac{\sin(\delta)}{\cos(\delta)} = \tan\delta \qquad (2\text{-}5)$$

$$E'' = \frac{\sigma}{\varepsilon}\sin(\delta)$$

Equation (2-5) shows the material loss factor or "tan delta". This quantity represents the ratio of energy dissipated to energy stored in one cycle of deformation.

The Rheometer is a specialized laboratory equipment capable of performing tests in shear. This machine has the capability to measure the materials viscous behavior. The measurements follow the Newton's law of viscosity [68]. Equations (2-6) and (2-7) shows the most common relationships.

$$G^* = G' + iG'' \qquad\qquad\qquad \eta^* = \eta' + i\eta''$$

$$G' = \frac{\tau}{\gamma}\cos(\delta) \qquad (2\text{-}6) \qquad\qquad \eta' = \frac{G''}{\omega} \qquad (2\text{-}7)$$

$$G'' = \frac{\tau}{\gamma}\sin(\delta) \qquad\qquad\qquad \eta'' = \frac{G'}{\omega}$$

where G*, G', G" are the modulus in shear, τ is the shear stress, γ the shear strain, η^* is the complex viscosity and ω is the frequency used during the experiment. When η'' is zero, η' represents an ideal liquid.

International associations define several standard tests, but they are only a mere indication to improve the data collection and researchers may or may not follow them. The Standard defines the

sample and the laboratory device specifications and requirements to obtain good accuracy and repeatability in the collected data. Also, the Standard explains the data processing or curve fitting that allows to characterize the material property. When a researcher applies another technique, the publication explains in detail the entire procedure to characterize the model parameters. Yousefi *et al.* [66] reviewed the cure kinetics, the rheological behavior and the most accepted test, measurements and models used in thermosets materials.

2.3.5 Glass Transition Temperature

During the cure of the thermoset polymers, the glass transition temperature T_g varies until a constant value that is representative of the solid material. This means that the T_g is a function of the cure degree.

The T_g defines the maximum in-service temperature for the composite part. This is because at temperatures above this temperature, the polymer changes to a rubbery material and its mechanical properties deteriorate considerably.

Researchers characterize this property with the rheological behavior and the heat flux released during the cure. The sample heats while it is mechanical loaded either in torsion or flexion. A sharp decrease in the storage modulus (E' or G') identifies the T_g. The ASTM E1640[69] standard describes this point as the interception of the two tangent lines in the storage modulus curve. But researchers also report this value as the peak in the tan δ. For this reason, it is evident that there is not agreement in the procedure. Either one temperature is valid, but the tan δ peak gives higher values. Figure 2.16, shows the two procedures.
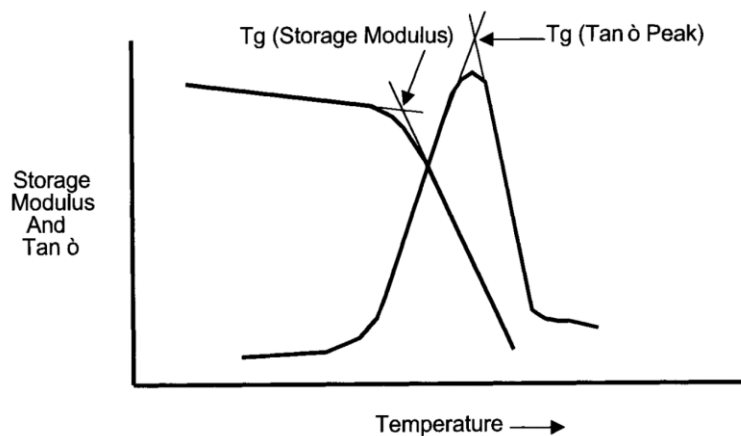
Figure 2.16: T_g in a dynamic mechanical analysis [41]

The reported data must include the load frequency and the heating rate. That is because the T_g shifts with those two parameters [70-72].

The heat flux data contains information about the glass transition temperature too [68]. Figure 2.17 shows that the T_g occurs as an inflection point in the derivative of the heat flow versus temperature data in a heating experiment.
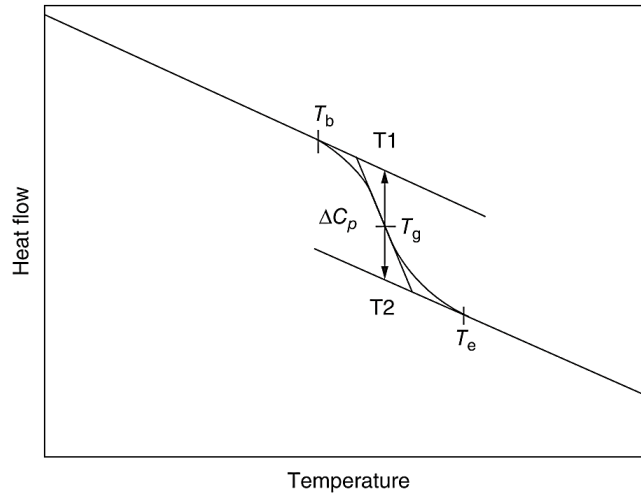
Figure 2.17: T_g in a Heat Flux data, endotherm down [68]

2.3.5.1   Cure-dependent Glass Transition Temperature

A dynamic mechanical analysis or a calorimetric experiment characterizes the cure dependency of the glass transition temperature. The experiment requires several samples with un-cure, partially cure and fully cured characteristics. To collect the data, researchers follow the next procedure [29, 73, 74]: First, totally cure a sample and obtain H_T. Second, partially cure a sample during a time t. Then, the sample is cooled as fast as possible to freezing temperatures (quenching). This process stops the chemical reaction. Now the samples are ready for the characterization of the glass transition, either by calorimetry or dynamic analysis as described in the section 2.3.5. Also, during the second heating cycle over the partially cure sample, the researcher obtains the residual heat H_R and use the Equation (2-8) to calculate the partial degree of cure.

$$\alpha = 1 - \frac{H_R}{H_T} \qquad (2\text{-}8)$$

Applying these experiments for different times t or degrees of cure, the cure-dependent glass transition temperature is modeled.

As suggested in [30, 50, 75] the T_g is typically expressed in terms of the degree of cure α using the Di Benedetto's equation (2-9) and the diffusion-controlled cure rates by a Williams-Lendel-Ferry WLF type equation (2-10).

$$\frac{T_g - T_{gO}}{T_{g\infty} - T_{gO}} = \frac{\lambda\alpha}{1-(1-\lambda)\alpha} \tag{2-9}$$

Where $T_{g\infty} - T_{gO}$ are the glass temperatures of fully cured and uncured resin respectively. α is the degree of cure and λ is a correction constant parameter ranging from 0 to 1. Researchers found values near to 0.4 for thermoset polymers.

$$\log a_T = \frac{C_1(\alpha)(T - T_g(\alpha))}{C_2(\alpha) + (T - T_g(\alpha))} \tag{2-10}$$

2.3.6 Gel point (α_gel)

The cure degree that marks the change from liquid to rubber is referred as gel point. In this point the viscosity has an abrupt increase and cannot flow anymore. It is important to characterize this point because marks the beginning of the mechanical properties [32]. ASTM D4473 [76] describes the procedures to obtain this point:

- For a resin system, the gel point is when the complex viscosity in equation(2-7) reaches 100 Pa.s.

- The gel point is the interception of the loss and storage modulus or were the loss tangent reaches the unity tan α (G''/G'=1).

Researchers found that the cure degree of the onset gelation is independent of the cure temperature, also the cure degree range between 58 – 62 % [29, 68].

Figure 2.18 shows an useful engineering map that describes the whole behavior of the thermoset, the time-temperature transformation diagram (TTT) created by Enns and Gillham [77]. The vitrification takes place when $T_g = T_{cure}$.
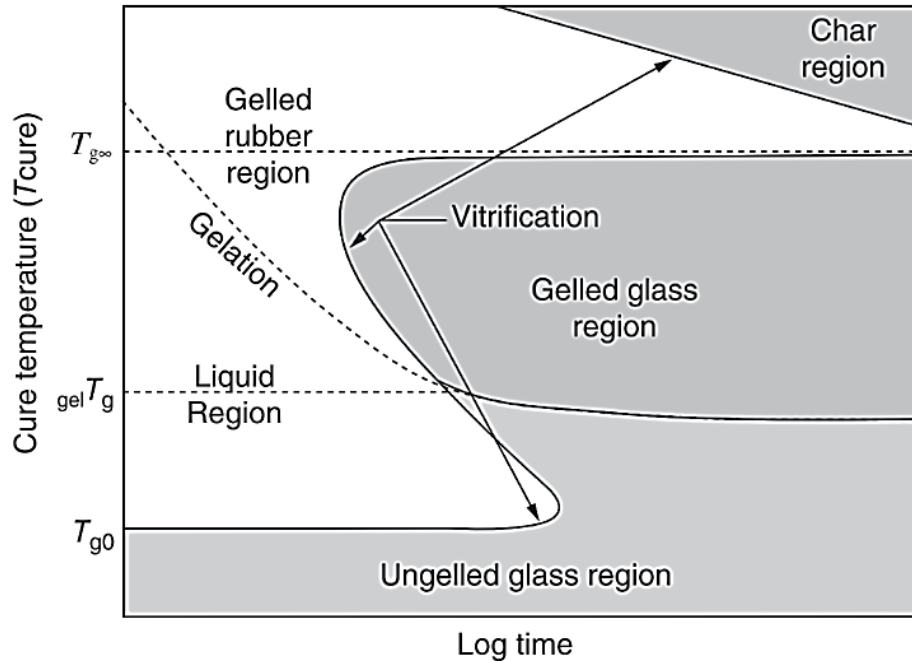
Figure 2.18: Generalized TTT cure diagram[68]

When choosing a cure temperature, a value higher than $_{gel}T_g$ ensures the on-set gelation of the resin. In contrast, lower values make the resin vitrify into and ungelled material, a desired state to store pre-impregnated fabrics because the chemical reaction rate greatly decreases. $_{gel}T_g$ represents the temperature where gelation and vitrification intersect. To map this diagram, researchers combine the data from gel times as function of the temperature, the glass transition as function of the cure degree and the variation of the cure degree with time. All of them described in the sections above.

2.3.7 Viscosity as function of the degree of cure

Halley *et al.* [31] reported about 19 models in their review for the rheological behavior as function of the cure degree. They contain empirical, gelation, molecular, statistical, Arrhenius and free volume models. To our knowledge, the most popular seems to be the gel model suggested by Castro and Macosko [78] and the modified WLF-type equation [31]. Either way, the models require to find a set of constants derived from the experiments described in the previous sections. Also, they assume that the resin behaves as a Newtonian fluid [79]. Figure 2.19 shows the typical viscosity behavior of a thermoset polymer. In section I, the effects of the temperature activate the molecules in the liquid resin. Therefore, the viscosity decreases. Section II contains the minimum viscosity

point. After this point the chemical reaction is important, and the resin viscosity increases to infinite in the solid stage of section III.
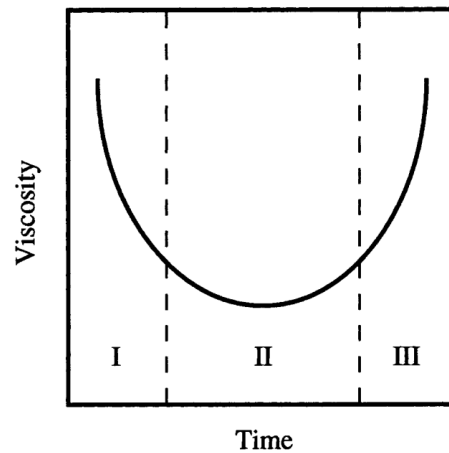
Figure 2.19: Typical viscosity behavior [31]

2.3.8 Volumetric changes during cure

Typically researchers embedded sensors into the composite structure, but sensors like strain gauges have an impact in the composite structure [28]. The problem decoupling the different effects of the temperature arises because during the cure, the fiber bonds into the resin. To fully understands the composite behavior, researchers require newer techniques. In general, they characterize the resin only. Then, mathematical models estimate the resin – fiber system behavior. The chemical shrinkage and the thermal expansion effects need to be decoupled. First, isothermal experiments measure the chemical shrinkage. Next, data from the volumetric changes are corrected with the shrinkage measurements. The result corresponds to the coefficient of thermal expansion CTE [80].

Figure 2.20 shows an overview of the volumetric characterization techniques. The experimentation challenges comprise errors induced by the resin sticking to the mold walls, too small samples or thermal gradients in large samples [28]. To prevent the resin from sticking to the mold, researchers cover the sample with layers of silicone or Teflon. This allows the material to expand or shrink without developing additional stresses. However, the effects and changes of this coupling agent require of additional calibrations [28].
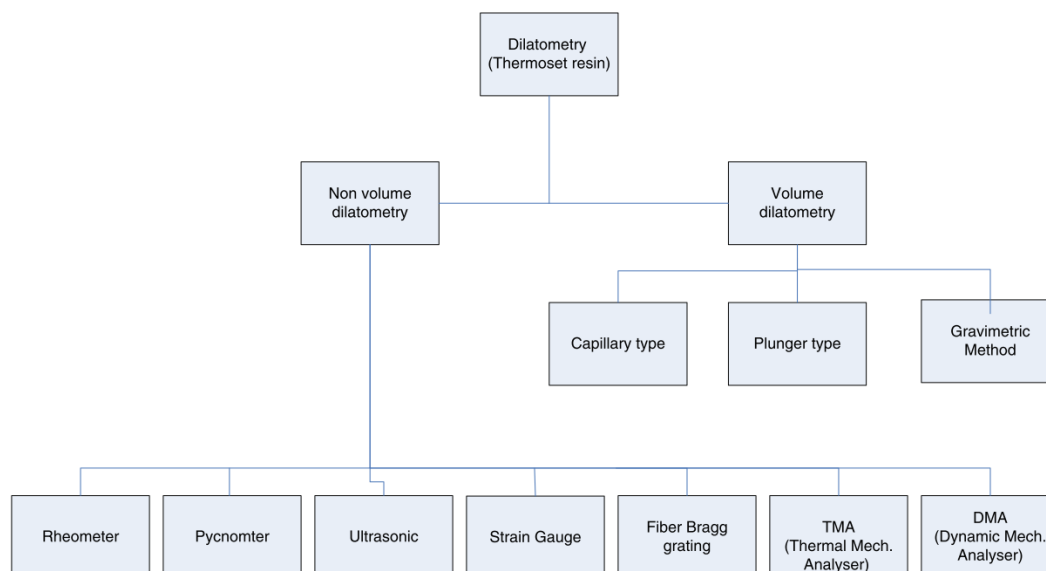
Figure 2.20: Shrinkage measurement techniques [28]

The chemical shrinkage occurs by phases divided by the gel point. Before gelation, the resin is in a liquid state with a slow chemical reaction kinetics. Resulting in a negligible shrinkage [27]. When the resin reaches the gel point, a small compressive force of typically 0.1 N guarantees the contact between the measuring device and the sample. The distance or "gap" measured by the device while the sample cures, constitute the shrinkage as function of the cure degree. Figure 2.21 shows the shrinkage in an epoxy–anhydride resin. Researchers assume a linear behavior neglecting the final curvature for simplification [36, 81]. Authors compare the results from a Pycnometer and a DMA using the same procedure [27, 82]. They found a difference of maximum 10% between the measurements taken with the two devices.
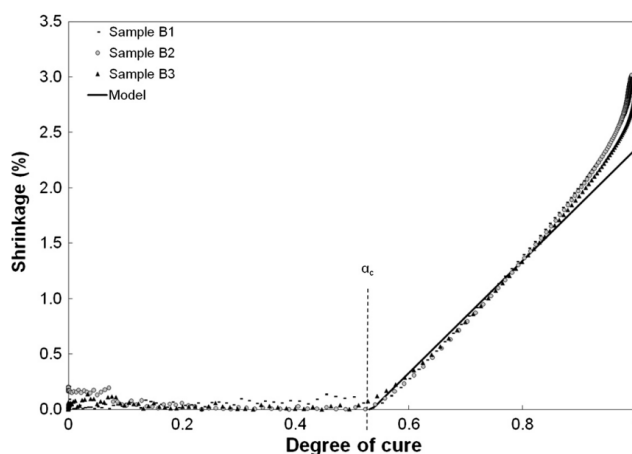
Figure 2.21: Resin shrinkage in an isothermal cure of 120 °C[36]

A TMA or a PVT piston-like device typically measure the CTE using the "gap" technique. Figure 2.22 shows the volumetric variations divided into four stages by Msallen et al. [29].
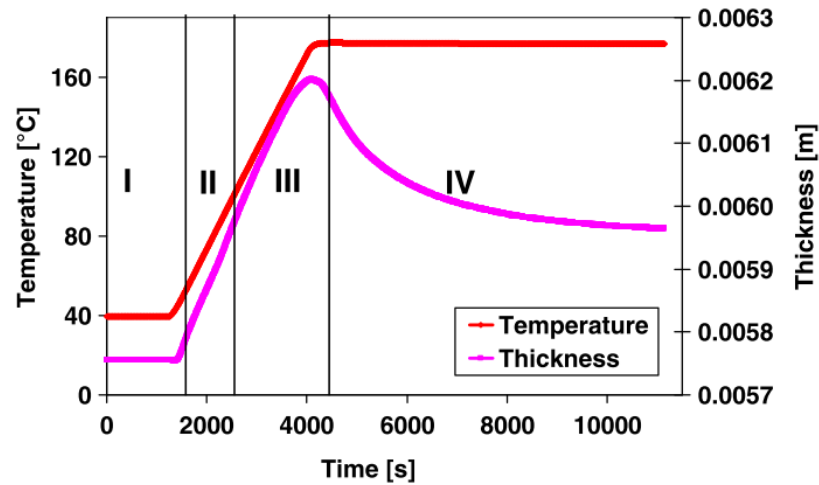
Figure 2.22: Sample thickness variations during a cure cycle[29]

I. Figure 2.23 shows the capsule made of a low modulus elastomer that covers the liquid resin inside the mold. Researchers found that elastomers act as an incompressible fluid [83]. Before heating up, the whole setup stands to a constant temperature (ambient or close) for thermal stability of the assembly.

II. A heating ramp increases the temperature. The shrinkage is negligible during the liquid state, so, the measured volume expansion matches the liquid thermal expansion.

III. In this stage, the thermal expansion and the chemical shrinkage develops at the same time, for this reason the thickness exhibit an inflection in the measurement.

IV. Finally, an isotherm ends the chemical reaction. After fully cure, cooling and heating ramps determines the final part CTE.

Figure 2.23: Elastomer capsule[35]

The resin chemical shrinkage and the elastomer CTE data obtained from separated tests rectify the material CTE characterization data.

Finally, Figure 2.24 shows the influence of the T_g over the fully cured material. The change of state from glassy to rubbery reflects a variation on the property value at high temperatures. At glassy state (temperature $< T_g$) the solid material limits the relative movement between molecules, the measure represents the usual CTE. On the other hand, the rubber-like state softens the material. Naturally, the molecules expand easily and the CTE value increases [30].
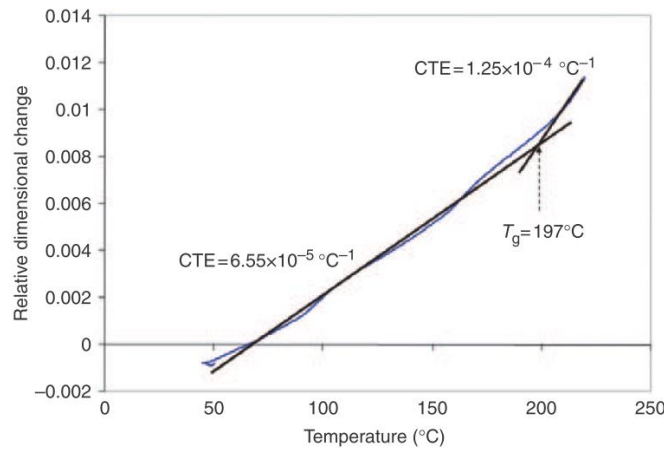
Figure 2.24: Dimensional change of a fully cure epoxy during a heating ramp [30]

2.3.9 Cure dependent Modulus

The mechanical property of modulus varies as function of the cure degree and the temperature. Researchers found that the mechanical properties begin to develop after the gelation point [30, 32, 50, 84]. For this reason, the traditional characterization methodology consists of curing the test samples after this point, then cool down the material as fast as possible to stop the chemical reaction. Section 2.3.5.1 describes this sample preparation procedure. After the sample setup, a three point bending or torsion test measure the modulus of the partially cure material [30]. The mathematical equations (2-4) and (2-6) combined with the cure degree measured with a heat flux sensor joins to find the cure dependent modulus development. Storage modulus E' and Shear storage modulus G' relates through the following material isotropic relation [30, 32]:

$$G(T,\alpha) = \frac{E(T,\alpha)}{2(1+v)} \qquad (2\text{-}11)$$

where ν is the Poisson's ratio measured from a fully cured sample at ambient temperature. Bogetti and Gillespie [49] found not differences if the modulus model takes into account the development of the Poisson's ratio during cure. They concluded that the Poisson's ratio does not have influence over the macroscopic properties of the PMCM or in the process induced residual stress. Figure 2.25 shows the modulus development as function of the cure degree.
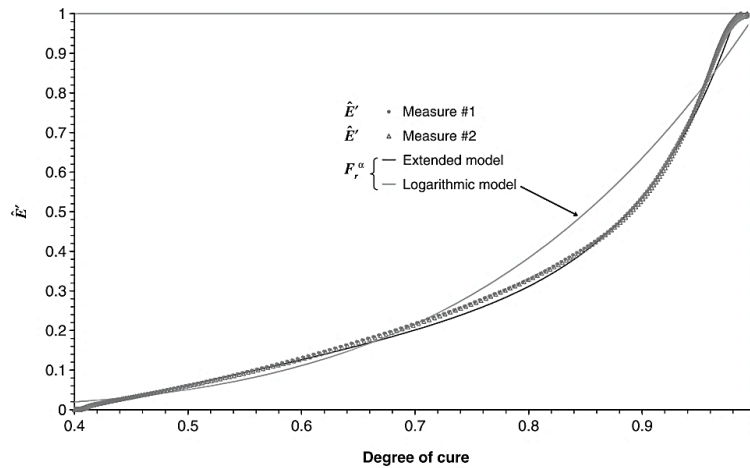
Figure 2.25: Storage modulus as function of the cure degree [32]

Figure 2.26 shows the "shift effect" measured by Johnston [50]. He measured the modulus development at two isothermal temperatures.
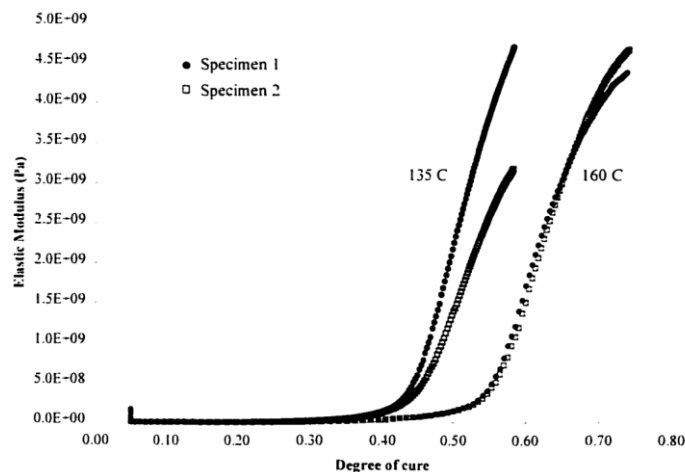
Figure 2.26: Shift effect in the modulus caused by the cure temperature [50]

Finally, the T_g decreases the mechanical modulus in a fully cured material. Figure 2.27 shows this phenomenon. From T_1 to T_2 the modulus decreases linearly. Then, from T_2 to T_3 the material has a

sharp reduction on the mechanical properties as the temperature approaches to T_g. At the end, a stabilization curve marks the change to the rubbery state where the modulus remains constant [30].
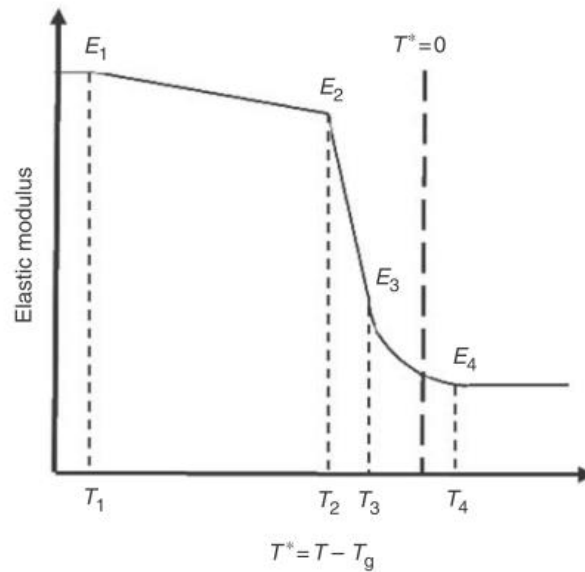
Figure 2.27: Modulus as function of the temperature [30]

All things considered, the traditional characterization methodology requires too many laboratory equipment and experiments. Even so, the tests require well trained personal capable to setup and interpret the collected data. Inevitably, the composite material community necessitates a better characterization methodology or device.

2.4 Single experiment devices for the characterization of multiple composite material properties

This section reviews the devices under development for the characterization of simultaneous properties during cure of PMCMs. Section 2.3 demonstrates the strong influence of the cure degree over the material properties. Also, from the traditional characterization methodologies we observed that the DMA and the Rheometer have the capability to measure the evolution of the mechanical properties as a function of the temperature. It is just logical to add to these devices the ability to measure the cure kinetics. Unfortunately, despite the improvements, the device limitations permit measure only the polymer part of the composite. In contrast, other researchers opted to build their own devices. For this reason, we divided these devices into two categories, attachments to traditional characterization devices and custom-made.

2.4.1 Attachments to traditional characterization devices

Usually, researchers measure the mechanical properties of polymer resin and thin composites with DMA or Rheometers. However, the labor intense sample setup (Section 2.3.5.1) leads to experiments hard to reproduce. Therefore, they reconfigure existing laboratory equipment to improve the measuring capabilities of the device, while taking advantage of the existing platform (sensors, force, data acquisition, reports, etc.). Despite the improvements, the device force remains the same. Thus, the characterization of thick composites continues to be a difficult task.

The following section presents the device attachments, their improvements and disadvantages, as well as the team and an approximate timeline of the development.

2.4.1.1 DMA Heat Flux

Polytechnique Montreal, CCHP and Metravib join to produce an attachment to a DMA test machine in Canada. Reports date from 2010 – 2013 [36, 85, 86].

A Metravib DMA +450 equipped with a custom-made mold an a Thermoflux heat flow sensor measure the mechanical properties as function of the temperature and cure degree [36, 85]. Figure 2.28 shows the attachment schematic. A closed mold with an injection port fits inside the DMA furnace. The existing displacement sensors allow to choose the desired sample thickness. The force controller applies the sinusoidal load while maintaining a central force to track the sample shrinkage.
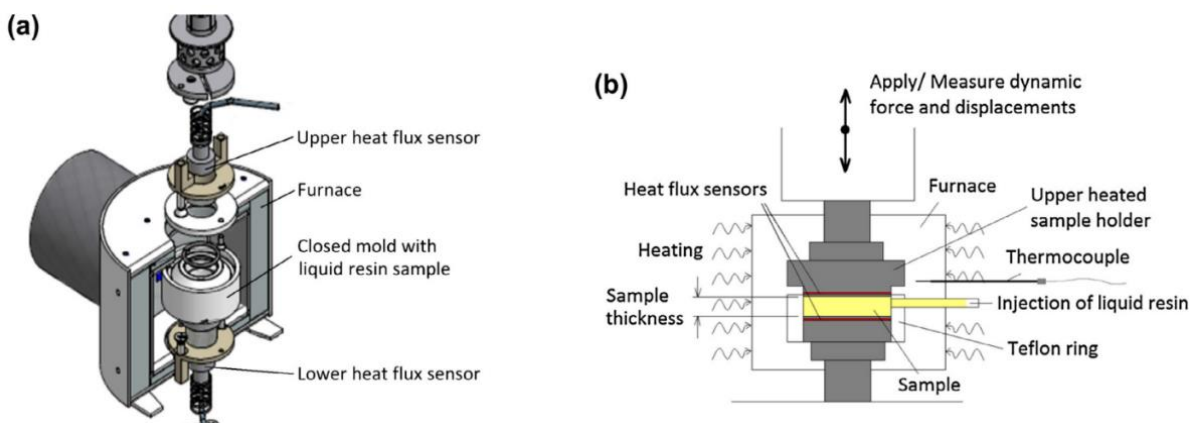
Figure 2.28: DMA Heat flux fixture [36, 85]

Overall, the improvement allows to include the polymer chemical reaction. But the device exhibits the next limitations:

- Figure 2.29 shows two perturbations in the temperature isothermal. In the first event, the temperature difference between the cold resin and the mold during the injection causes a decrease in the furnace controlled ambient. And second, an exothermic peak from the chemical reaction. As a result, the researcher requires to find an optimal sample thickness. At low resin mass the sensor is not able to take the measurement. On the other hand, too much mass and the furnace controller could not stabilize the temperature.
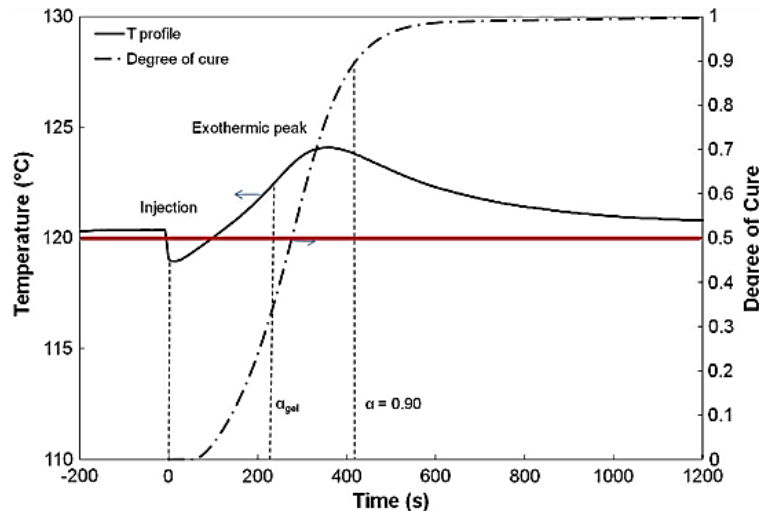
Figure 2.29: Isothermal test at 120 °C[36]

- The Teflon holder serves as a mold with an injection port, but this piece needs to be very tight to prevent resin leaks. To put it differently, the mold is not optimal decreasing the reproducibility of the test.

- Despite the researchers' claims, they do not report the characterization of a composite material.

- Properties measured: cure degree, shrinkage, Stiffness, gelation point, loss modulus, storage modulus, viscosity.

2.4.1.2 RheoDSC

Research Foundation Flanders (FWO), TA Instruments and the University of Vrije in Brussels produce a combined device in Belgium. The approach combined two TA commercial devices, the Q1000 T_{zero} DSC and the AR1000 Rheometer. This research date from 2007 to 2013 in the literature [87-91].

Figure 2.30 shows the RheoDSC hybrid device. They remove the DSC flux sensor capsule and adapted it to the rotatory Rheometer as a custom fixture.
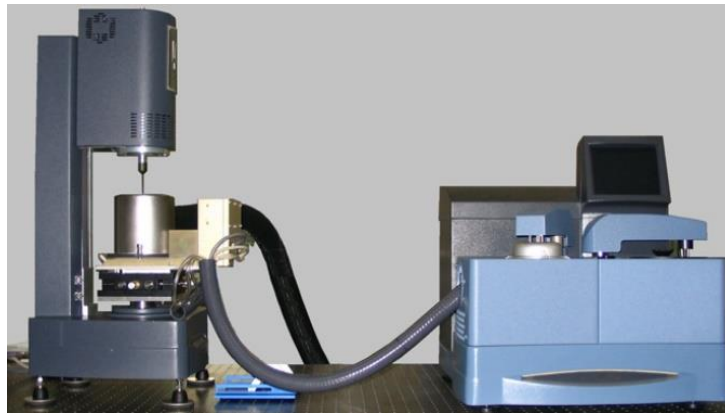
Figure 2.30: RheoDSC made of AR-G2 Rheometer and a Q2000 DSC [87, 91]

From the review, the hybrid device displays the following challenges:

- The RheoDSC uses the DSC's sample pan, which result in a very small sample size typically 5 – 20 mg [68].

- As a matter of fact, the DSC sample size is very susceptible to thermal gradients in DSC measurements [68], which is why the attachment requires of a meticulous calibration. Figure 2.31 shows the temperature gradient in the hybrid attachment, where the rotor acts as a heat sink. Indeed, great part of the publications deal with the device calibration and data validation [89]. All things considered, the thermal lag and the difficulty to predict the influence of the rotor over the test makes this device operative under very special circumstances. Only very qualified personnel could take advantage of this device.

- Properties measured: TTT, G', G'', η^*, degree of cure, gel time and T_g.

- Authors do not report composites or volumetric changes.
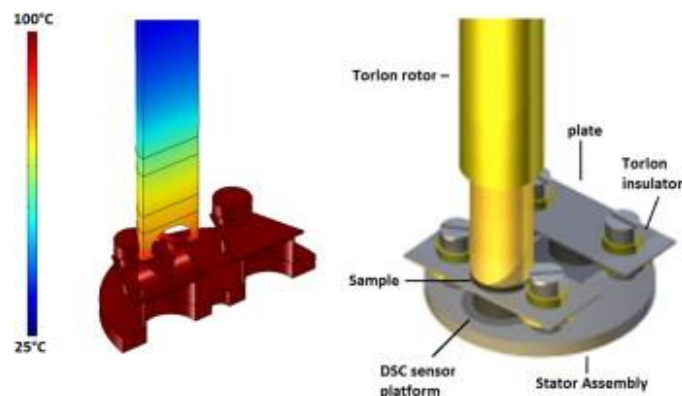
Figure 2.31: Rotor temperature gradient [90]

2.4.1.3 Dielectric Analysis DEA-Rheology

NETZSCH Company develops this hybrid device mixing a Rheometer with a reusable dielectric sensor. The dielectric sensor uses the sample dielectric characteristics as a capacitor and measure the phase lag between the applied voltage and resulting current. This research was found online in 2014 [92], but was finally published in 2018 [93]. Figure 2.32 shows a dispensable dielectric sensor on the left and the DEA-rheology attachment on the right.

Device challenges:

- Frequency swap and frequency dependent properties. The device requires of a specific calibration and software. Also, the device limits to the characterization of polymer with good polarizability. Filler and reinforcements affect the measure [68].

- Researchers found difficult to relate the polymer physics with the dielectric data. Known models are not applicable.

- Unfortunately, researchers do not measure the cure kinetics. In that case, the device requires more study.

- Properties measured: Viscosity, G', G'', Tg and Gel point.
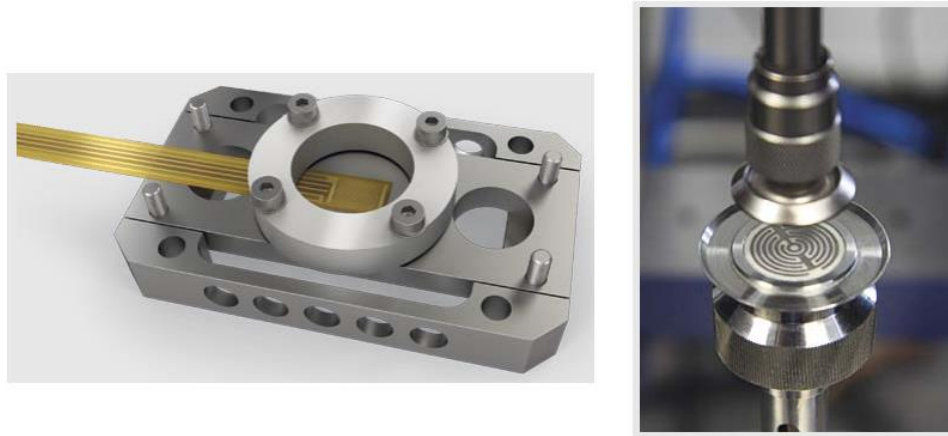
Figure 2.32: DMA-DEA hybrid device [92, 93]

2.4.1.4   Rheo-ultrasonic

In this occasion, the University of Salento in Italy made a Rheometer coupled with an ultrasonic emitter and receptor. The device was tracked from 2004 to 2013 [94-97]. Ultrasonic sensors measure the frequency response of the sample to an ultrasonic wave. The data relate directly to the sample mechanical properties. Moreover, the ultrasonic waves cause mechanical vibrations which propagate through the sample material. Equation (2-12) shows the mathematical relations when the wavelength (λ) of the propagating waves is λ/2π<<1 [94]:

$$L' = \rho c^2; L'' = 2\rho c^3 \frac{a}{\omega}$$
$$\omega = 2\pi f$$

$$(2\text{-}12)$$

where ρ is the material density, c is the ultrasonic velocity, a the attenuation coefficient, f is the frequency and ω the angular frequency. L' corresponds to the elastic modulus and L'' is the loss modulus. Equations (2-13) [94, 98] present the mathematical relationships to the bulk and shear modulus from the traditional mechanics:

$$L' = K' + \frac{4}{3}G'$$
$$L'' = K'' + \frac{4}{3}G''$$

$$(2\text{-}13)$$

This device delivers non-destructive and non-intrusive measurements of the molding process. In addition, the measure of the dynamic mechanical properties does not require of high force actuators. One of the major challenges in the characterization of stiff composite materials.

Despite all the advantages, the device has the next limitations:

- Researchers must make their own ultrasonic transducers and data acquisition. The test setup requires of proper alignment and contact to the sample.

- Figure 2.33 shows the Rheo-ultrasonic setup. The rheometer warrants the sensor alignment and the contact to the sample. At the same time, it measures the sample shrinkage. Although they perform air couple experiments, contact and coupling agents produces better data. Common coupling agents come in liquid or gel form, but they have influence on the resin cure kinetics.

- Custom-made ultrasonic sensor made from piezoelectric materials gives low resistance to industrial environments, like high temperature and pressure.

- The interface matrix – fiber reinforcement decreases the ultrasonic wave propagation. In other words, it is not possible to characterize composite materials because the fiber interferes with the collected data.

- Properties characterized in resin systems: Gelation, vitrification, loss modulus, storage modulus, cure degree, volumetric changes.
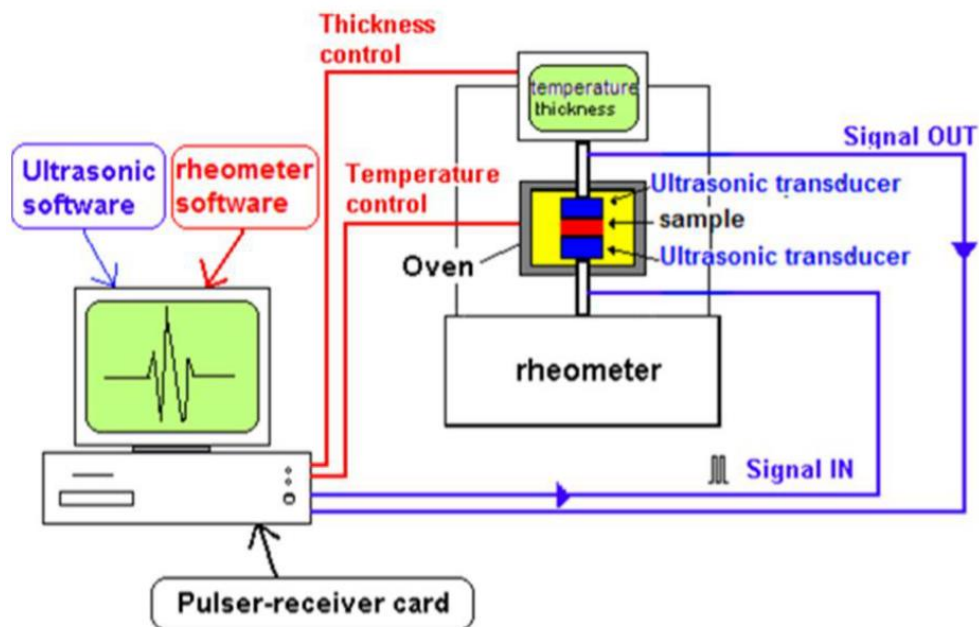
Figure 2.33: Rheo-ultrasonic device [94]

2.4.2 Custom-made

Custom-made devices implement an electric press to apply the force. But they go one step further. The new device or mold does not rely in an existing platform. As shown in the last section, the attachment to traditional equipment carries the original machine limitations. Essentially, researchers untie their designs from existing platforms to gain more control over the experiment. In fact, even with the collaboration of big manufactures, the existing platform is too close to the scope of the new custom-made devices.

2.4.2.1 PVT

A force piston with a displacement sensor and a heated mold cavity setup a *Pressure – volume – temperature* machine. Figure 2.34 shows a TMA device diagram. It is in fact a PVT machine; the only difference relies in the amount of force applied during the test. TMA test applies a negligible force to measure the volumetric changes as function of the temperature. Constant, ramps or modulated temperatures measure the material properties by means of the change in the free volume. This device uses small samples, generally to prevent thermal gradients. Researchers characterize materials with thickness of 0.5 to 2.5 mm with heating rates ranging from 1 to 5 °C/min to decrease the thermal effect [68].
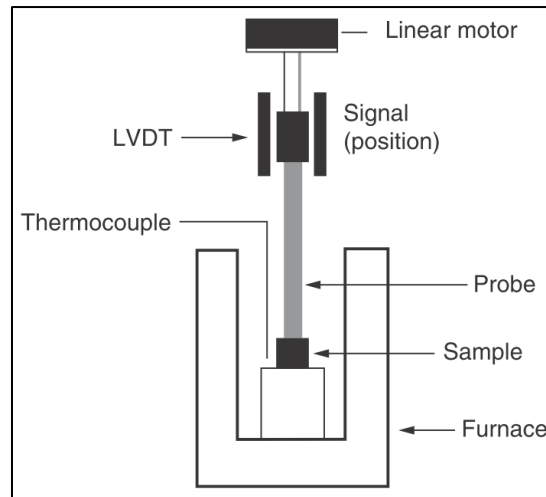
Figure 2.34: TMA instrument [68]

In comparison to TMA, PVT devices have the capability to apply massive pressures of up to 250 MPa [99]. Researchers could also call them high pressure dilatometers. Their pressure capacity makes them ideal to test thermoplastic polymers properties. Injection machines mold this type of material under high pressure due to their high viscosity. Wang [100] review these devices, he found custom machines as old as from 1976. All of them attach a hydraulic pump to a piston. In other words, they put a small sample inside a mold and compress it with a hydraulic piston. In general, researchers classify them into two main categories: piston die and confining fluid. Their main difference is that in the confining-fluid mold, the liquid applies a hydrostatic pressure in all directions, but the fluid used is mercury which makes this experiment non-viable according to modern environmental restrictions. In the case contrary, the piston die is easier to setup, but the sample could stick to the walls, introducing errors in the measure. Either way, researchers found a 4% of difference between measures from one device to the other [100].

Naturally, the specific volume depends of the temperature and the pressure. Figure 2.36 shows the PVT tests on a polymer at different pressure conditions. The section denoted by A-B-C represents the T_g and how the pressure displaces and distorts the linear behavior of the volume and the glass transition.
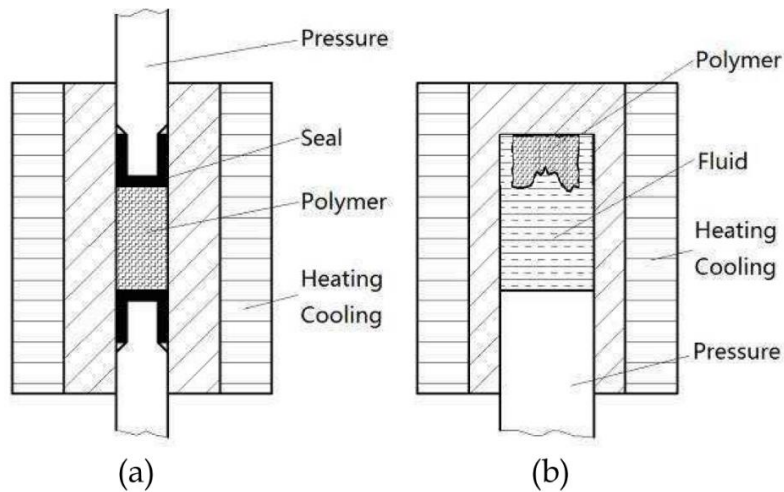
Figure 2.35: Mold categories. (a) Piston-die. (b) Confining-fluid [99]
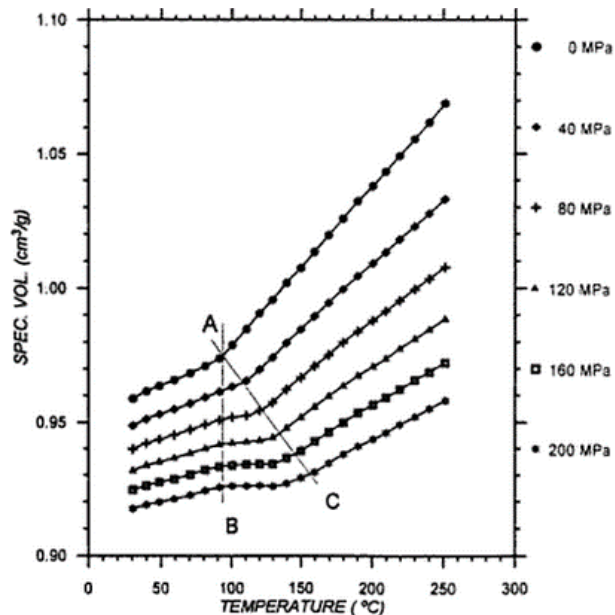
Figure 2.36: PVT tests on polystyrene under isobaric conditions [101]

Finally, Ramos *et al.* [74] study the influence of the pressure over the cure degree on an epoxy-amine system. They obtained the cure degree from the specific volume variation in an isothermic and isobaric PVT test. Figure 2.37 shows that the pressure has very low influence over the resin cure kinetics. Fortunately, in the manufacturing of thermoset composite materials the consolidation pressure is near 600 kPa [41] which compared to the 20 MPa from the test makes the influence of pressure in the cure of PMCM molding process negligible.
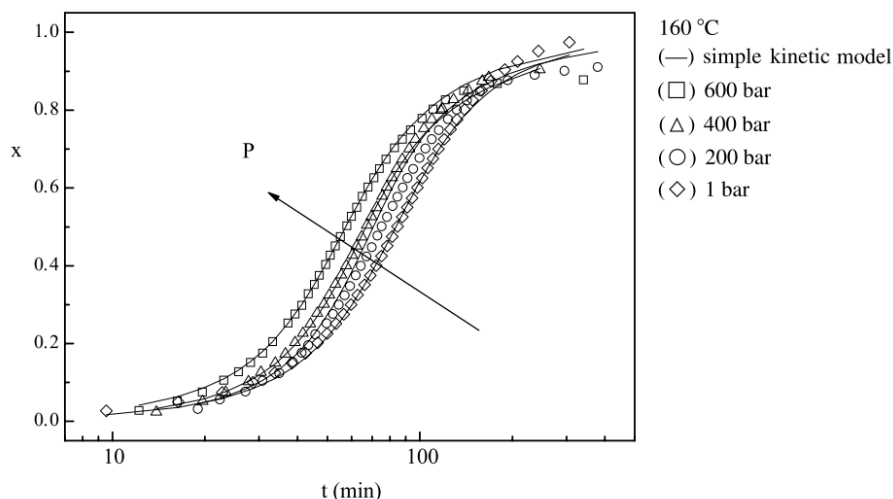
Figure 2.37: Cure degree vs time at different isobaric pressures [74]

2.4.2.2 PVTα and PTV-HADDOC

2.4.2.2.1 PVTα

The PVTα device originally developed from the Nantes University in France from 2003 to 2013 [33-35, 83] is the most active and reported in the literature reviewed about custom-made devices. They made a variation of the PVT piston die device. A mold equipped with a heat flux sensor and an electric press allows the characterization of thermoset polymers with a diameter of 40 mm and variable thickness. The PVTα allows the characterization of simultaneous properties as the material cures. The heat flux sensor obtains the properties as function of the cure degree in a single experiment. Figure 2.38 shows the schematic diagram of the mold. A displacement sensor provides the feedback to measure the volumetric changes during the test. They reported the CTE, cure shrinkage, bulk modulus and cure degree properties.

The device presents the following challenges:

- Heat losses in the mold and thermal expansion of the LVDT sensor.

- The applied dynamic force was not completely sinusoidal, less than 0.5 Hz which makes not possible to obtain the mechanical properties directly.

- A thermocouple embedded inside the sample allows to measure the thermal gradients inside the sample. The data represent the thermal conductivity of the thick sample.

- A silicone capsule covers the sample to prevent the resin to stick to the mold cavity. For this reason, the sample injection and the setup of the middle thermocouple is the challenging part of the test.
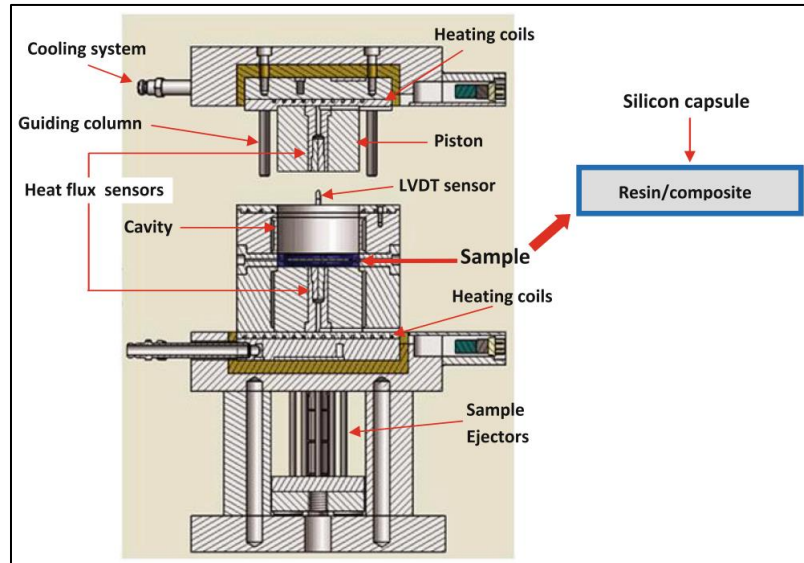
Figure 2.38: PVT-α sketch

2.4.2.2.2 PTV-HADDOC

The PTV-HADDOC is the latest improvement of the Nantes University team with alliances with Airbus Group. This device was recently presented in 2017 [37]. Figure 2.39 shows the new device. It is a confining fluid PVT type. They put a sample of 105 mm x 105 mm and a variable width inside a mold cavity surrounded by silicon oil. Both liquid and a specialized Instron E10000 electrical press maintain a constant pressure inside the mold. The displacement sensor in the piston with the profilometer measures the sample volumetric changes. Researchers measure the volumetric changes in all directions and the cure degree in the same experiments. They test two composite materials, a Glass/Polyester with short glass fibers randomly oriented and a Carbon/Epoxy with plies unidirectional oriented. In both cases the volumetric CTE and volumetric cure shrinkage measure was very close as the one measure with the through the thickness on the PVTα. In the case of the composite with oriented fibers, the researchers observed no influence of the reinforce over the chemical shrinkage.
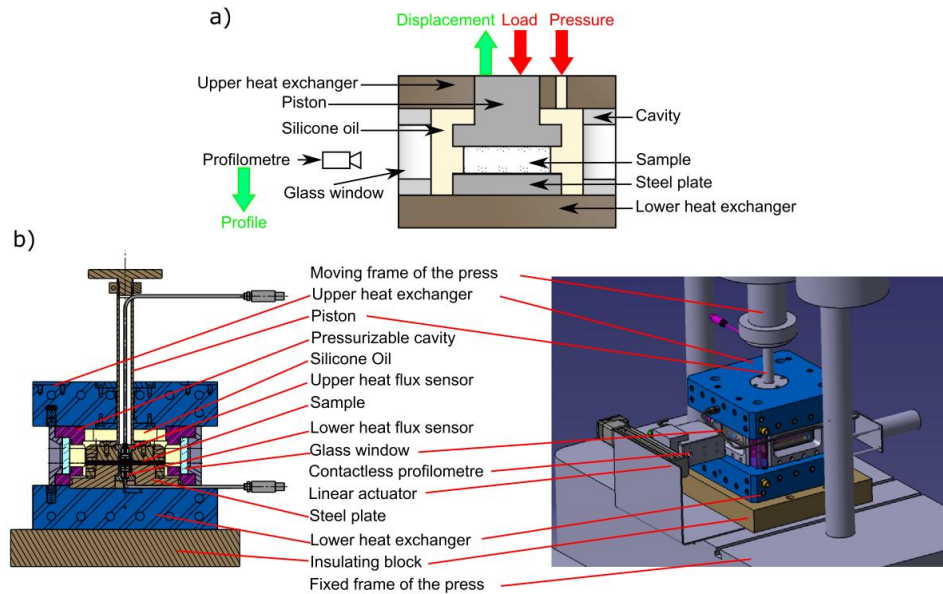
Figure 2.39: PTV-HADDOC Windowed mold design [37]

The device presents the following challenges:

- Synchronize the piston and fluid pressure. This requirement makes possible the hydrostatic pressure.

- The mold and sensors require of a special fine-tune and corrections.

- No significant improvement over the piston die technique. In fact, the challenges on the confining fluid PVT imposes too much work with no beneficial results.

- Despite the addition of a high-end Instron press, researchers have not presented dynamic mechanical tests.

2.5 Conclusion

This chapter contributes to responding to the first objective (OB1) by identifying the laboratory equipment limitations. In specific, we found that the characterization of the fiber impregnation uses a known constant viscosity liquid different from a thermoset. Also, the nature of the PMCMs does not permit to define a unique material model for all composites. Phenomenological models are more suited to describe the material property because a small change in the material composition has big influence over the resulting properties. For example, changing the fiber percent makes a totally different composite. In terms of chemistry, adding less catalyzer will change the cure rate,

one of the most important manufacture properties. This is a big issue for the design because makes unlikely to infer the evolution of the material without a progressive characterization of the constituent materials. In other words, the characterization requires to know before hand the fiber impregnation and compaction to inject the resin. Also, the evolution of the resin viscosity to temperature is important to prevent gelation and polymerization in critical parts of the device and take advantage of the minimum viscosity point during the injection. Another property that requires a good number of tests is the evolution of the T_g. The characterization methodology makes clear that is impossible to find the TTT diagram using only one experiment. In addition, separated the chemical shrinkage from the thermal volumetric changes requires at least one experiment under an isothermal cure. Finally, to the best of our knowledge no device includes the void content and void formation in their test. This is primarily because the test sample is too small to observe the influence of the void content in the material.

The characterization of PMCM is a science in development where traditional techniques compete with custom-made machines. Traditional equipment has the precision and proven procedures, but they cannot characterize a full composite structure due to the small sizes involved in the test. On the other hand, the custom-made devices require of constant calibration.
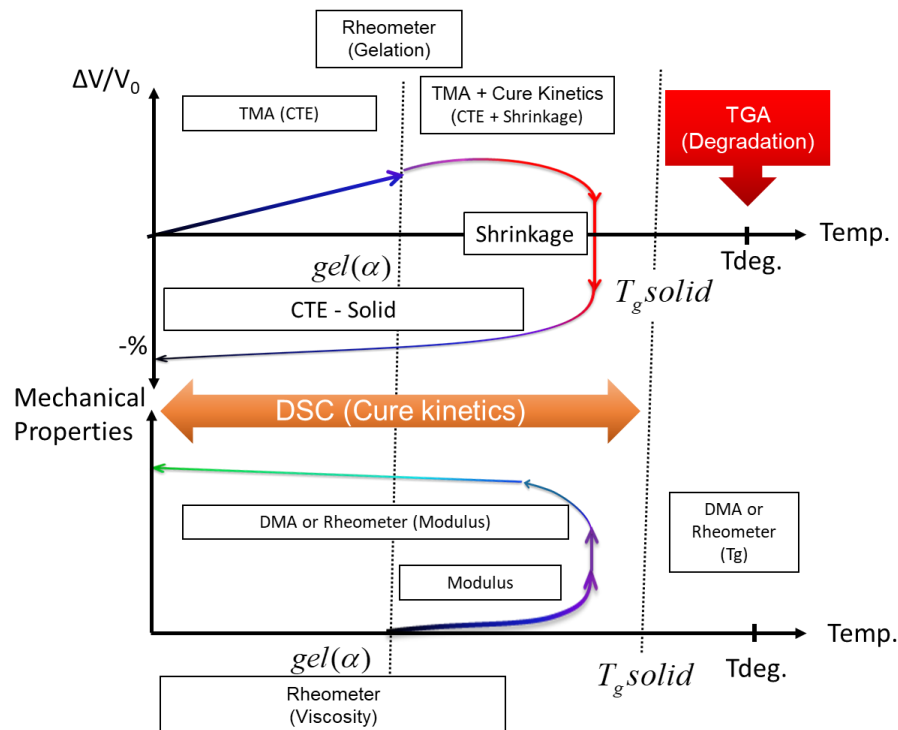
Figure 2.40: Properties development during a cure cycle

Figure 2.40 sums up the transformations that undergo the PMCM during their manufacturing. It also shows the traditional laboratory equipment required to fully track the material history. Unfortunately, the methodology and the number of models and test require to correlate the information from multiple techniques makes this methodology difficult to reproduce.

A custom-made device could improve the characterization of PMCM. PVT devices equipped with heat flux sensors shown promising results. But there are still many challenges to solve. Among them, prevent the resin from sticking to the equipment, the injection of the polymer into the mold, thermal gradients and find out how to apply a dynamic force to a thick composite.

Table 2.1 sums up all the devices reviewed in the literature. Consider that in general researchers do not mention the difficulties they have to produce the data and only show their best results. An despite that fact we were able to collect the information that will lead to a better design. Also, the table will help to understand the challenges that could be faced by the researchers during their own studies. To the best of our knowledge, the dynamic thermo-mechanical characterization of a thick composite material during a manufacturing cycle is still not possible with the traditional and reviewed devices.

Table 2.1: Devices in the literature review

Device	Team	Sample	Test type	Test Characteristics	Properties Measure	Challenges	Project Time Span	References
DMA Heat Flux	Polytechnique Montreal, CCHP and Metravib	Cylindrical 20 mm diameter, 2 mm thick, 0.9 g.	Linear, Dynamic 1-100Hz, Optimal 10 Hz, maximum deformation 20um. Thickness gap method	Isothermal 120 °C	Cure degree, shrinkage, Stiffness, gelation point, loss modulus, storage modulus, viscosity	Sample holder leaks, thin composites, limited force, thermal peaks.	2010 - 2013	[36, 85, 86]
RheoDSC	Research Foundation Flanders (FWO), TA Instruments and the University of Vrije in Brussels	Typical 5 -20 mg. Reported: Epoxy 188 gmol-1 with amine 49.5 gmol-1	Oscillatory shear force: displacement 5e10-3 rad with frequencies 0.079 Hz to 2.5 Hz	Modulated, isothermal 170 °C and ramps 5 Cmin-1	TTT, G', G", degree of cure, gel time and Tg, n*	Too small sample, thermal gradients, thermal lag, calibration. The attachment serves as a heatsink.	2007 - 2013	[87-91]
DEA-Rheology	NETZSCH Company	Diameter 25mm, 1mm thick. Epoxy – Amine	Rheometer displacement 2.5%, angular frequency = 7.5 rads-1, Torque 10 mNm. Dielectric test from frequencies from 1 Hz to 1 MHz	Ramp 0.5, 1 and 1.5 Kmin-1. Range 28 to 208 °C.	Viscosity, G', G", Tg, ε', ε", Gel point.	Cable connector have influence in the measurement. Mechanical and dielectric data hard to couple. Not enough known properties models. Resin only.	2014 - 2018	[93]

Table 2.1 (continued): Devices in the literature review

Device	Team	Sample	Test type	Test Characteristics	Properties Measure	Challenges	Project Time Span	References
Rheo-Ultrasonic	University of Salento in Italy	Thickness: 1.4mm. Test I: Unsaturated polyester resin. Test II: Epoxy 190 gmol-1 with amine.	Ultrasonic wave in the range of 1-10 MHz. Rheometer: contact force to measure thickness	Isothermal at maximum 50 °C	Gelation, Vitrification, Loss modulus, Storage Modulus, cure degree, volumetric change	Custom made ultrasonic transducers prone to damage at high temperature and pressure. Custom hardware and software required. Coupling agent (liquid or gel). The fiber distorts the ultrasonic waves.	2004 - 2013	[94-97]
PVT	-	Polymers, mostly thermoplastics. Sample in the mg range	Pressure, Temperature, Volume	Isobaric up to 120 MPa, Isothermal up to 350 °C. High cooling rates.	Free Volume, Tg, Melting Temperatures, CTE	Leaks in the sample chamber, low pressure resolution, small sample. Hazards enclosing fluid like mercury, the sample could mix with the enclosing fluid. No composites.	Since 1976	[68]
PVTα	Nantes University in France	Diameter 40mm, variable thickness. Epoxy vinyl ester	Pressure, Temperature, Volume	Isothermal and heating ramps up to 180 °C and 4 Cmin-1. Force about 0.75 Mpa.	CTE, cure shrinkage, bulk modulus and cure degree. Thermal conductivity	Heat losses in the mold and thermal expansion of the LVDT sensor. Not a truly dynamic load. Embedded sensors in the sample. Thermal gradients inside the sample. Sample setup	2003 - 2013	[33-35, 83]

Table 2.1 (continued): Devices in the literature review

Device	Team	Sample	Test type	Test Characteristics	Properties Measure	Challenges	Project Time Span	References
PTV-HADDOC	Nantes University in France and Airbus Group Innovations	105 mm x 105 mm, variable thickness	Pressure, Temperature, Volume	Isobaric, hydrostatic pressure of 1 MPa. Temperature 200 °C and heat rate 16 Cmin-1 maximum.	CTE, cure shrinkage, cure degree.	Piston force and liquid pressure synchronization. Hard to calibrate. No significant improvement over regular PVT. No dynamic force.	2017	[37]

CHAPTER 3   UNDERSTANDING THE MANUFACTURING PROCESS

3.1 Introduction

Before implementing the mechatronic design techniques, it is imperative to have a deeper understanding of the manufacturing process in order to comprehend the challenges faced in a real-world setting. Most of the academic research in this field tends to cut off failures and errors from their results, this gives an oversimplified picture of the problematic at hand. For that reason and to obtain experience on the manufacturing steps, a collaboration with the Engineering Research & Flow Technology (ERFT) company provided us with a laboratory scale RTM mold apparatus capable to accurate reproduce the molding process of PMCMs.

These experiments will complement the information found during the literature review. Ensure that we face similar manufacture problems will aid to fully answer the first research objective (OB1) that is to identify the laboratory equipment limitations and manufacturing challenges in the characterization of PMCMs properties.

Figure 3.1 shows the laboratory scaled RTM molding device. The device has an injection pot, a mold and a "catch pot". Also, ball and 3-way valves manually choose the pressure direction.
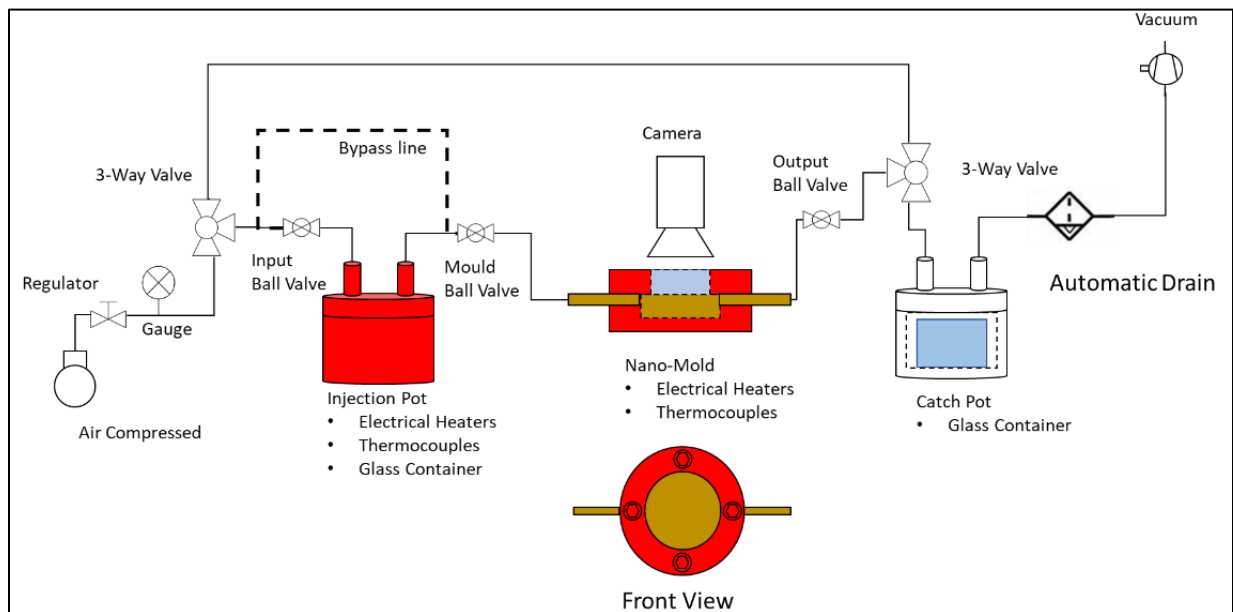
Figure 3.1: Laboratory scale RTM apparatus schematic diagram

The device has a cavity mold of 45 mm x 15 mm. To cure a composite, the operator must follow the next steps with or without minor changes using high temperature gloves:

a. Mold setup: Clean the mold with acetone to remove any dirt or residue from previous injections. Then, apply at least three layers of release agent to prevent the piece from bonding to the mold walls. Each layer requires to wait at least 45 minutes between each coating. Finally, carefully assembly the mold and prepare the device components.

b. Pre-heating: With the Omega controllers, heat the mold, the pipes and the injection pot to the desired temperature. The pipes and the valves that conduct the resin require and specific temperature to prevent any thermal shock. An abrupt change in the temperature of the resin can solidify it and block the injection.

c. Resin preparation: Mix the polymer resin and the catalyst in a glass container that fits inside the injection pot. After thoroughly mixing the components, put the glass container inside the injection pot. Make sure that the injection pot remains completely closed.

d. De-gas: prior to the injection, select the proper vacuum pressure direction with the manual valves. Open the input ball valve to remove the gas inside the injection pot. The catch pot serves as a liquid trap. Additionally, an automatic drain filter gives the extra protection to the company facilities.

e. Injection: Manually choose the injection direction, making sure that the input ball valve remains close. Place the mold so the resin enters from the bottom of the mold. This ensures proper mold filling and fiber impregnation. Set the desire injection pressure and open the valve to push the resin inside the mold. At the end of the injection turn the mold 90 degrees to a horizontal position and close the input - output valves.

f. Consolidation pressure: Use the quick connectors to bypass the injection pot as shows in the dotted line of the Figure 3.1 select the consolidation pressure, close the output valve and open the mold valve to apply the consolidation pressure to the mold.

g. Cure: maintain the temperature until fully cure the material. Then, turn off the heaters and let it cool to near-room temperature.

h. De-mold. Disassemble the mold and remove the piece.

Figure 3.2 shows a detailed exploded view of the mold. Pupin et al. [102] work in the same device in parallel to our work in the ERFT company. They present their results in 2017 and demonstrated that this device and image processing techniques can characterize the influence of the consolidation pressure in the voids formation. But unlike them, this PhD project focuses on finding the device limitations and the manufacturing challenges. It is important to separate them to understand the requirements of the mechatronic device to be developed and contribute to reaching our main objective to integrate multiple characterization laboratory equipment into a single device for PMCMs. This abstraction is discussed in detail in section 3.3.
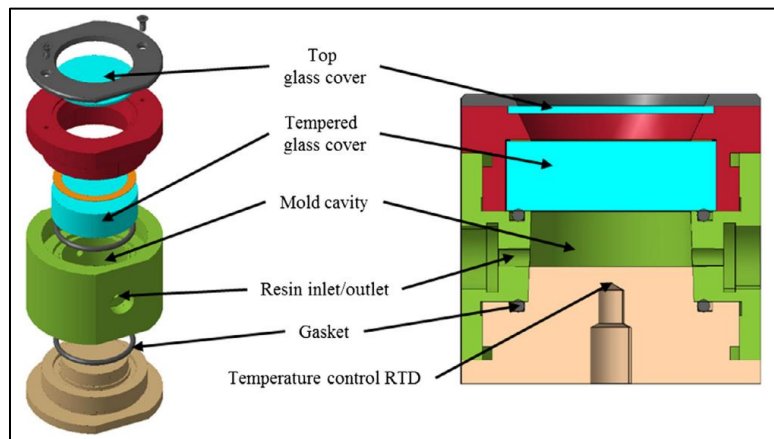
Figure 3.2: Laboratory scale RTM mold [102]

3.2 Materials and methods

The manufacturing steps could vary from one injection to the other and represent a general view of the manufacturing process. As described, the production of composite materials is labor intense and involves many manual operations. Choosing the pressure direction, open and closing valves, adding and removing pipes require of skilled personnel. Even so, it is prone to human error that can spoil hours of preparation. Figure 3.3 shows the difference between a bad and a successful process. An aged seal or malfunctioning quick pipe fitting could promote air pockets that lead to problems during the injection.

During the experiments we carried out, some tests were a total failure and the next injection was postponed one day due to the three hours of time required for cleaning and the application of the release agent coating. Also, some well-cured parts broke during the de-molding step.
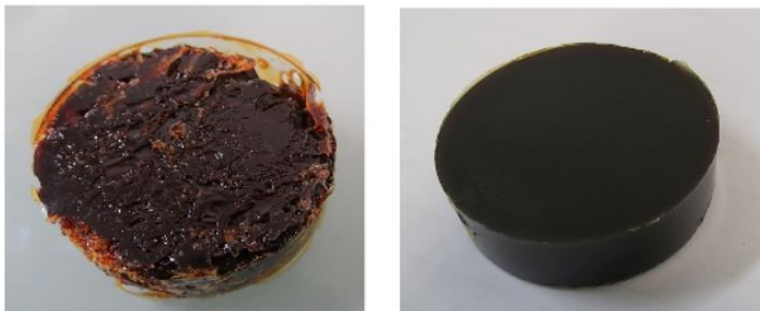
Figure 3.3: Left, Failure test. Right, good cured part

The injected polymer resin was an epoxy DGEBA (Diglycidyl Ether Bisphenol A) or D.E.R. 383 mixed with Methyl Tetrahydrophthalic Anhydride (MTHPA). A catalyst in the form of 1,2-Dimethylimidazol+2-Ethyl-4-Methylimidazol started the chemical reaction. Figure 3.4 shows the polymer viscosity from the data sheet. Also the fully cure T_g for the resin mixed with MTHPA state by the manufacturer is 148 °C [103].
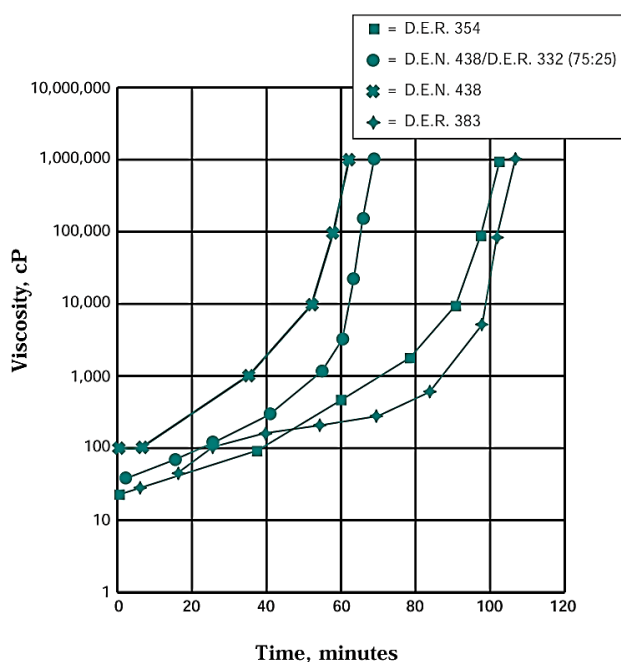
Figure 3.4: Resin viscosity at 85 °C and MTHPA curing agent [103]

From the literature review section 2.3.6, we found that the cure temperature should be lower than the fully cure T_g value to ensure proper gelation. For this reason, the process temperature was selected to be 140 °C. Also, to maintain the resin at low viscosity, the injection time must be between 20 - 40 minutes at 85 °C. For a real-world setting we limit the information of the material

to the manufacturer datasheet, one academic publication and the staff experience. Limit information and operator experience is the challenge faced by composite parts manufactures. In this respect we choose the work of Ivankovic *et al.*2003 [73]. They studied an Epoxy/Anhydride similar to the resin using during this research. Their results presented in the Figure 3.5 shows that with a heating rate of 5 °C/min, the cure degree remains almost zero for about 18 minutes, confirming the datasheet information.
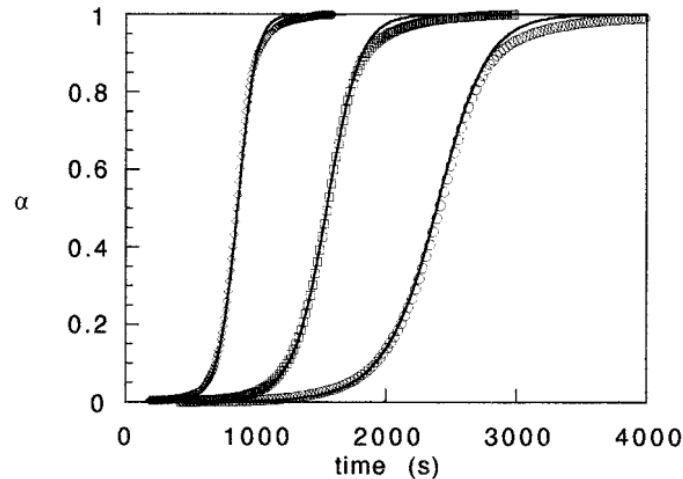
Figure 3.5: Resin kinetics. From right to left: 3, 5 and 10 °C/min [73]

The maximum heating rate measured in the device was approximately 6 °C/min. With the resin data and the device characteristics, a corrected cure cycle was performed: First, the mold was heated to 140 °C. At the same time, the injection pot was maintained at 70 °C. Then, the polymer mixture was put inside the container where it was heated as fast as possible to the temperature of the mold. When the temperature inside the resin reached 100 °C, around 5 to 7 minutes, vacuum de-gas it. Finally, the injection was made upon reaching 140 °C, considering a 15-minute restriction inside the heating ramp to maintain the cure degree negligible.

The collected data from the video camera and the temperature recorded from the data loggers were analyzed from two successful tests. The video data is helpful in the synchronization of the temperature measurements with the process steps. In fact, it also allows the identification of bubbles or air pockets presented in bad injections. Although the video information was only qualitative, we found this information complementary to the data from the temperature sensors. Figure 3.6 shows a special characteristic of the chosen epoxy. The resin change colour during the gelation which permits to identify the gelation time from the video recording.

Figure 3.6: Color change representative of the liquid to gel transformation

Figure 3.7 and Figure 3.8 shows two cure cycles with similar temperature profiles. Although the device was maintained at a uniform temperature, at the time of the injection, the resin creates a disturbance in the mold. At that time the control increases the power of the heaters to compensate, but because the chemical reaction releases heat, it cannot compensate for the temperature. As a result, the temperature exceeds the predetermined value. To correct it, manual adjustments by trial and error were made. This peak coincides with the gelation of the material. From that time, the molding continues until complete 80-90% degree of cure, or a total 30 minutes, according to the measurements of Ivankovic *et al.* [73]. Finally, it is safe to de-mold the piece missing less than 20% of cure since the remaining chemical reaction continues at room temperature in the solid state. By doing so, we save around 45 minutes, but in massive PMCM parts, this could represent hours. This is a procedure routinely used in the industry because does not affect the final properties of the material.
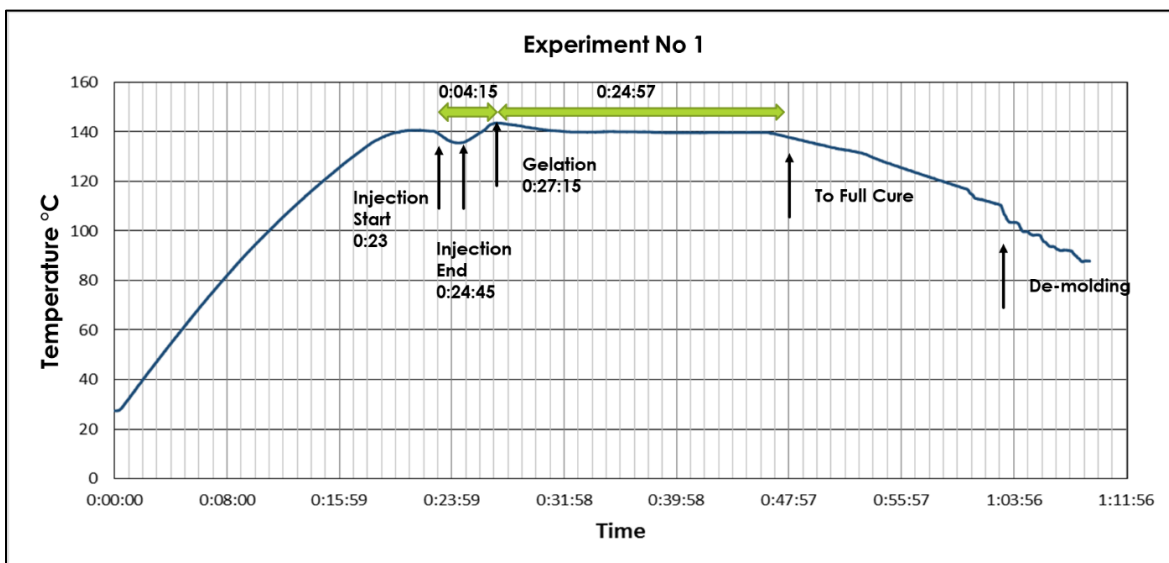
Figure 3.7: Mold temperature and video interpretation from experiment 1
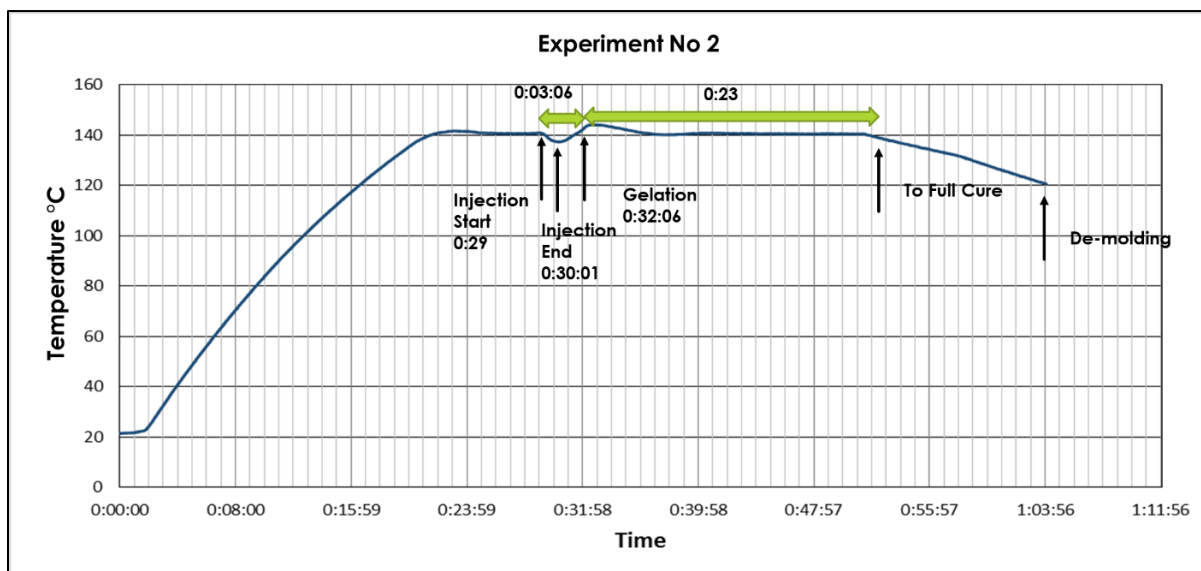
Figure 3.8: Mold temperature and video interpretation from experiment 2

From the video and the change of colour in the resin, a gelation time of 4:15 and 3:06 minutes was obtained, values very close to the 3:30 minutes obtained by Ivankovic *et al.* [73]. The difference of one minute between the two injections is because they were made a day apart. And although we follow the protocol of storing the resin at -15 °C, the chemical reaction continued in the time interval required to cool and thaw the material.

3.3 Results and discussion

The dedication and care in the configuration of the process require not only the knowledge of the device but also the details of the steps to follow. It is also necessary to understand the chemistry of the resin and the time allowed to process it. Increasing the temperature decreases the molding time, but it becomes difficult to maintain a uniform temperature across the device, this is because not all the heaters respond at the same speed. By decreasing the molding time, an impact on the decision-making and concentration on the operator was observed. Consider that he must follow the process program and at the same time he has to remove the gloves to adjust the temperature controllers and put them on again to handle the hot parts. This represents a latent danger. In this sense, we believe that the device requires at least two well-coordinated people to handle it. However, a computer-aided process will provide the basic tools to coordinate the machine, record the data and provide the operator with warnings or visual cues that contribute to the decision-making.

Continuing with the observations, we found that prior to the mixing, the resin has a consistency like the one of glycerine. As we continue stirring the mixture and the components are integrated, the viscosity decreases obtaining a consistency of corn syrup. If under-mixing is presented, the final part becomes fragile due to uncured spots where the resin was not catalyzed properly. In this context, the consistency of the liquid is a good indicator of the mixture status.

Regarding to the injection, the combination of compressed air and glass containers is very convenient since they allow to keep the injection pot clean and the device safe from the resin. Also, they are easily replaced or cleaned with a solvent. However, a minimum pressure is necessary to push the resin out of the injection pot. Due to the increase in temperature the resin is very watery which causes it to flow very quickly. A sudden increase in the pressure can cause the resin to flow from one end to the other, leaving the mold completely empty. In other words, the pressure range is very limited and difficult to control with the regulating valves and the operator could miss the opportunity to close the outlet port of the mold. To this purpose, the resin volume increases to allow the material to flow after filling the mold in a process called bleeding. The idea is to allow the resin to fully impregnate the fiber, remove air pockets and give time to the operator to close the pipes. As a result, the amount of resin to inject increase, and in the same way the waste.

In general, the temperature controllers reach the desired temperature, but we had to adjust the set point as many times as required to obtain a close value. For instance, if the required temperature was 140 °C, at the end of the cycle the set point was between 3 and 8 °C more than that value. Despite fine-tuning the issue persisted, it may be necessary to increase the heat capacity of the heaters or add proper isolation. As a matter of fact, these upgrades will improve the controller capabilities and increase the actual maximum temperature ramp of 6 °C/min. Although it is necessary to consider the amount of mass (mold + sample) to be heated, which can hinder to reach higher rates of heating.

Finally, removing the sample from the mold is extremely difficult, the release agent helps to this purpose but results not effective for the sides of the mold. The problem is that upon completion many parts of the device end up filled with polymerized resin. As result, tubes, quick connectors, ball valves must be replaced. The mold filling ports are not an exception and the resin from a pair of polymer pins that holds the molded part in place. Figure 3.9 shows the part with the pins that

must be broken with a rubber mallet to free the molded piece. Inevitably, the impacts could also break the piece and the filling holes needs to be re-drilled after each process.
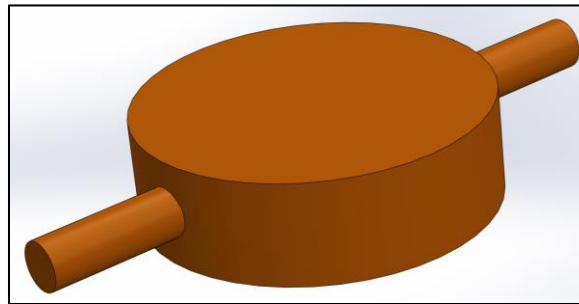
Figure 3.9: Sketch of a molded material with the solidified filling ports attached

Table 3.1 summarizes the manufacturing and design challenges obtained from the industrial experience we carried out. They were also dissociated from the RTM laboratory scale device limitations and grouped into typical manufacturing evaluation criteria.

Table 3.1: Mechatronic device design challenges

Challenge	Evaluation Criteria	Relevance to the project
Ensure resin mixture	Quality	It is under the user responsibility but adding a mixer will increase the success rate.
	Functionality	Variation on the viscosity and injection flow. Heating and injection force must compensate.
	Production	A batch of resin for a series of experiments could be made to maintain the mix uniform but requires storage at negative temperatures to decrease the chemical reaction rate. The reaction does not stop.
Resin stickiness and solidification outside the cavity mold	Maintenance	Plastic tubes and containers should be replaced. Valves, quick connectors can be cleaned but the solvents will damage the sealing. The injection reservoir must be empty.
	Functionality	Solid resin inside the tubes could block the injection.
	Production	The ports in the mold will solidify and should break at unmold without damaging the part.
	Environmental	Strong solvents required to clean the resin are being banned in some regions due to their toxicity.

Table 3.1 (continued): Mechatronic device design challenges

Challenge	Evaluation Criteria	Relevance to the project
Open and close device ports	Functionality	Ball valves are easy to handle and perform well blocking the flow, but they must be replaced too often. Clamping the tube is other solution but the tube could deform or damage. Also, air compressed clamps exist but they are bulky.
	Ergonomics	Synchronization and selection of the resin path is a key aspect of the process. It should not require of two people to work with the device.
	Safety	Handling hot surfaces always implies a burning hazard.
Maintain and uniform temperature across the device	Functionality	Thermal shock could suddenly solidify or degrade the resin. Tubes and valves represent the major challenge for reaching this objective. A good number of temperature sensors may be required. Also, high power heaters and good isolation of the parts contribute to the temperature uniformity.
	Ergonomics	Heaters, power and sensor cables could be on the way of the operator.
Mold release layer	Working principle	It is not possible to verify the proper application of the release agent. Also, an elastomer layer requires of calibration to correct the collected data. Either way, an operative protocol must be defined, which must ensure proper functioning of the equipment.
Add a glass window to the device	Functionality	Image processing gives feedback of the process and voids formation information, but high-processing computing power is required to process the information online.
	Working principle	The glass prevents the addition of heaters or other sensor types in the upper side of the mold. It also prevents obtaining a uniform unidirectional heat flow, which is generally achieved by heating the upper and lower part of the mold.
Reduce the human intervention	Ergonomics	A computer air-assisted increase the success rate and reduce the operator decision-making during the molding process. The device must be operated by one operator.
	Safety	The operator will be safe behind the automation, but all the risk will be translated to the device. In case of failure the device could finish with polymerized resin. In that case critical parts must be protected for this eventuality.

Table 3.1 (continued): Mechatronic device design challenges

Challenge	Evaluation Criteria	Relevance to the project
Easy to unmold the part	Assembly	Glass window, heaters, cooling, sensors, isolation and wires are all in the mold. At the same time the design must deal with the polymerized ports to easy unmolding the part.
Prevent resin leaks	Assembly	Seals, quick connectors, O-ring and mechanical seals are inspected as part of the setup. Even after visual inspection and proper assembly, it is difficult to detect failing seals unless all are brand new.
	Cost	Valves, quick connectors, seals could be cleaned and reuse. But knowing the number of tests until failure could not be possible. Instead is easier changing them. This increases the molding costs.
	Functionality	Proper sealing is required to obtain accurate and repetitive results.
Resin bleeding	Production	Allow the resin to flow after filling the mold increases the amount of resin used in one injection.
	Environmental	Increases the material waste.
Injection	Working principle	It is necessary to know the resin viscosity behavior and the fiber impregnation before attempt to inject. Properties tested in a separated test.

3.4 Conclusion

After careful examination of the manufacturing of PMCMs, we conclude that the idea of the catch pot provides a protection layer to the device that should be implemented. Also, having a glass window in the mold and image processing from the video recording will provide the device with vital information about the process. It will allow and help the operator to observe the mold filling or fiber impregnation, understand and measure the voids formation during cure [102] and detect gelation time. We acknowledge that all tests were made with resin only, but it is expected that the fibers will be confined to the mold cavity. Two potential problems could arise; first, the fiber content, wettability and compaction could increase the injection pressure to a value higher than the available. And second, if the mold is filled with short fiber content, it could be pulled out during the injection.

In respect to the device design we found that having a critical view of the manufacturing process allowed us to separate the limitations of the RTM scale device from the manufacturing challenges. Considering these potential problems during the design stage will improve the device functionality.

In a broader context, we were able to reach the first objective (OB1) of identifying the laboratory equipment limitations and manufacturing challenges. In particular, the conclusions presented during the literature review are now supported by the experimentation in the RTM laboratory scale device. We face the manufacturing challenges and problems by ourselves which give us the experience and information to complete this first objective. Moreover, we identify the challenges and organized them in terms of quality, functionality, maintenance, etc. All the information compiled in Table 2.1 and Table 3.1 will serve as a source to obtain the device design requirements.

CHAPTER 4   INTEGRATED MECHATRONICS DESIGN METHODOLOGY (IMDM)

This chapter relates to the second objective of this PhD project (OB2) that is to develop an integrated mechatronic design methodology. First, we explore the mechatronic design challenges and propose an integrated methodology to solve them. Second, we apply the methodology to the design of the mechatronic system for the characterization of PMCMs.

4.1 Introduction

Multiple disciplines converge in the development of mechatronic products. Each one makes the necessary contribution to obtain the final product. In this situation a proactive integrated approach produces better results [2]. A better planning in the initial stages of the project allows the team to focus on the device requirements [104]. Essentially, the team must avoid redesigning or perform expensive corrections at final design stages which could lead to an imminent failure. The intense collaboration required by different disciplines makes a holistic vision of the system necessary[1]. Obtaining a high degree of abstraction on the requirements and functions is an arduous task that requires an integrated methodology [12].

To overcome the challenges in the mechatronic design of the characterization device, this research proposes an integrated methodology composed of five complementary approaches. The main core follows the V-shaped mechatronic design methodology from Gaussemeier *et al.* [15] which divides the design into requirements, system design, domain-specific and system integration steps which must be performed in loops until the final product is obtained. Section 1.1 described this methodology in detail.

To complement the design methodology we adopted the results from Torry-Smith *et al.* [1] and Mohebbi *et al.* [12, 104]. They found that the main challenges involved in the design of mechatronic systems lies in the multi-criteria decisions that the multidisciplinary teams carry-out during the design and development of the product. Most important, the methodology must provide the tools to evaluate the candidate solutions against the device requirements and if required make adjustments on each design loop or iteration. Table 4.1 describes how the methodologies selected contribute to solving the design challenges. Inevitably, each one intends to solve one aspect while leaving behind others, but together the full spectrum is covered resulting in an integrated

mechatronic design methodology (IMDM) that solves the principal problems faced by multidisciplinary design teams. No methodology is perfect and must evolve with the project, since the project is in the initial phase, the proposed methodology focuses on the first two stages of the VDI V-shape design: requirements and system design. After that, the team could follow a traditional approach to embody the detailed design and the system integration steps. It future iterations is possible to support the design with an artificial multi-criteria decision learning models like the one proposed by Mohebbi *et al.* [12, 104] in 2018. This is because the requirements and system functional model can be simply transferred to the automated decision-making platform.

Figure 4.1 shows the proposed integral mechatronic design methodology. Due to the complexity of the mechatronics systems, the methodology requires of many loops as possible to self-optimize the product. In the same way, the added techniques need to have the capability to evolve with the project. Furthermore, they must be able to track the project evolution and the changes made through the timeline of the project.

As described in the Table 4.1 the VDI methodology is not strong by itself and only defines the steps that the team must follow. To define the device requirements we used the task clarification of Pathl *et al.* [105]. It allows to extract the requirements for the device and group them into demands and desires. As the requirements are clarified, they are organized in a form that allows the traceability of the changes made. The team must focus on the demands, while deciding how important the wishes are, and if worth the effort. Consequently, it is required to evaluate the previous list in a quantitative way. For this, the Quality function deployment (QFD) [106] allows to classify the requirements through a scale of importance. Then, the requirements go into a matrix of compatibility. It makes possible to find the interrelations between the components of the equipment. In addition, by assigning a weight to each characteristic, the QFD permits to calculate which components have greater importance and therefore has the greatest influence on the functioning of the device. These components must be developed with a higher order of priority than the others. The two methodologies establish a common ground for the multidisciplinary team. They define the requirements using a common language and a quantitative matrix that makes possible to the teams known how one requirement affects the others.

Table 4.1: Proposed design methodology and its contribution to the research. Adopted from [1]

Influence	Strong	Medium	None	Challenges							
Solutions				Lack of common understanding	Difficulty in assessing consequences	Lack of common language	Modeling/controlling multiple relations	Controlling multiple functional states	Different mental models	Knowledge transfer between domains	Complexity as generic problem
Process model containing activities for the development process, VDI Gausemeier *et al.* 2003 [15].										Medium	Medium
Controlling design activities through requirements managements. Pahl *et al.* 2007 [105].						Medium			Medium		
Relationship management - QFD Terninko 1997 [106].					Strong		Strong		Medium	Medium	Medium
Informal description consisting of a number of modeled/described aspects to specify systems. Buur 1990 [107].				Strong	Medium	Medium	Medium		Strong	Medium	Medium
Functional approaches and functional decomposition, heuristic methodology. Stone 2000 [7].				Strong		Medium	Strong	Strong	Medium		Medium

Next, the teams translate their mental models into functional models that are finally put together in a product architecture. During the system design, the functional modeling of Buur [107] describes the device behavior with the Function – Means approach. Here, the team uses simple words to define the system functions and they think on the means to perform it. Once all agrees and understands the functional model, the architecture of the system could be uncovered. The functional decomposition or heuristic methodology of Stone [7] takes the Function – Means model and groups it into a modular and more flexible representation.

With the information collected in these stages, the system should be fully described, and the team can begin with the specific design. As the project progress and loops are performed, the forms, the QFD matrix and the functional diagrams must be updated appropriately.
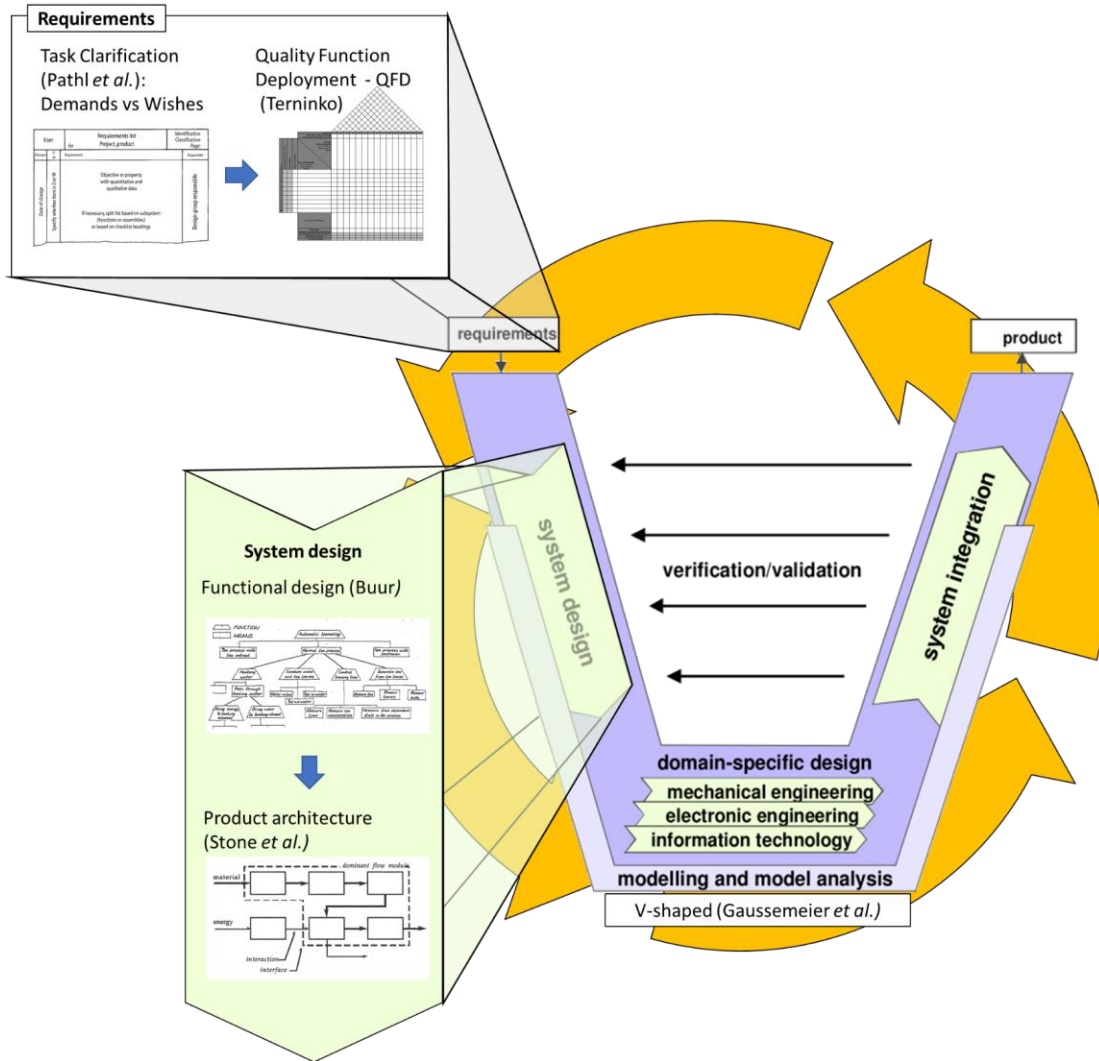
Figure 4.1: Proposed integrated mechatronic design methodology. Adopted from [7, 15, 105-107]

With the general overview of the proposed methodology we proceeded to explain and implement the requirements and system design steps.

4.2 Requirements definitions

4.2.1 Task clarification

Pahl et al. 2007 [105] organize the product requirements into demands and wishes. It is important for task clarification to filter the requirements list. The teams must focus on those elements that the system must meet no matter the circumstance (demands). On the other hand, wishes would add more value to the product but they could be implemented in a future version.

To reach a good level of abstraction, the requirements follow the next three-step process [105]:

- Statement. Here the team define a requirement in a simple phrase that sums the product needs. It must describe a problem, an expectation or a constraint in a general way.

- Development. Now the team focuses on listing as a checklist the steps necessary to comply with the statement.

- Refinement. Finally, the focus is described in detail the technical aspects of each item of the list from the development. If possible, precise quantities must be introduced. Also, they could contain qualitative statements.

This is probably the most difficult step in the whole design stage, not only because it requires a lot of experience but also the consent of all parties. At the same time, this list of requirements is used to measure the capabilities of the product. When the team reaches a consensus on the requirements of the product and the level of abstraction required, all information is placed in a form that can be updated in future integrations. Figure 4.2 shows the requirement list form that contains all the definitions that allow the tracking of the product evolution.

Figure 4.2: Requirement list form [103]

By implementing this strategy, the teams express their different mental models about the project using a common language. By consolidating the requirements, the team gains knowledge about the operation of the device. The Figure 4.3 shows a list of items that can be used to obtain the system requirements.

Main headings	Examples
Geometry	Size, height, breadth, length, diameter, space requirement, number, arrangement, connection, extension
Kinematics	Type of motion, direction of motion, velocity, acceleration
Forces	Direction of force, magnitude of force, frequency, weight, load, deformation, stiffness, elasticity, inertia forces, resonance
Energy	Output, efficiency, loss, friction, ventilation, state, pressure, temperature, heating, cooling, supply, storage, capacity, conversion.
Material	Flow and transport of materials. Physical and chemical properties of the initial and final product, auxiliary materials, prescribed materials (food regulations etc)
Signals	Inputs and outputs, form, display, control equipment.
Safety	Direct safety systems, operational and environmental safety.
Ergonomics	Man-machine relationship, type of operation, operating height, clarity of layout, sitting comfort, lighting, shape compatibility.
Production	Factory limitations, maximum possible dimensions, preferred production methods, means of production, achievable quality and tolerances, wastage.
Quality control	Possibilities of testing and measuring, application of special regulations and standards.
Assembly	Special regulations, installation, siting, foundations.
Transport	Limitations due to lifting gear, clearance, means of transport (height and weight), nature and conditions of despatch.
Operation	Quietness, wear, special uses, marketing area, destination (for example, sulphurous atmosphere, tropical conditions).
Maintenance	Servicing intervals (if any), inspection, exchange and repair, painting, cleaning.
Recycling	Reuse, reprocessing, waste disposal, storage
Costs	Maximum permissible manufacturing costs, cost of tooling, investment and depreciation.
Schedules	End date of development, project planning and control, delivery date

Figure 4.3: Requirements list guidelines [103]

4.2.2 Quality function deployment (QFD)

There exists a vast literature about QFD. Chan *et al.* [108] reviewed it since its inception in Japan in the late 60s. It is important to note that in its origins, QFD measured the quality of products, but due to its intrinsic capabilities, the industry has used them to analyze the customer needs. In the 90s, the technique was implemented in the design of products. In this area of knowledge, QFD contributes to the "quality design", where a strategic planning and a proactive approach at the beginning of the product development had produced excellent results. In engineering, it allows to establish the relationships between product specifications (how) and customer needs (why). It also allows us to define priorities and make decisions by imposing a measure weight. Finally, it is possible to understand how a change in one design criterion affects others and to what extent. Now days, it is possible to find templates, software and video tutorials to make the so-called "house of quality".

Figure 4.4 shows a general description of the QFD and the steps to follow:

A. The requirements collected are translated as a list of needs. Also, the team weight the items in an importance scale and calculates the relative importance of each element.

B. The planning matrix allows to compare the product in development to the competitors. But, for this initial stage this step is omitted.

C. During the task clarification the team identifies the technical aspects, these relate how the demands or wishes could be achieved. These items go as columns in the technical measurements arrangement.

D. The most important step in the QFD is the matrix of relationships that correlate the needs (rows) with the technical aspects (columns). The matrix defines the relationship on a qualitative scale that ranges from none, weak, moderate or strong. At this stage could be a lot of debate because mental models emerge, for example, how does the cost of the car relate to the weight of the car? It can be argued that the relationship is strong because that means more components or materials, so the resulting product should be expensive. Then, another team argues that if the car is made of advanced materials such as lightweight composites, the cost skyrockets, so the weight is not directly related, and it is necessary to

specify new relationships. This example shows how subjective and important is the consensus among the teams.

E. The "house of quality" roof represent the technical correlation matrix. It relates how each technical aspect affects others. It really depends on whether the team objective is to minimize or maximize the item in that column. Then, the team debates what happens with a neighbor technical column if this column maximizes or minimizes. In general, the description uses a correlation scale of strong negative, negative, positive and strong positive.

F. A difficulty scale from easy to extremely difficult weights the technical aspects. The relationship between difficulty over importance from the step (A) tells the teams where to focus in the project, expending more energy on those aspects that have bigger weight will conduct the design in the right direction.
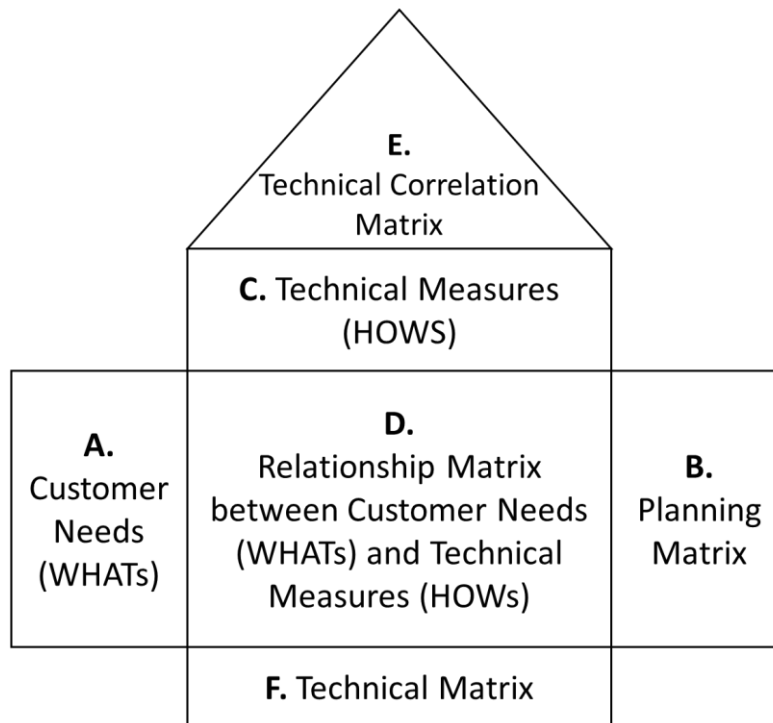
Figure 4.4: QFD overview [109]

No matter the scale, the QFD form will contain the symbols and grades used to interpret it.

4.3 Requirement for the mechatronic characterization system

4.3.1 Demands and wishes

In this section we put into practice the techniques presented to define the device requirements. We begin by abstracting the information for the Chapter 2 Literature review, Chapter 3 Understanding the manufacturing process, group meetings and our experience.

The Table 2.1 describes the equipment limitations and challenges to characterize the composite material properties. In this context and with the meetings to organize the laboratory scale experiments, we refined the requirements list for an ideal test. Table 4.2 defines the design requirements for the test. All begins with the test sample size. We saw that is the most important aspect for the design. In particular, the volume defines the amount of material. The sample must be big to represent the composite structure, but small so the required dynamic force for the experiment remains in a manageable range. Once the team agrees in how big the sample must be, we translate the test requirements in the form of a PVT machine. We choose this machine type due to their promising results discussed in the literature review and instead of just copying a design and improving it. We decided to make a hybrid between the RTM laboratory scale device (Figure 3.1) and a PVT (Figure 1.5).

Table 4.2: Requirement list linked to the test
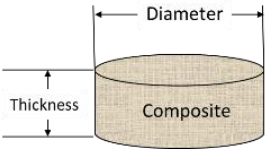
ERFT Composites		Requirement list for the mechatronic system – Test requirements	6th Issue on 2017/12/11
Changes	**D W**	**Requirements**	**Responsible**
		Test Sample:	ERFT staff
		Geometry: dimensions of the test sample.	
2017/12/11	D	Thickness: up to 20mm.	
2017/12/11	D	Diameter: 38.1mm (1.5 inch).	
	D	Volume: up to 23 μm^3 (23 ml).	
		Material:	
	D	Thermosets: Epoxy, Polyamides, Polyester, etc.	AGRU
	W	Thermoplastics, polymer blends.	
	D	Pre-pegs, long fibers and 3-D textiles and fiber compaction.	
	W	Short fibers, Nano-composites.	
	W	The resin impregnates uniformly the fibers at lowest viscosity possible.	

Table 4.2 (continued): Requirement list linked to the test

		Test Kinematics:	AGRU
	D	Linear with a vertical motion.	
	D	Precise thickness selection.	
	W	Thickness resolution: 1 µm.	
	D	Automatically close the mold, and fast.	
	D	Applied load with a piston.	
2017/12/11	D	Fixed and oscillating load.	
	D	Always maintain contact with the sample.	
	D	Stroke 100 mm.	
	D	Compression typical displacement ±10 µm.	
2017/12/11	W	Maximum test displacement ±50 µm.	
	D	Displacement resolution ≤ 1 µm.	
	D	Sinusoidal load frequency up to 10 Hz.	
	W	Variable frequency from 1 to 100 Hz.	
	W	Automatic de-mold.	
	D	Compact the fiber prior to the injection.	
		Force:	
	D	Variable force up to 2580 N.	ERFT staff
		Energy:	
	D	Electrical 115 VAC 50 – 60 Hz.	AGRU
	W	The composite cures uniformly, no thermal gradient.	
2017/12/11	D	Temperature test room 25 to 350 °C.	ERFT Staff
2017/12/11	D	Isothermal and heating ramps.	
	W	Heat capacity ≥5 °C/min.	
	W	Cooling up to -5 °C/min.	
		Autoclave pressure range 50 – 200 psig [41].	
		Thermoplastic composites molding pressures 100- 500 psig [41].	
2017/12/11	D	A middle ground pressure of up to 362.5 psig (25 bar).	ERFT Staff
		Signal:	
		Input:	
	D	Temperature profile	
	D	Initial sample thickness	ERFT Staff
	D	Piston displacement and frequency	
		Output:	
	D	Heat flux released.	
	D	Piston displacement	
	D	Resulting force.	
	D	Video camera.	ERFT Staff
	W	Test time approximate 60 min.	

Table 4.2 (continued): Requirement list linked to the test

		Properties to measure:	AGRU
	D	Chemical Shrinkage and CTE.	
	D	Degree of cure.	
	D	Gelation point.	
	D	Modulus development.	
	D	Complex viscosity.	
	D	Void formation.	
	W	Void size and form.	
	W	Void contents, percent.	
	W	Tg, TTT and vitrification.	
	W	Fiber impregnation	
		Controllers:	
	D	Temperature, displacement and force.	
		Datalogger:	
	D	All the signals must be recorded and stored.	
	W	External storage.	
		Display:	
	W	On-line properties graphs.	
	D	On-line signals graphs.	
	D	Signals and synchronized video.	
	W	Warnings and status.	
		Production:	
	D	At least two tests per day.	ERFT Staff
		Replaces 5th Issue of 2017/07/24	Signature

Table 4.3 shows the design requirements relate to the injection system. One crucial aspect of the new proposed device is the capability to analyze the void formation. As a consequence, an automatic injection system comes into play. In that case, the PVT gain the capability to emulate the RTM manufacturing conditions but at the same time we impose the challenges found in Table 3.1. In particular, the requirement of knowing the fiber permeability and the resin viscosity before injecting. This knowledge allows the system to avoid the gelation inside the injection container and to calculate the injection pressure. Those requirements could make impossible to reach a functional device, for that reason are included in the form of wishes.

Finally, Table 4.4 relate the company requirements. They are not directly related to the characterization, instead they are linked to the device structure and functions. Essentially, they

reflect the experience gathered for the company and its engineers when working with other characterization devices and in other design projects.

Table 4.3: Requirement list linked to the injection system
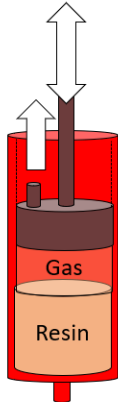
ERFT Composites		Requirement list for the mechatronic system – Injection system	6th Issue on 2017/12/11
Changes	**D W**	**Requirements**	**Responsible**
2017/12/11	D W D D D W W	**Material:** Volume: the amount of resin must fill the mold to the selected sample thickness and allow to perform the bleeding. Possibility to inject oils for other tests. Fiber capillarity and permeability. Fiber percent and compaction. No resin inside the injector at the end of the process. Apply vacuum to remove gas (-14 psig). Flow rate up to 16.2 x 10^{-6} m^3/s [110].	AGRU
2017/12/11	D D W	**Kinematics:** Piston injection to avoid compress air. Injection at constant pressure or constant flow rate Mixing the resin with a rotative motion or stirring system	AGRU
	W	**Force:** Dependent on the relationship between the piston radius and the output radius. Resin is considered to be Newtonian fluid.	
	D D D D W	**Energy:** Electrical 120 VAC 50 – 60 Hz with Max 12 Amp. Temperature uniform with the mold. Isothermal and heating ramps up to 5 °C/min or more. Typical RTM pressure 0.03 – 0.07 MPa [110]. Note: Mold clamping pressure Injection pressure to maintain a linear flow rate and follow Darcy's law. This also relates to the decrease on the permeability due to the compaction pressure [110].	ERFT Staff
2017/12/11			AGRU

Table 4.3 (continued): Requirement list linked to the injection system

		Signal:	
		Input:	
	D	Temperature profile	
	D	Selected sample thickness	ERFT Staff
	D	Flow rate or injection pressure	
	W	Gelation time or time limit for injection	
		Output:	
	W	Degree of cure.	
	W	Viscosity	
		Controllers:	
	D	Temperature, injection pressure, flow rate.	
		Datalogger:	AGRU
	D	All the signals must be recorded and stored.	
	D	External storage.	
		Display:	
	W	On-line viscosity and resin temperature.	
	W	On-line signals graphs.	
	W	Injection evolution.	
	W	Warnings for the onset gelation.	
		Operation and maintenance:	ERFT Staff
	D	Easy to load the resin.	
	D	Reusable with minimal cleaning	
		Safety:	AGRU
	W	Cover hot surfaces and moving parts.	
	D	Compliant with international IP ratings.	
	D	Piston free of friction and prevent it from being stuck inside.	
		Ergonomics:	
	D	Easy to access the resin chamber	ERFT Staff
	W	Quick connectors.	
	D	Metric tools.	
		Assembly:	
	D	Logical assembly and easy to access the barrel and piston for cleaning.	ERFT Staff
	D	Common seals, tight but easy to remove.	
	D	Compact with syringe body.	
	D	Solid structure.	
	W	Rotative barrel.	
	W	Removal and reusable resin cartridge.	
		Replaces 5th issue of 2017/07/24	Signature

Table 4.4: Requirements linked to the device characteristics
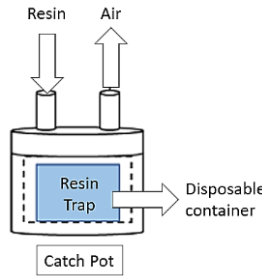
ERFT Composites		Requirement list for the mechatronic system – General Assembly	6th Issue on 2017/12/11
Changes	**D W**	**Requirements**	**Responsible**
	D W D D D D	**Machine Geometry:** Table desk size: Width: 120 cm x Depth: 76 cm Maximum Height 2 m. Tubes and wires in fixed position. **Mold Geometry:** Cylindrical shape. Glass window in the upper side. Good clearance to the video camera.	ERFT Staff
	D D	**Kinematics:** Heavy duty adjustable feet leveling. Vibration free.	
	D W W W D D D	**Energy:** Only electricity allowed. American / European connector. Vacuum pump. Heating elements. Cooling. Piston force load. Reduce the energy consumption with good isolation. Tubes, injection container, mold uniformly heated and isolated.	ERFT staff
	D D D W	**Material:** The resin flows from the injector to the mold. Include a resin trap to protect the device. Note: The resin will solidify in the pipes. De-molding agent. Avoid embedded sensors inside the molded material.	

Table 4.4 (continued): Requirements linked to the device characteristics

		Signals:	ERFT staff
	D	Proprietary data acquisition system to convert signals produced by outsourcing company in Montreal.	
	D	Proprietary software framework made by ERFT programmers.	
	D	Proprietary human machine interface made by ERFT programmers.	
	D	Search for best database platform for store the test results.	
	W	Remote monitoring the machine or share data using the internet of things.	
	D	Proprietary controllers to gain full control of the signal and actuators.	
	D	Noise filters and state of the art signal conditioners.	
	W	Reports and easy to export data to external storage devices	
	D	Fully automation and synchronization of the test.	
	D	Auto tune and well-defined calibration protocols.	
	D	User-friendly software interface.	
	D	Shielded wires and connectors.	
		Safety:	AGRU
	D	The software interface must solve errors and warnings.	
	D	Search for laboratory standards and guidelines to follow.	
	D	User isolated from the heat and moving parts.	
	D	Reduce the human intervention during ongoing tests. The machine software interface provides warnings and alarms can ask for human feedback.	
		Ergonomics:	AGRU
	D	A single operator is required to perform the test.	
	D	User-friendly, manuals available in digital format.	
	D	Well defined protocols, steps and limitations.	
	D	Parts, screws and quick connectors easy to reach.	
	D	Resin, fiber, mold, sensors, etc. Accessible and easy to load and reach.	
	D	Ventilation ducts away from users.	
		Production:	AGRU
	D	At least two tests per day.	
	D	Standard metric parts in the assembly.	
	D	Prevent leaks and provide leak protection to critical parts.	
	D	Include connectors with the required IP rating.	
		Quality control:	AGRU
	D	Explain calibration protocols.	
	D	Search for standard calibrations required in the used sensors.	
	W	Sanity check and test cycle of the machine actuators, heating/cooling, sensors and start up or before a test.	

Table 4.4 (continued): Requirements linked to the device characteristics

		Assembly:	AGRU
	D	Quick connectors in the resin lines, sensors and cables.	
	D	Easy to remove the molded material.	
	D	De-molding pins that break the solidified injection ports.	
	W	Intuitive assembly add pin guides to help alignment and proper fit.	
		Operation	AGRU
	D	Quiet operation.	
	D	Smooth and fast mold closing.	
	D	Leak proof and safeguard for hot resin.	
	D	Automatic resin direction, open and close of the tubes.	
		Maintenance	AGRU
	D	Identify the parts that could be clean and what are consumables?	
	D	Sensors, wires, isolation are properly covered and have well-identified place to be held.	
	D	Keep the machine clean before each test to prevent contamination. Establish cleaning protocol and hazard warning for the cleaning solvents.	
	D	Define cleaning and maintenance protocol (instructions) and recommendations.	
	D	Provide proper guarding from dangerous parts.	
	D	Detail the safety accessories required for maintenance.	
		Recycling	
	D	Define waste disposal of cured tubes, unused or failed molding, valves, seals, etc.	
	D	Reduce the test consumables, like tubes, valves, seals.	
		Cost	ERFT Staff
	D	Production cost 30 000 USD	
	D	Non-commercial software or external licensing.	
		Replaces 5th issue of 2017/07/24	Signature

4.3.2 Finding the design relationships through the QFD

Most of the design teams start the design based on the requirements sheet. This is known as a reactive design. This type of design meets the requirements as a checklist. The problem lies in the fact that the impact of the decisions made by the teams are not discovered until a late state of the design. Also, it is not possible to know how one requirement influence others. This makes the reactive design inefficient and expensive. Consider that during the integration these relationships emerge in the form of changes in something already designed.

The QFD allows to find the relationship between the design requirements in an early stage of the project. With this proactive approach a higher level of abstraction is required. Figure 4.5 shows the QFD for the mechatronic device. We use the Excel template from QFD Online[111] .

First the requirements are organized into "WHATs". "WHATs" groups several requirements from the list into one category expressed in one phrase. For example, it is required a 1µm of displacement resolution. Also, we intend to design a characterization device, for this reason all the tests need of the best type of sensors. In turn, what we required is "High measuring accuracy and precision". The principal idea is to abstract quantities and to group the requirements into a broad category that represent "What" is really required.

We abstracted the requirements and group them into test, technology and Operation subcategories. We found that these subcategories make easy the abstraction. Second, we discussed the importance of each item and give them a value between 0.0 and 5.0. In this respect, "High measuring accuracy and precision", "Get multiple properties in one experiment" and "State of the Art control" score the highest importance. In the same way, "Use only proprietary software" has a high mark.

"HOWs" are related to the engineering, parameters that we can control, measure or design. In this context, the team decide the direction of improvement. From the QFD in the Figure 4.5, it is demanded to maximize the sample size, minimize the actuator force, hit the demanded temperature, etc.

At this point the QFD can be filled with the correlation scale and the relationship weight scale. The designer or teams discuss how one parameter affects the other and relates them with the strong, positive, negative, strong negative correlation. For example, if we increase the sample size, the type of resins and fibers will be more representative, in the case contrary, if we decrease the sample size, we may not be able to use complex fiber mats. Next, if we increase the size and maintain the injection flow rate and injection pressure constant the injection is affected, we may be able to inject but not in the same way in the case of a smaller sample. So, negative but not strong negative because we can continue injecting to a certain degree. In the case of the force, the relationship is straight forward, with a bigger sample, bigger test force. But the design criterion is to minimize the amount of applied force. For this reason, the relationship is strong negative. We must evaluate the relationship backwards. Upon reducing the force, what should we do with the sample size? Of course, reduce the size to meet the test requirements, this has and strong negative impact in the

goal to maximize the sample size. The roof continues in the same way as described. It is expected a lot of debate and good agreement to fill this step.

Finally, we apply the relationship weight, this step unveils what are the most important design parameters that the teams should accomplish at the beginning. To do so, we apply the relationship scale in the matrix to relate each row with their respective column. After that, each relationship weight multiplies the respective relative row weight. The total sums of columns/rows go to the weight/importance row and a relative weight of the design parameters is calculated.

All things considered, the QFD tell us that the test force, the computing power and the linear displacement have the higher score. Indeed, the dynamic mechanical part of the test have been elusive to the characterization of composite materials. Moreover, the amount of control and signal to process suggests high computing power. In the next category, we obtained the design and engineering time competing with the machine production cost. Looking the QFD roof, we see an un-denied reality. In order to reduce the engineering load and reach the market fast, it is required to make a big investment to the same extent. In the case contrary, if it is required to reduce the investment we must give the engineers more development time.

It is important to maximize the Linear displacement resolution; hence, we focus in on the negative aspects of the roof. In this case, the sensor resolution and the acquisition electronics must meet the expectations, but this also means more computing power, engineering time and cost.

Continuing with the design task map, to reduce the test mechanical force, we may have to reduce the sample size, this could be our last resort after several iterations. In a broader perspective this also relates the fiber compaction and injection pressure in the case of the injection system. In the case contrary if the maximum force is reduced we see that the impact to the other parameters in positive so we must ask, could we be able to meet the required force, or should we reduce it? As we can see in the roof, this is not an easy decision because by doing so, the electronics, computer, development time and cost are greatly reduced. But in turn we could not meet the main objective to integrate multiple characterization laboratory equipment into a single device.

Finally, we have the computing power which relates to the device controllers and degree of automation. Particularly speaking we can say that the requirement to develop a custom software framework is perhaps the most proper way to gain full control over the device. Unfortunately, it is the aspect that requires the most engineering time for development but is at the same time the most

unattended-for task in design. For example, you can have the best software or library but if it is hard to understand or bad documented future programmers just prefer to do all the program again. Another aspect is the programing language and their standard libraries. It is not the same to call a MATLAB function to program it from scratch. At the last aspect is the engineer feeling, if we do not feel safe trusting our product to others 100 000 lines of code, we may be better producing all the code by ourselves.

Legend

Symbol	Meaning	Value
⊙	Strong Relationship	9
O	Moderate Relationship	3
▲	Weak Relationship	1
++	Strong Positive Correlation	
+	Positive Correlation	
—	Negative Correlation	
▼ (filled)	Strong Negative Correlation	
▼	Objective Is To Minimize	
▲	Objective Is To Maximize	
x	Objective Is To Hit Target	

Column #	1	2	3	4	5	6	7	8	9	10	11	12	13	14	15
Direction of Improvement:	▲	x	▲	x	▼	▲	▼	x	x	x	▼	▼	▼	▼	▼
Functional Requirements or "Hows"	Sample size	Types of Thermoset polymers	Fiber compaction and percent	Injection flow / Pressure	Resin viscosity	Linear displacement resolution	Linear force	Linear speed	Maximun temperature	Heating rate	High resolution and fast adquisition electronics	High resolution Video Camera	Computer Power and storage	Design and engineering time	Low machine production cost

Customer Requirements or "Whats"

Row #	Max Relationship Value in Row	Relative Weight	Weight / Importance 0.0 to 5.0	Requirement	1	2	3	4	5	6	7	8	9	10	11	12	13	14	15
1	9	10.8	4.0	Test wide range of composites	O	⊙	⊙	O	⊙	▲	⊙		⊙	▲		▲			
2	9	13.5	5.0	High measuring accuracy and precision	⊙		⊙	▲		⊙	⊙	O	O	▲	O	▲	⊙	⊙	⊙
3	9	9.5	3.5	Wide range of manufacturing parameters combinations	O	O	O	O	O	⊙	O	O	O	O	▲	▲	▲	▲	▲
4	9	13.5	5.0	Get multiple properties in one experiment	⊙	⊙	⊙	▲	O	⊙	⊙	O	O	O	⊙	O	⊙	O	▲
5	9	12.2	4.5	Use only proprietary software.				▲		▲	O	O	▲	▲	O	⊙	⊙	⊙	⊙
6	9	13.5	5.0	State of the art control				▲		⊙	⊙	⊙	O	O	⊙	▲	⊙	⊙	⊙
7	9	8.1	3.0	Automatic test without human intervention	▲	O	O	O	⊙	O	▲	O	O	O	▲	▲	⊙	⊙	O
8	9	8.1	3.0	Safety Hazards	▲	▲	▲	O	O	⊙	O	▲	⊙	O					▲
9	9	5.4	2.0	Easy to clean, maintain and setup	▲	⊙		O	⊙				▲						⊙
10	9	5.4	2.0	Minimize material waste	⊙	⊙	▲	⊙	⊙				O	▲					

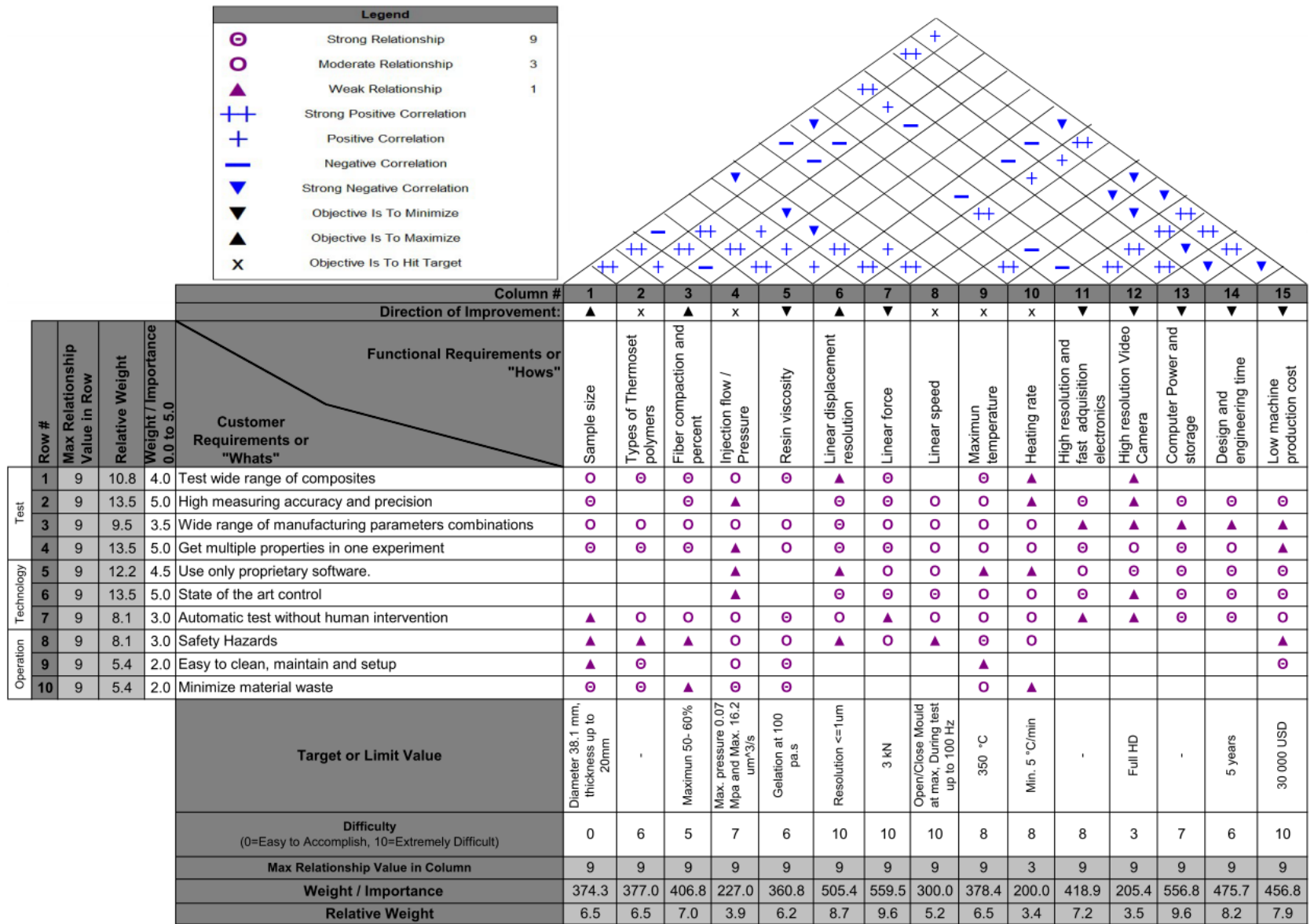|	1	2	3	4	5	6	7	8	9	10	11	12	13	14	15
Target or Limit Value	Diameter 38.1 mm, thickness up to 20mm	-	Maximun 50-60%	Max. pressure 0.07 Mpa and Max. 16.2 um^3/s	Gelation at 100 pa.s	Resolution <=1um	3 kN	Open/Close Mould at max, During test up to 100 Hz	350 °C	Min. 5 °C/min	-	Full HD	-	5 years	30 000 USD
Difficulty (0=Easy to Accomplish, 10=Extremely Difficult)	0	6	5	7	6	10	10	10	8	8	8	3	7	6	10
Max Relationship Value in Column	9	9	9	9	9	9	9	9	9	3	9	9	9	9	9
Weight / Importance	374.3	377.0	406.8	227.0	360.8	505.4	559.5	300.0	378.4	200.0	418.9	205.4	556.8	475.7	456.8
Relative Weight	6.5	6.5	7.0	3.9	6.2	8.7	9.6	5.2	6.5	3.4	7.2	3.5	9.6	8.2	7.9

Figure 4.5: Mechatronic characterization device QFD

4.4 System design

4.4.1 Functional design

After the product requirements, it is the time to define the device functions. Functional modeling is an extensive field and the amount of literature is high. Particularly, Unified Modeling Language (UML) and Systems Modeling Language (SysML) [112, 113] attempts to establish a common platform to model and optimize the design process. Their advantage is that provide a software platform to work with. Sadly, groups refuse to implement them because of the extra work required to get use to all the conventions and components defined in such as languages. Above all, the solution must be able to represent a global vision of the system. Also, the resulting model must be easy to read by any member of the team. For this methodology, the function/means tree from Buur [107] was implemented.

Figure 4.6 shows an example of a function/means tree model. It contains a hierarchical structure from top to down. The vertical model contains two main blocks. A trapezoidal shape, representing the system functions and a rectangular shape that contains the means to realize the function.
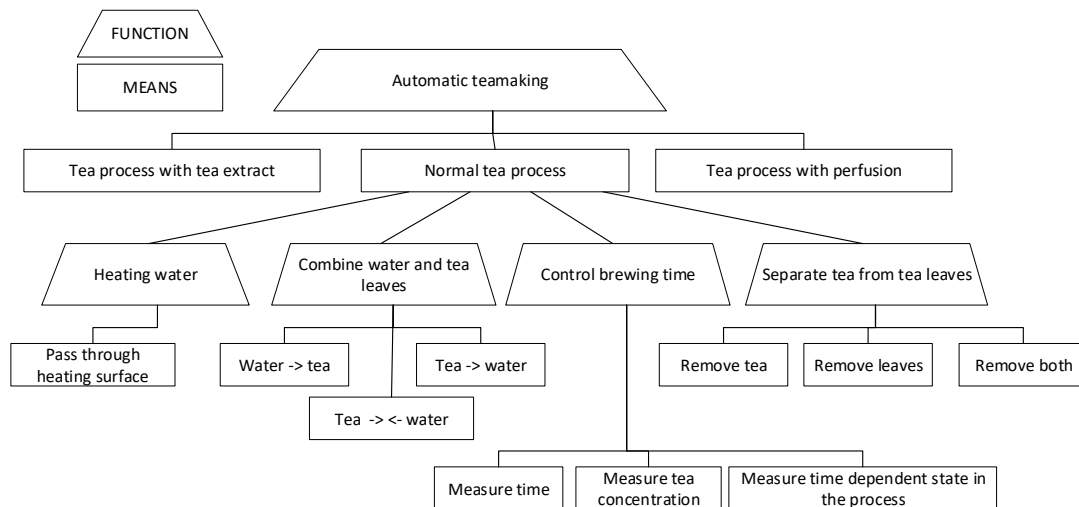

Figure 4.6: Function/means tree model of an automatic teamaker [107]

The model represents the tasks undertaken by the product using levels. So, to read it, we begin from top to bottom. "Means" have congruent lines, they represent a set of optional alternatives (like a logical OR). On the other hand, sub-functions are mandatory and required fully completion (like a logical AND).

Buur 1990 [107] developed the function modeling using the Law of Vertical Causality. The principle states that one function requires a series of means to be achieved. In turn, a means requires a set of sub-functions at a lower level. Following with this trend, the functional model grows in an organic way with the system integrations.

4.4.2 Product architecture

Finding the product architecture may require many prototypes and user feedback. However, as the functional model evolves, the teams begin to observe similarities in the function blocks. In this respect a modular design could reduce the production cost and the flexibility of the system. To this end, in this research and to complement the functional model the heuristic method from Stone [7] allows us to identify the product modules and architecture.

Figure 4.7 shows the first task in the product architecture. Derived from the functional model, the team translate it to an energy, material and signal flow model beginning from the black box identifying the input and output flows.
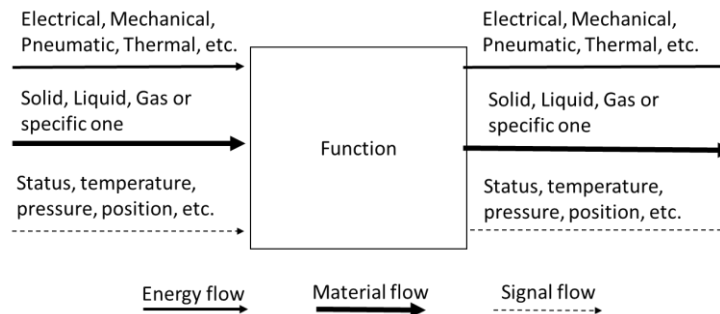
Figure 4.7: Black box model. Adopted from [7]

The process continues as the teams divides the function into more detailed sub-functions. Once the model reaches a good level of detail, it is possible to begin with the architecture analysis. After applying the methodology and the modules emerge, the team could continue adding sub-functions to optimize the design with every integration loop.

Figure 4.8 describes the first cue to find a module. A dominant flow goes through a set of sub-function unchanged and does not divide into branches. A dashed shape surrounds the identified group as a dominant flow module. Any flow that crosses the module interface requires an interaction that the team should be aware of during the implementation stage.

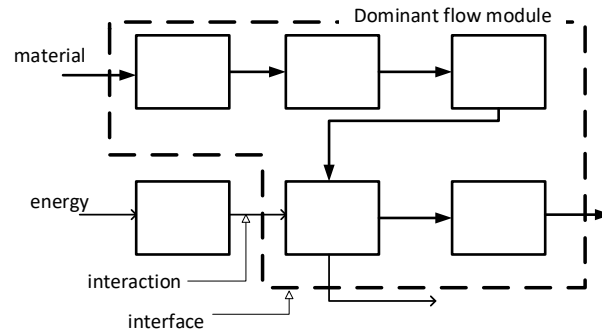Figure 4.8: Dominant flow module [7]

Figure 4.9 shows how to identity a branching flow set of modules. In this case the principal flow divides in a set of parallel chain functions. The parallel branches define a sub-module or branch module of the principal one. Essentially, they represent buses, attachments or interchangeable elements of the machine. While the principal branch could be a physical connection common to the modules.
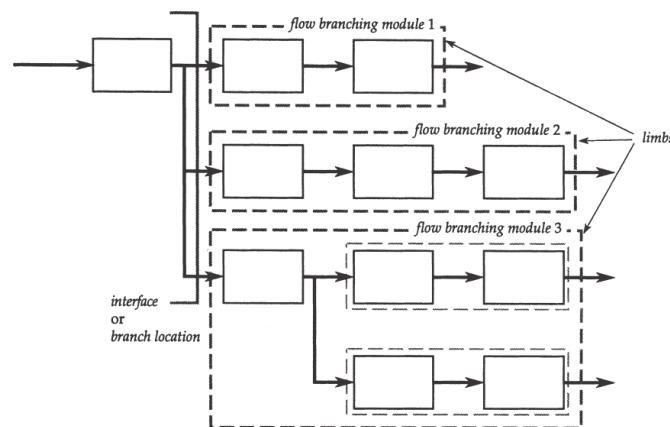
Figure 4.9: Branching flow parallel modules [7]

The final identification technique relates the material or energy flows. Figure 4.10 shows the conversion/transmission module identification. Conversion blocks differ from regular verb functions because transforms the incoming flow to another. It could be possible to find a pair of blocks that converts and transmit the new flow. Finally, if three blocks convert, perform a function and transmit the flow, they form a conversion – transmission chain. In general, any conversion – transition arrangement of blocks from a module.
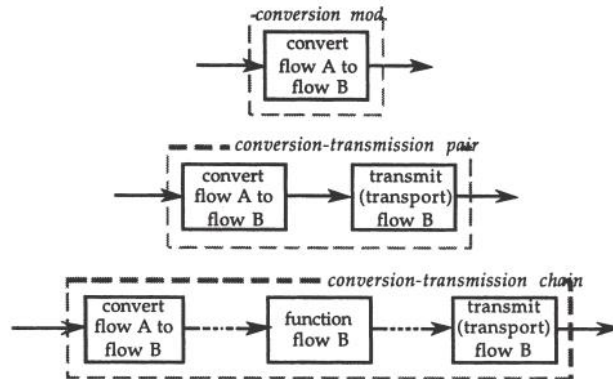
Figure 4.10: Conversion – transmission modules [7]

4.5 Functional model for the mechatronic characterization system

The functional model supports the requirements stage from the previous section. The main objective is to provide the means to unify the mental models, understand the functions and logical states in the automation, in a broader context increase the common understanding of the mechatronic device.

This stage aims to convert the system requirements into a functional model and a product architecture.

4.5.1 Functional model

The functional model tree is described by levels. To maintain the tree easy to read, we divided it into four figures. Figure 4.11 shows the principal functional model. Here, we present the main objective of the characterization device, characterize a composite. To reach that objective, it is required to obtain the reinforcement, resin and in the end the composite properties.
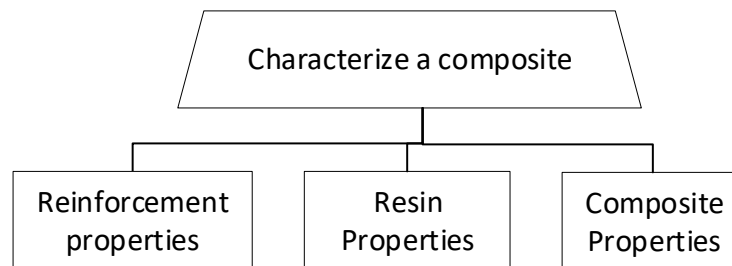
Figure 4.11: Principal functional model three

Next, we develop each of the means. For the reinforcement properties we investigate the literature review in the section 2.3.1 that describe the fiber impregnation. For the resin and composite properties we rely in the description of the typical characterization devices of section 2.3 and the experience of Chapter 3.

Figure 4.12 describes how to obtain the reinforcement properties. In this stage we discuss the difficulty to obtain the reinforcement permeability, for that reason we include the literature as a source. Another path could be measuring the properties directly in an attachment or specific test. After the test, the result will be stored in the device database and can be selected as a source during the composite characterization. In this case, the three sources of material information are mutually exclusive, and the user can only choose one source during a composite test.

Figure 4.12: Reinforcement properties functional model tree

Figure 4.13: Resin properties functional tree

Figure 4.14: Composite properties functional tree

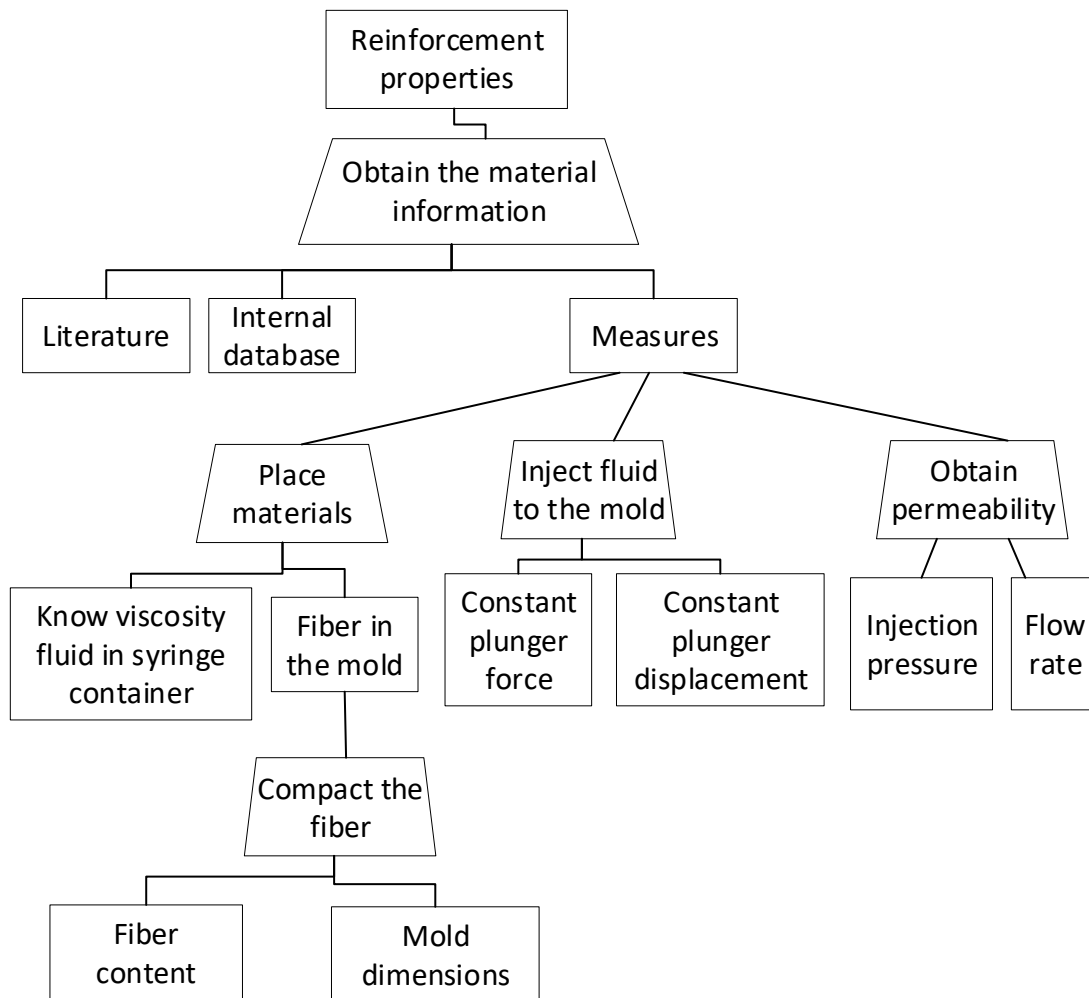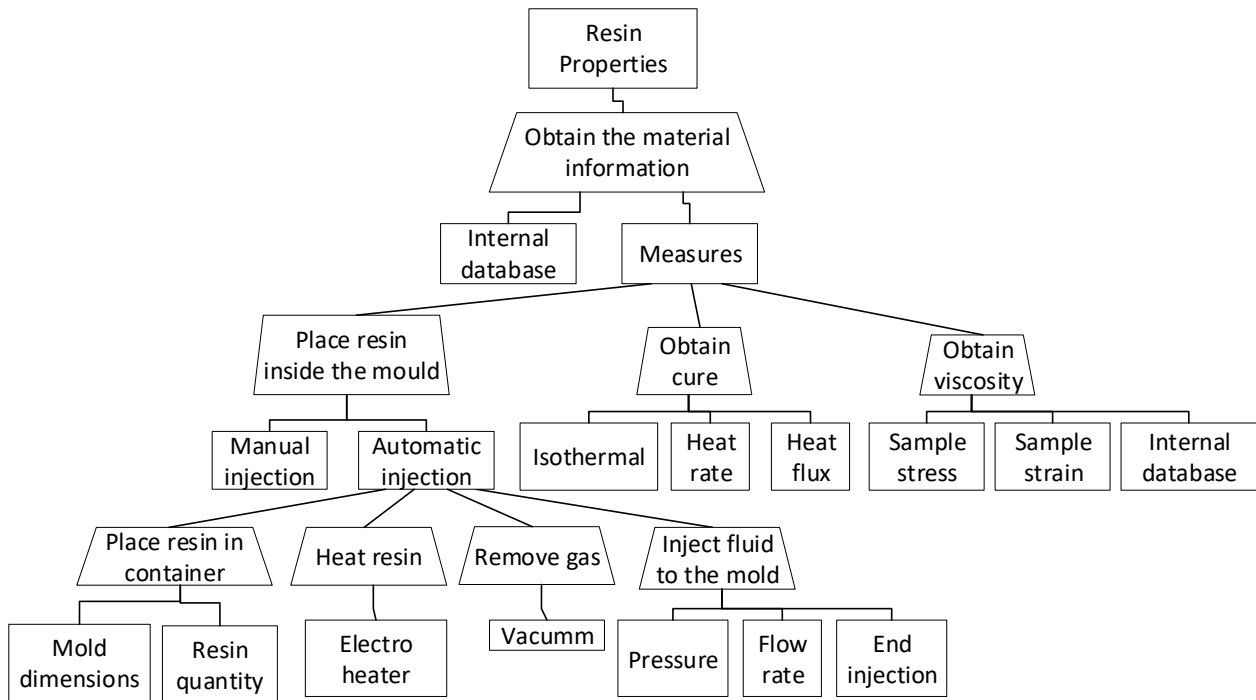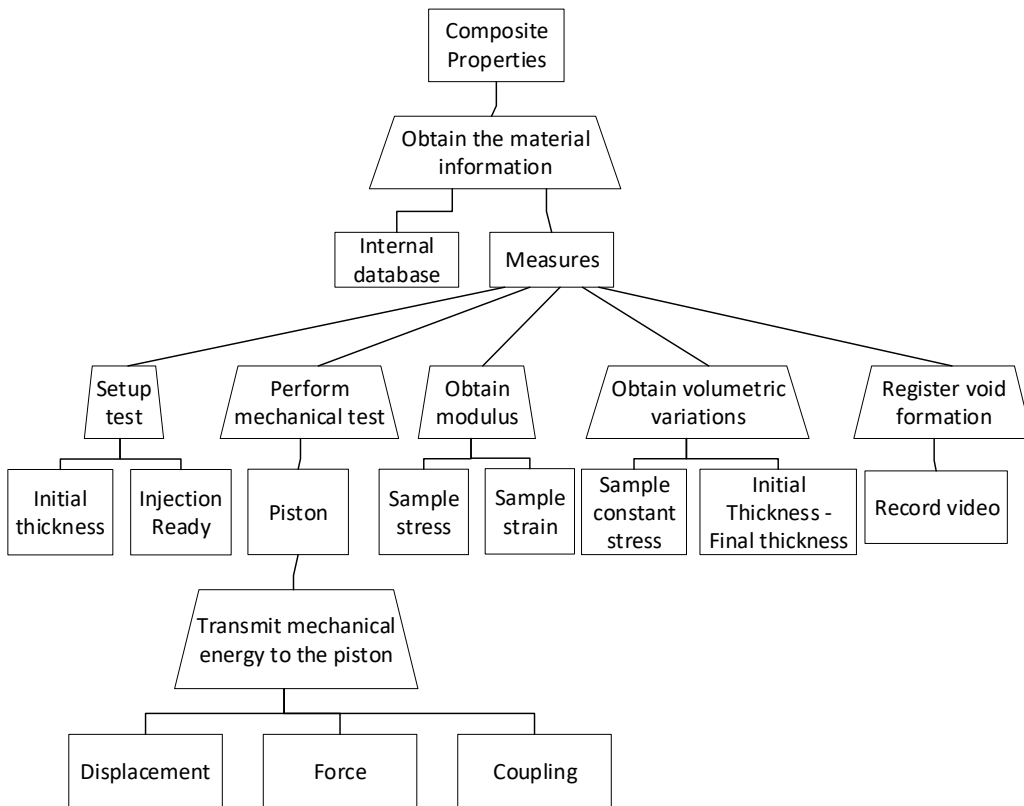Figure 4.13 shows the functional model tree for the characterization of the resin. Here, the viscosity is the most troublesome property. To overcome the requirement of a prior test we include the internal database to acquire the information.

Figure 4.14 indicates the last functional tree required to fully characterize a composite material. The procedure is covered with the principal functional model tree (Figure 4.12). In that case the "means" form an ORed structure. In other words, each of the functional models of properties must be completed in order to fully characterize the composite.

Sometimes all the "means" are required to complete a function and sometimes one is enough to do it. It depends on the scenario and the team interpretation. For example, Figure 4.15 shows the steps to recover the characterization properties from the device database.
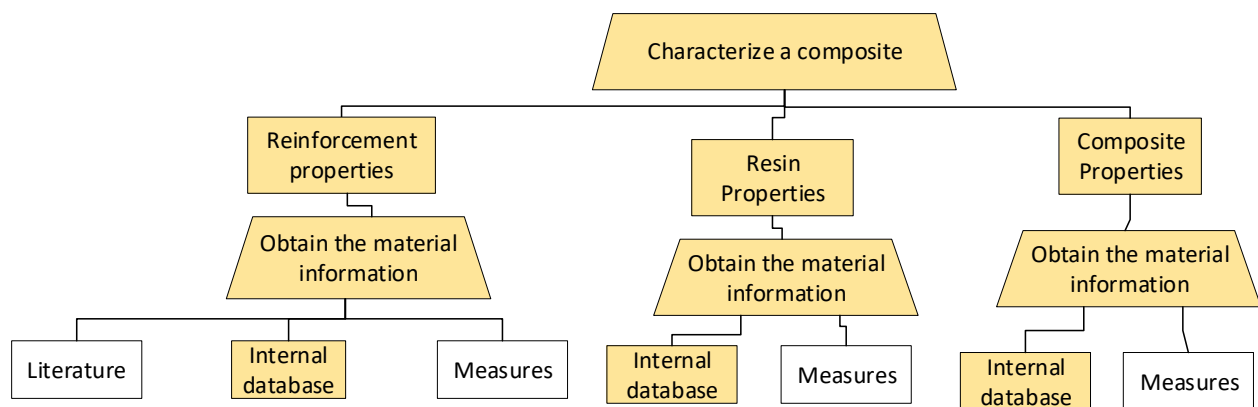
Figure 4.15: Retrieve composite information from the database

We put to test the functional model in different scenarios and cover all the possible combination to obtain the material properties. Surprisingly the functional model integrates all the traditional characterization devices but at the same time it can create substructures to create a less powerful but versatile equipment. For example, Figure 4.16 shows a specialized TMA for characterize composites derived from the principal functional model. This device require much less force to operate and only constant force, in turn, the development time and cost is greatly reduced according to the QFD in Figure 4.5. Also, we removed the injector to a manual injection. Maybe a port to be filled with a syringe will work well for this simplified device.

To sum up, the functional model gives the tools to express in detail the device functions. As we demonstrated, it can also be used to derive a set of tests that could be stored in the device memory for future purposes or even create a product family.
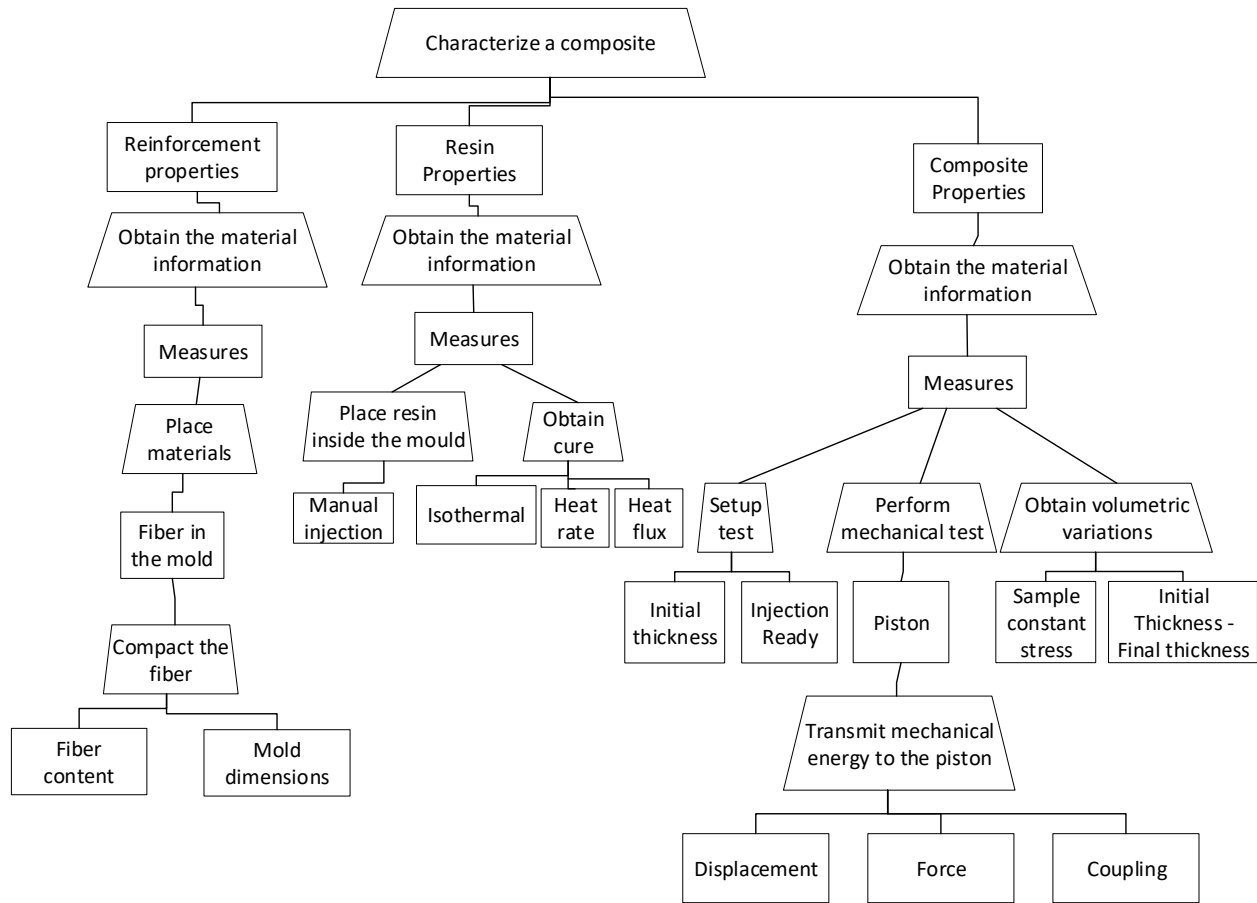
Figure 4.16: Composite TMA device functional tree

4.5.2 Product architecture

Although we found the functional model a versatile tool, it fell short to describe the device signals or interactions between the device components. To this purpose, the product architecture technique will complement the functional model. Figure 4.17 shows the starting black box model for the mechatronic characterization device made from the information of the Table 4.2 in the signal group.
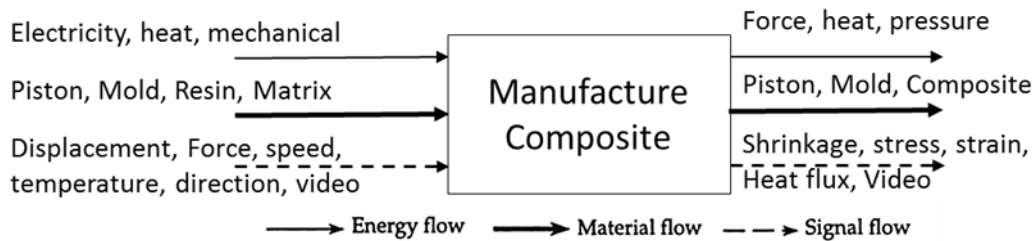
Figure 4.17: Black box model for the mechatronic characterization device

Then, we take the functional model and translate into the functional block of the Figure 4.18. The model represents the input signals and controlled parameters in the form of arrows and interactions that are grouped into modules. The interactions described in the section 4.4.2 allow us to analyze the signal flow to group the elements together. In the diagram, we found two conversion blocks or "conversion-transition" blocks. "Convert-electricity to force" and "Convert-electricity to heat/cool". The first one could represent an electrical motor, a hydraulic cylinder, etc. And the second, a heating source of any kind. In other words, a physical device or actuator capable of convert the source energy into the other, each block represents a module to develop.

As we could estimate from the functional model developed in the last section, the functional block model reveals a force as well as a heat/cool modules. As a matter of fact, they are the two main driving signal flows or parameters in the characterization device. The electricity module depends of the conversion-transition modules. For example, a DC motor will require an AC to DC current converter.

The measure module takes all the signals and converts them into the desired property. It could be related to the sensors, analog to digital converters, data conditioners and the processors. The importance of the functional block is that describe the required input signals, this helps the teams to define the electronic device inputs – outputs.

The injection module is not well defined and can be formed with the "put the matrix in the mold" and the "wet the matrix with the resin" blocks. That is because at this early stage of design is not possible to define how the permeability and resin viscosity prior to the injection are going to be measured. Finally, the video module is straight forward and does not interact with other signals.

The functional block model can continue to evolve as the team advances and find solutions to the macro models, that is the case of the injection system. In general, we found that this type of model complements the functional model and consolidate the team mental models which at this point will have the knowledge and confidence to begin finding solutions to the path traced by the mechatronic design methodology proposed.
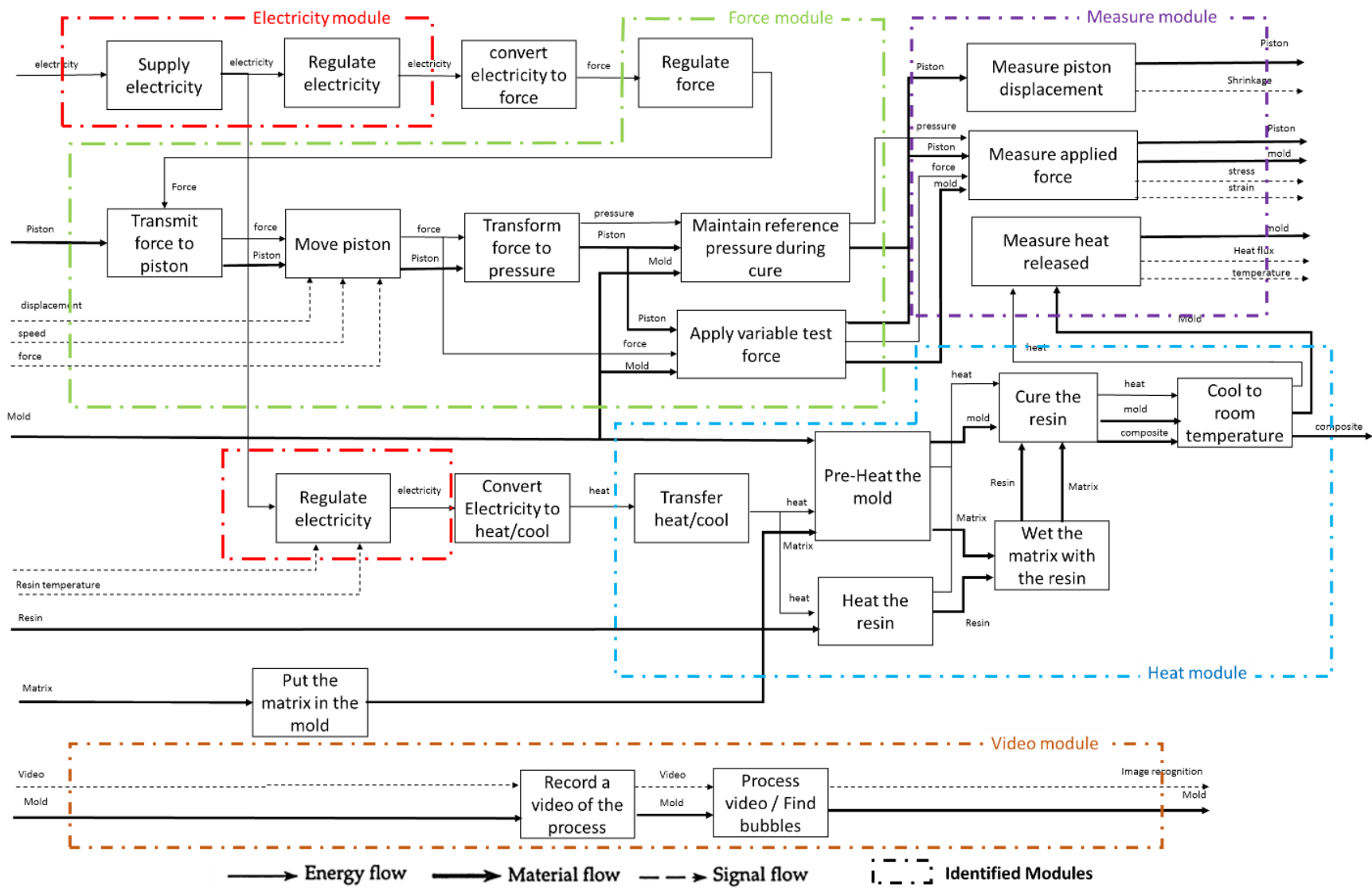
Figure 4.18: Functional block model and modules identification

4.6 Discussion

In order to achieve the second objective of developing an integrated mechatronic design methodology, we carefully analyze the most common mechatronic design challenges reported in the literature. Then, we assembly an integrated mechatronic methodology composed of five progressive techniques to extract and define the project requirements. Moreover, practical platform permits to define the system functional model and product architecture. As the design loop converges in the integration step, changes and updates refine the final product.

In particular, we can only express our impressions about the implementation of the proposed methodology during the realization of this PhD project. We found that the methodology implemented traced the path to follow during the mechatronic device design. First, the information gathered in the literature review and the manufacture experience was compiled and verified with the ERFT company engineers. Specifically, we found a common ground and language with the "demands and wishes" forms. The QFD gave us a tangible and quantitative way to evaluate the project dependencies. As the functional model and architecture emerged, the team was confident to propose changes and upgrades to the design. This showed that we gained a deeper comprehension of the device. When a change in the requirements was needed, we found a good "deal" between the involved engineers. This was because all the parts knew the influence on other people's activities, and by acknowledge the impact of their decisions, all the changes were for the best of the project. Finally, it is in our best aspirations that the course of action proposed, serve to inspire future integrations and the project continues growing to a fully functional characterization device.

4.7 Conclusion

For the particular design task to be carried out in this project, a new design methodology is needed to respond to the specific need of the lack of standard design knowledge in the field. This advanced strategy must meet the specific requirements for this multidisciplinary mechatronic device and our main objective to integrate multiple characterization laboratory equipment into a single device for PMCMs. A simple methodology is unable to meet or organize the complexities of this project. And a methodology assisted by genetic algorithms is too sophisticated to be applied in a mechanism where the minimum details have not yet been defined. We have observed that the proposed

methodology allows to manage the economic resources and organize the human resources. We can also say that the methodology allows a self-optimization which improves the product on each iteration. The advantages of following the suggested steps in addition to being potentially economical are also organizational, since having a project traceability and a holistic view of the system, the product becomes easy to improve or update even by a totally new team. All things considered, we can be sure that the second objective (OB2) for developing an integrated mechatronic design methodology was thoroughly covered with a well-defined and applied design strategy.

CHAPTER 5   EMBODIMENT DESIGN

5.1 Introduction

The purpose of this chapter is to complement the conceptual design presented in the requirements and system design stages of the VDI V-shape design methodology into the detailed design phase (embodiment). Upon completing, we will provide the appropriated design solutions for the critical components that will allow the characterization of multiple PMCM properties using a single device, our main PhD project goal.

In general, a mechatronic design requires of several design iterations to obtain a final product. Although in this section we are dedicated to the most important aspects, Appendix C shows parts of those design iterations.

According to the results of the QFD on section 4.3.2 and the product architecture of section 4.5.2, the team must focus in finding the proper force actuator with the proper linear displacement resolution to perform the characterization test. In particular, the development team must determine the preliminary layouts and technical solutions. In this context, the specific design should meet the demands and wishes of the product obtained in the section 4.3.1. We expend this chapter exploring these challenges. In here, we will be presenting the proposed solutions that will lead to a final product and the fulfillment of the third objective (OB3), identify the most critical machine components for design embodiment.

5.2 Challenges Related to Linear Actuators

The starting point of the design is the form, scale and layout of the machine. In other words, the mechanical design. Given that the device will be a hybrid of the laboratory scale RTM device presented in the Figure 3.2 and a PVT machine type, we focused on designing a mold with a piston. Figure 5.1 shows the 3D model (Catia) designed mold and piston derived from the requirements list. It requires a thick quartz glass window to withstand the high pressure applied to the sample and a second thin glass to create an air gap to provide isolation to the camera. Ideally, the piston

would maintain this simplified configuration, but with the addition of sensors and wires, the sensor placeholder will require of deeper design.

Figure 5.2 shows the leak-proof system. The piston will require a guiding ring to hold the piston in place during the displacement. To improve the leak-proof protection, an asymmetrical seal is included in the design. In this case, the seal allows free movement when the piston is not in the presence of the resin. When the resin fills the gap, the pressure pulls the seal to the mold wall. Because the high-pressure part of the test requires displacements in the range of µm, we expected a minimum of interference by the seal in the test.
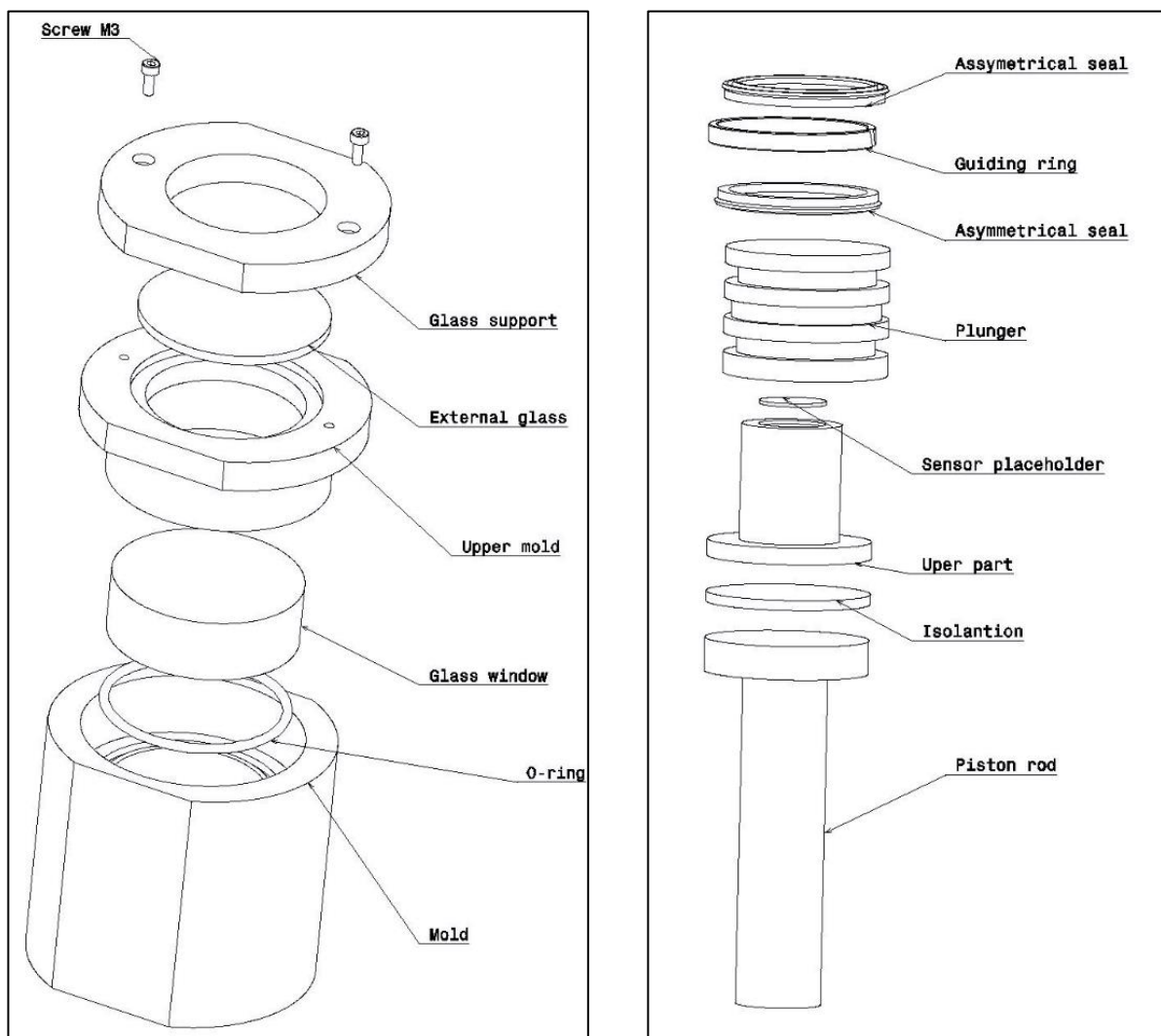
a. Mold exploded view.   b. Piston exploded view.

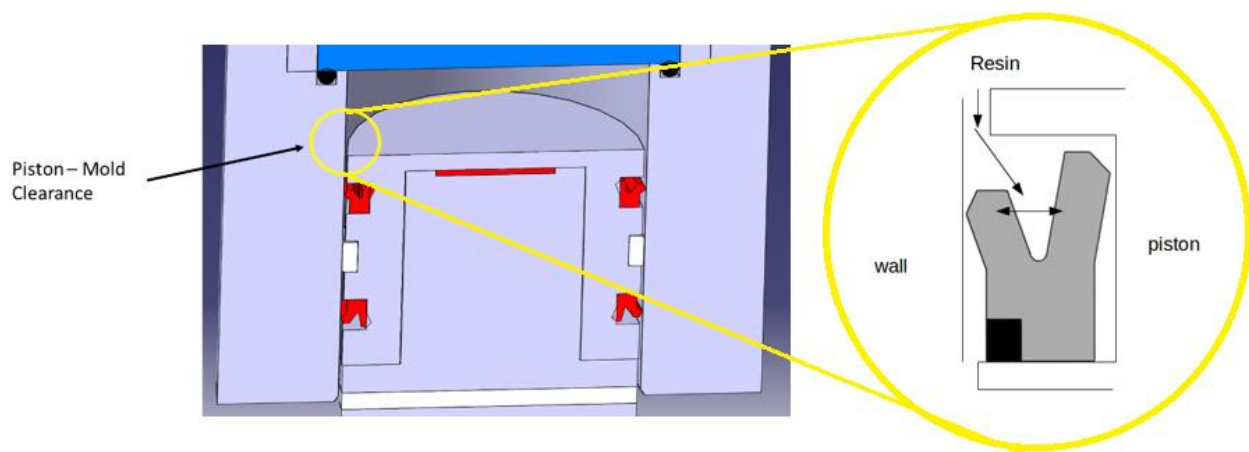Figure 5.1: Mechatronic device mold and piston assembly

Figure 5.2: Leak proof mold

Table 5.1 shows the materials used in the manufacture of the piston seals. The material determines the service temperature range and the application type. In this context, the requirement of 350 ºC in Table 4.2 is impossible to meet. Likewise, and to the best of our knowledge the maximum allowed temperature for tubing (injection system) is the silicone food grade material which also has a service temperature of 260 ºC. In summary, in a future iteration the team should revaluate the possibility to decrease the temperature to 200 ºC and study the implications of that change. For the time being, we will continue searching for the best sealing materials.

Table 5.1: Seals materials, adopted from [114]

Seal Material	Max Service Temperature °C	Description
Fluorocarbon elastomer	-20 to 210	Resistance to chemicals, organic compounds and heat.
Polytetrafluoroethylene or Teflon	-200 to 260	Chemical resistance and low coefficient of friction. Not good for dynamic applications and water.
Glass 15%, Molybdenum Disulphide 5% filled with polytetrafluoroethylene	-200 to 260	Resistance to cold flow, good for hydraulic seal. Not good for dynamic applications and water.
Carbon 25%, Graphite 5% filled with polytetrafluoroethylene	-200 to 260	Wear and chemical resistance. Good in water and emulsions. Good mechanical properties.

Table 5.1 (continued): Seals materials, adopted from [114]

Seal Material	Max Service Temperature °C	Description
Glass fiber with polytetrafluoroethylene	-200 to 260	Wear and chemical resistance. Improved mechanical properties. Seal for high mechanical stress. Low friction
Bronze reinforce with polytetrafluoroethylene	-200 to 260	High compressive strength and good mechanical properties. Low friction.
Nitrile butadiene rubber	-25 to 100	Good mechanical properties. Chemical resistance to hydraulic fluids. Widely used in seals.
Methyl silicone rubber	-55 to 210	Use in hot air, streams. Medium mechanical properties. Chemical resistance.
Polyoxymethylene	-60 to 100	Good mechanical properties and chemical resistance. Stable in water. Low moisture absorption. Used in precision and close tolerance.

5.2.1 Linear actuator vs. the force

The heart of the mechatronic device is in the force actuator (See QFD on section 4.3.2). In order to obtain the device layout, it is imperative to define the force actuator and their dimensions. Pure linear actuators are preferred due to their linear behavior, just apply an electric energy and the resulting force and displacement will be proportional. Unfortunately, this type of actuators has limited displacement in the range of mm and are very bulky. Figure 5.3 shows the DMA 450 from Metravib. The information was gathered from their training material presentations [115]. To overcome the limited stroke, the user must manually setup the machine initial position. As shown in the figure, the actuator is an electro-dynamic actuator or electro shaker, the working principle of this device is similar to an audio speaker.
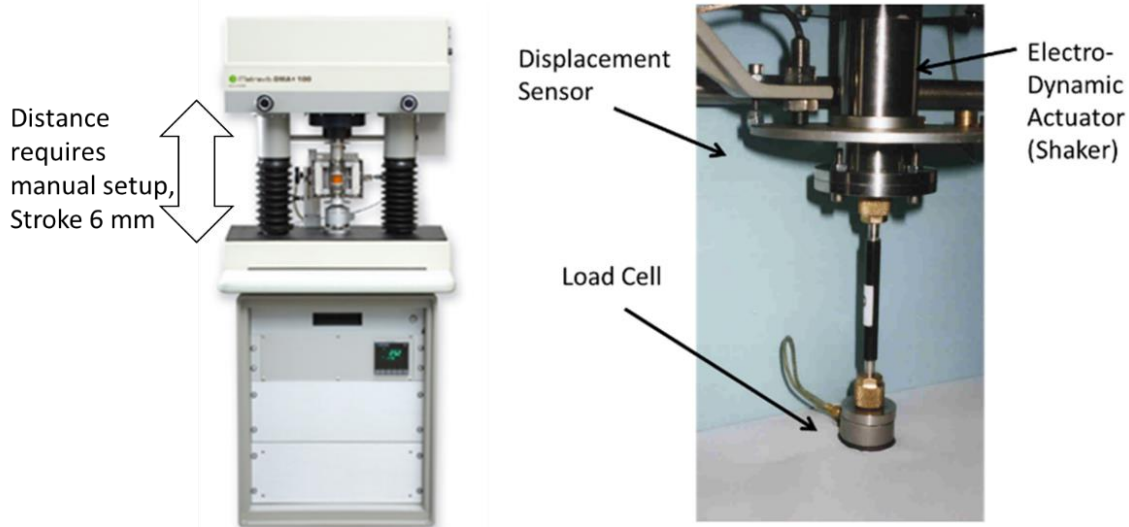
Figure 5.3: DMA 450 from Metravib [115]

To draw a comparison between existing devices and the required actuator, we look for an actuator with identical working principle. Figure 5.4 shows an electrodynamic shaker with 2.2 kN of force, the device cost is around 40 000 USD and required 5200 VA. Inevitably this type of device will not comply with device requirements of tabletop mounting and another working principle needs to be reviewed.

Force	2.2 kN
Max Displacement	25.4 mm
Frequency	Up to 4500Hz
Weight	215 kg
Size	53H x 35W x 35D cm

Figure 5.4: Electrodynamic shaker from Vibration Research group [116]

5.2.2 Piezo stacks, good things come in small packages

Piezo stacks are not a new technology, but recently they are being used to produce Nano-meter positioning systems and micro motors. In this respect, they could solve the mechatronic device force problem. Figure 5.5 shows the internal structure of this linear actuator. It forms from layers of piezoelectric material bonded and connected electrically. When a voltage pass through the stack it expands with a linear behavior [117, 118].
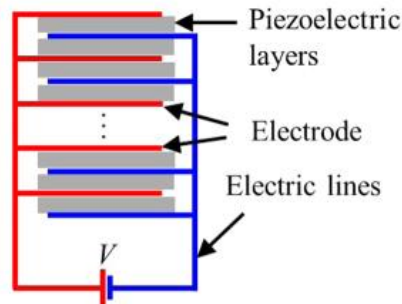
Figure 5.5: Piezo electric actuator internal structure [118]

The actuator requires voltages in the range of 100 – 1 000V, but because the current is in the range of mA the power drivers are relatively small. Figure 5.6 shows the piezo stack acquired from the PiezoDrive company [119], in the figure a pen provides the comparative means to visualize the devices size. The piezo stack has 1.8 kN of blocking force, 70 µm of stroke and 36 kHz of resonance frequency. The driver requires a power supply of ±12V and provides a peak current of 300 mA. To drive the piezo stack a signal of ±10V is proportionally converted to ±150V. For size comparison, Figure 5.7 shows a piezo stack with 70 kN of force. In connection with the device requirements, Table 4.2 tells us that the test needs are ± 10 µm of strain, 10 Hz of sinusoidal load frequency and 2.5 kN of force, quantities in the range of the presented piezo stacks.

Figure 5.6: PiezoDrive Piezo stack actuator with the voltage driver board
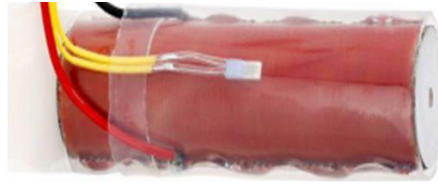
	Displacement	Diameter OD	Length L	Blocking force	Stiffness	Electrical Capacitance	Resonant frequency
	µm	mm	mm	N	N/µm	nF	kHz
P-056.90P	180	56	169	70000	390	21000	7

Figure 5.7: PICA power piezo actuator, adopted from [120]

Tzen *et al.* 2003 [117] tested the dynamic behavior of a piezo stack preloaded with a spring. In an open loop configuration and with a sinusoidal input signal of 10 Hz, the actuator error was about 1 µm. Then, they repeated the experiment in a closed loop configuration and achieved about 0.15 µm of tracking error. Figure 5.8 shows the close loops test results. In fact, the tracking error is not critical in our case because we required to measure the stress response of the material to the applied strain, that is independent of the lag between the commanded signal and the actuator response. The important is that the strain frequency and magnitude remain in the desired levels. However, the dynamic response of the presented piezo stack is exceptionally good. Sadly, they do not describe the imposed load which gives us some uncertainty about the results and the applicability to the mechatronic characterization device.
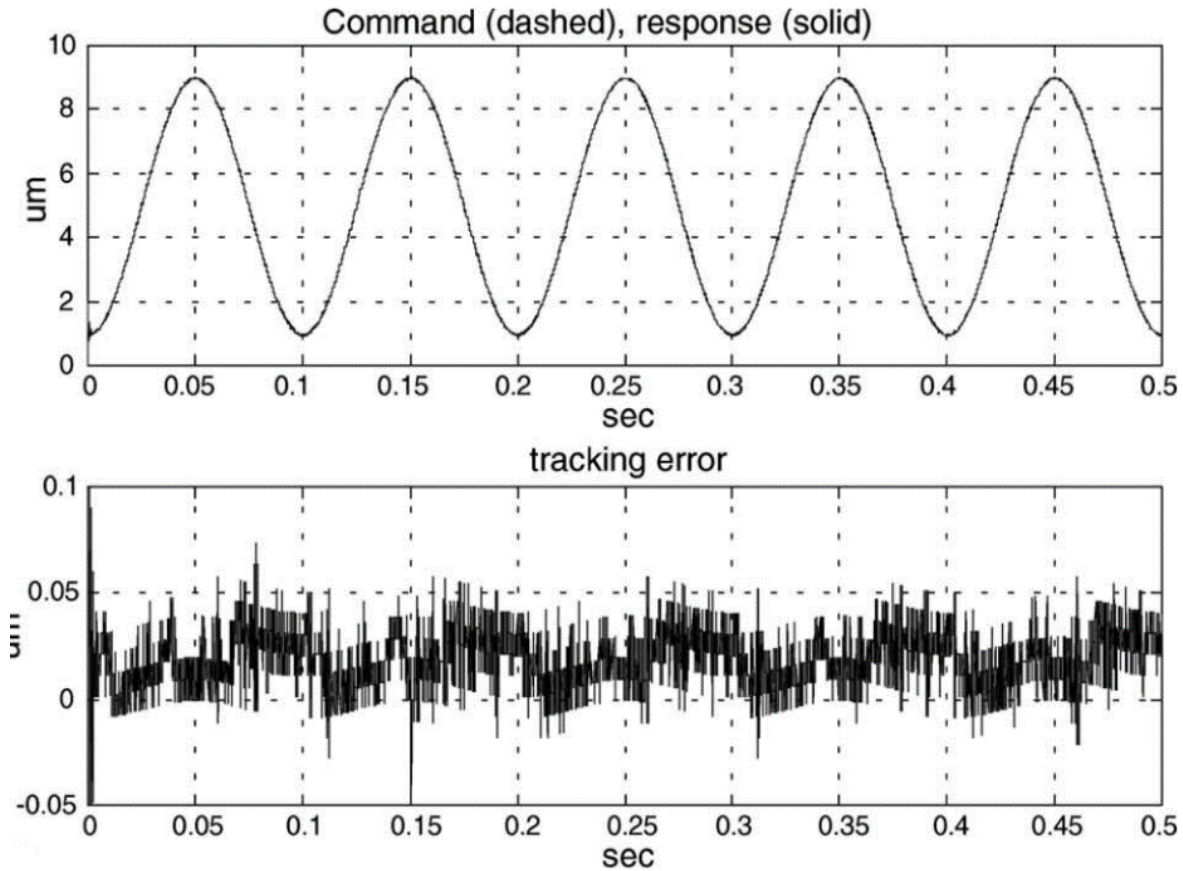
Figure 5.8: Piezo stack under close loop control [117]

Regarding the displacement vs. force capabilities, Tran *et al.* 2016 [118] showed an interesting test setup to test the blocking force of a custom-made piezo actuator. Figure 5.9 shows that the piezo stack lifts a fixed load, the laser displacement sensor measures with high degree of precision the movement. After collecting the data, the load increases to repeat the test.
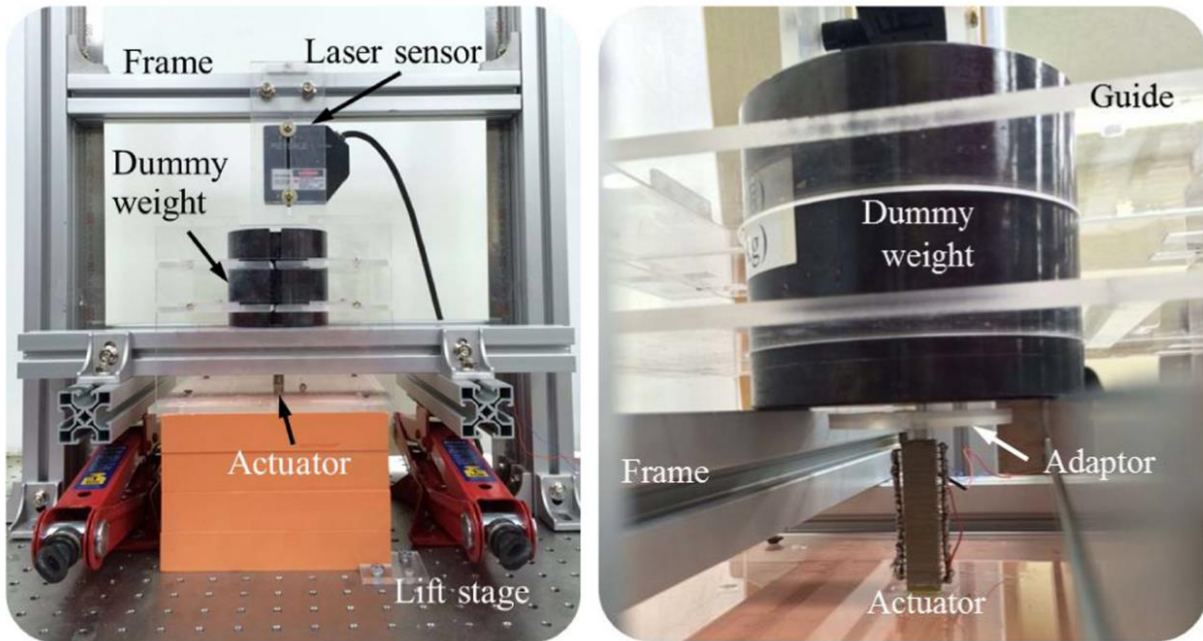
Figure 5.9: Piezo stack blocking force setup [118]
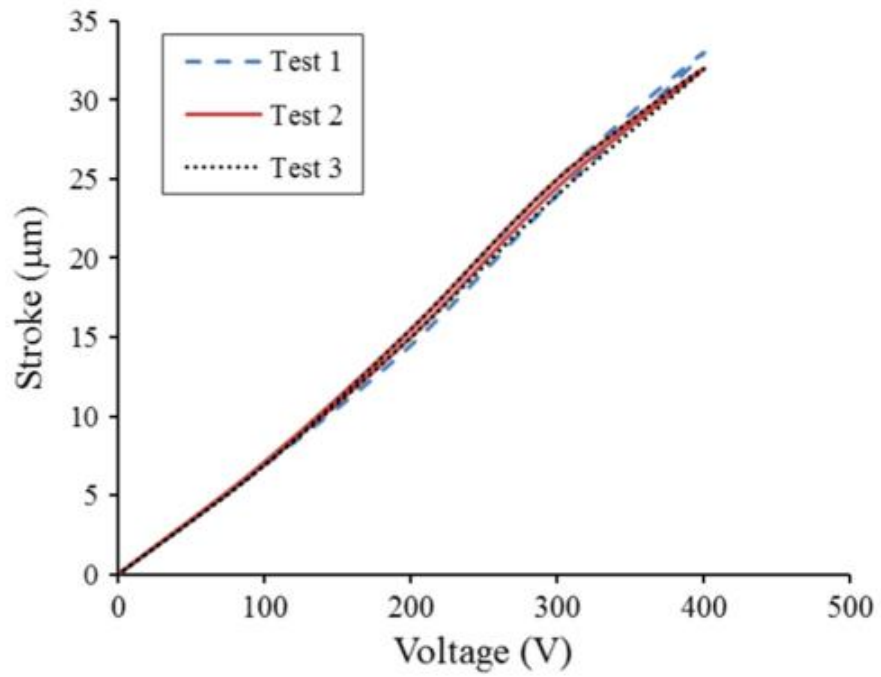
Figure 5.10: Piezo stack hysteresis curve, no load [118]

a. Weight 2 kg.

b. Weight 4 kg.
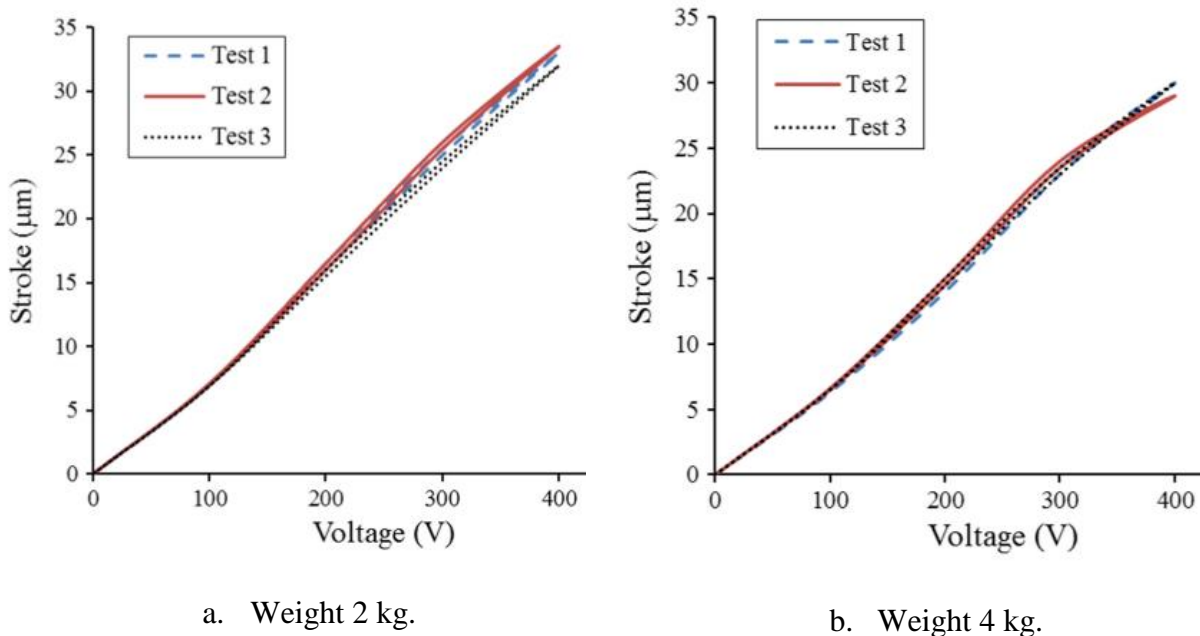
Figure 5.11: Piezo stack hysteresis curves under load [118]

Figure 5.10 shows that the custom-made piezo actuator has a stroke of 32 µm. In the same way, Figure 5.11 shows that under load, the piezo stack keeps moving reaching 25 µm without a problem. During the last 7 µm, at 4 kg the actuator presents some difficulties. But in general, the custom-made device maintains the linear behavior under load.

Taking into consideration the results in the two-works presented and the promising capabilities of the commercial piezo actuator in Figure 5.7, we can hypothesize that the device could meet the mechatronic characterization device requirements. Unfortunately, that is not enough to answer the following questions necessary to take design decisions:

*What are the piezo stack stroke, blocking force, stiffness and resonance frequency optimal values required to apply a dynamic compressive force of 2.5 kN with a maximum amplitude of 20 µm with a sinusoidal frequency of 10 Hz? How can these properties be characterized? What are the recommended setting conditions to increase the actuator durability and reliability? And more importantly, how many working cycles can the device withstand under the desired test conditions?*

All these questions are relevant to the development of the mechatronic characterization device and requires of a scientific approach to solve them. Another solution could be simply buy the patented

actuator of an Instron machine to unveil their industrial secrets but that could cost too much, bear in mind that an Instron E3000 3kN machine cost about 250 000 USD. However, judging for the piezo stack prices in Table 5.2 and the possibility to develop a custom-made device, this solution is attractive from an academic point of view and rentable from an industrial perspective.

Table 5.2: Piezo Stack prices

Company	Product, reference, stroke, force	Price in USD
Kinetic Ceramics	D050120 – 120 µm, 4500 N D075120 – 120 µm, 10000 N D100120 – 120 µm, 18000 N	$1,975.00 $2,945.00 $3,975.00
Physiks Instruments	P-887.91 – 30 µm, 1850N P-225.2SV – 30 µm, 12500 N, high temperature P-025.80 – 120 µm, 16000N	$503 $3,312 $3,435

5.2.3 A first overview of the mechatronic characterization device

As the design iterations progressed two designs layout were proposed and evaluated. Figure 5.12 shows the two typical machine configurations for universal machine testing (UTM). The single column is predominant in low force machines ($\leq$ 10 kN), in the other hand, twin column covers the high force range ($\geq$10 kN).

Single column.

Twin Column.

Figure 5.12: Universal test machines typical configurations [121]

The first machine layout follows the single column trend and was proposed bearing in mind the piezo stack as the principal component. On the contrary, the second layout considers a ball screw actuator as the only source of force guided by two linear bearings.

We begin the analysis with the single column design layout. This configuration produces more compact structures for tabletop mounting, which is demanded in the Table 4.4 of requirements. Because the piezo stack possesses a stroke in the range of µm, the design requires an additional linear displacement actuator. From the test requirements Table 4.2 , the maximum piston stroke value was defined as 100mm to open and close the mold. Figure 5.13 shows the Nook ND8-12-20-B chosen device. It has the demanded stroke and the force is in the same range as the required in the carried-out test.

Product Info	Screw Type	Ball Screw

Details		
	Voltage (Vdc)	12
	Gear Ratio	20:1
	Speed at no load (mm/s)	17
	Speed at full load (mm/s)	14.3
	Dynamic load (N)	4500
	Static load (N)	13600
	Currents (A)	16

Figure 5.13: Ball screw linear actuator [122]

Figure 5.14 and Figure 5.15 shows the first proposed mechatronic characterization device. Here, the linear actuator closes the mold to the desired sample thickness. Them, the linear bearing guides the piston inside the mold which is pushed by the piezo stack actuator. Finally, a load cell measures the applied force.
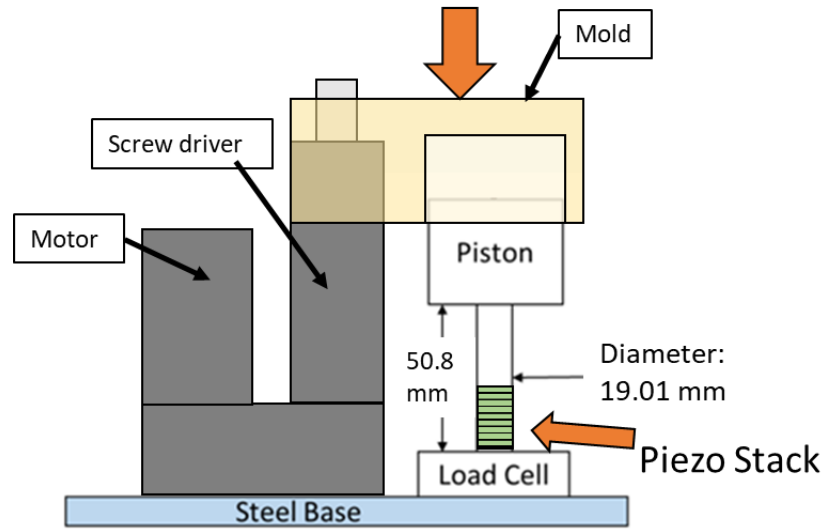
Figure 5.14: Mechatronic device sketch
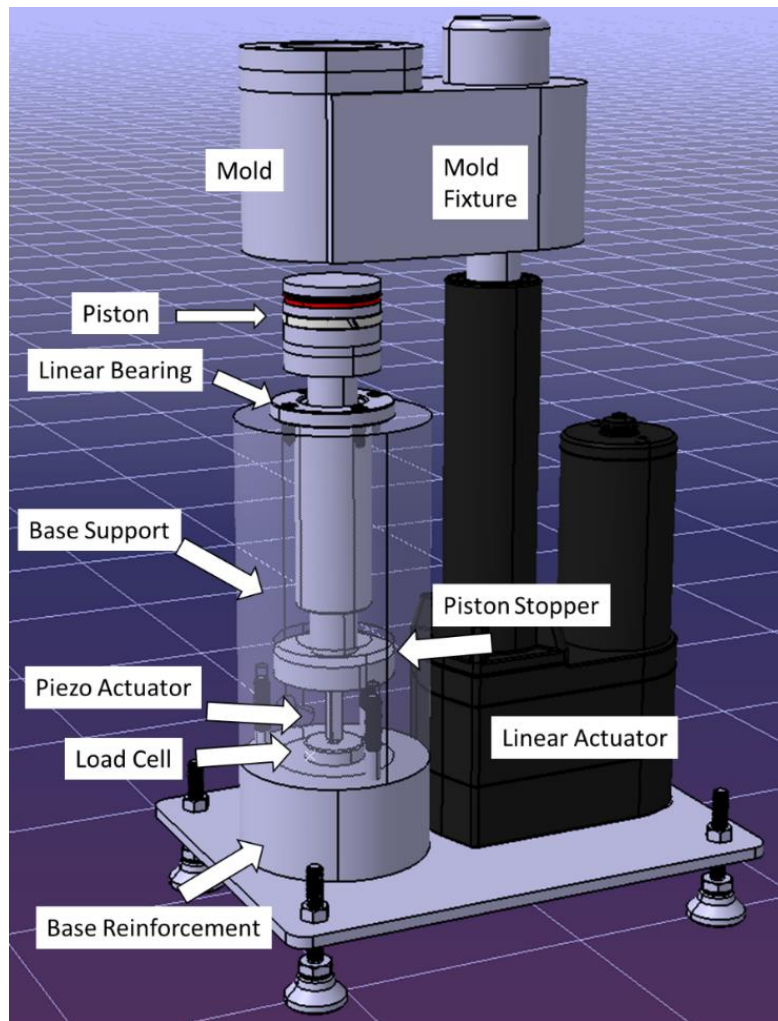
Figure 5.15: First proposed mechatronic characterization device, Catia 3D Model

Figure 5.16 describes in detail the piezo stack fixture. This design requires that the piston compresses the piezo actuator with the linear actuator. In other words, the ball screw motor applies a constant force through the experiment, at the same time, the piezo stack will provide the sinusoidal stress – strain to perform the test. Synchronize the two actuators will be a mayor challenge to solve for the future design team. At the end of the test, the linear motor pushes the mold up, in that case, the piston will touch the piston stopper. If all goes as planned, the piston should have separated from the mold and the user can remove the mold from their fixture. Unfortunately, the amount of force to separate the piston from the sample is unknown.
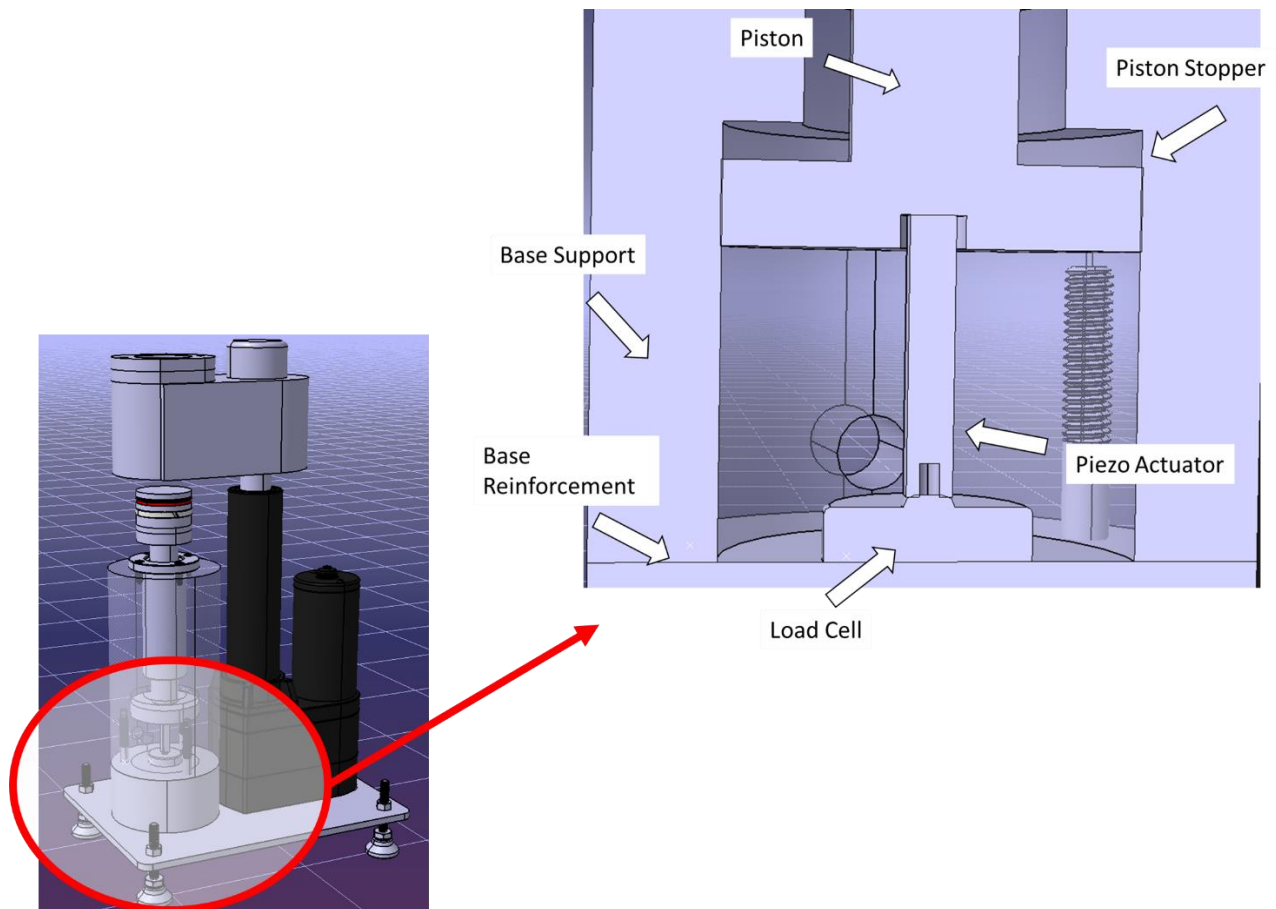
Figure 5.16: Piezo actuator support, detailed view

At this point of the early design, there are many choices and decisions to make. One example of that is how apply the heat to the mold. In the proposed design we have not considered the space to the electrical heaters. Figure 5.17 shows the most promising choice. A band heater will be just screwed in place and is already isolated. The problem is that the mold is running out of space. Considering that the bottom side is for the piston, the upper side is required to the glass window

and finally, all the mold sides will be covered by the heater band. In turn, we have not space for the injection ports. In this context, the future team must perform a set of design iterations and careful evaluate the mold design or discard the band heater from their selections.
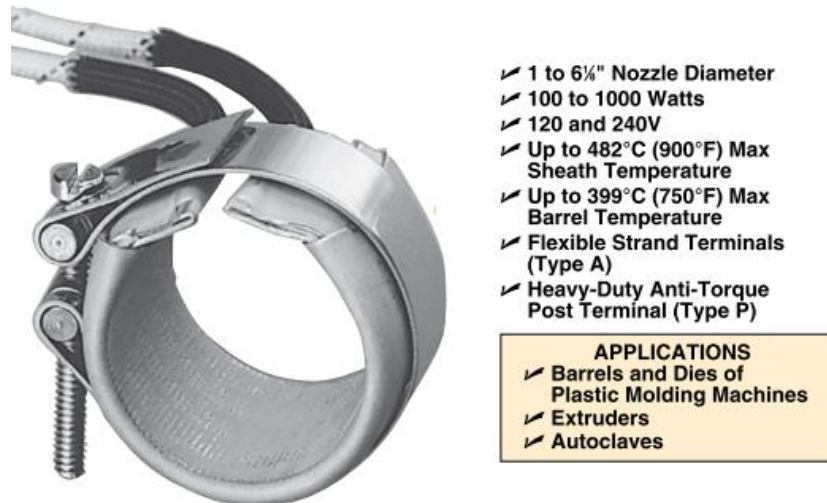
Figure 5.17: Insulated band heater [123]

Because this first design layout requires synchronizing two actuators and it also requires two sets of sensors and controllers. We build the second proposed layout in Figure 5.18 because resembles an UTM testing machine. These devices are well known for material testing due to their excellent performance.

Upon arrival of the load cell, we verify the sensor calibration. Far that purpose, we compress the device in an hydraulic UTM machine MTS 50 kN from the laboratory of micro-characterization of composites at Polytechnique Montreal. Figure 5.19 shows the testing setup. Once applied the force, a multimeter displays the measure voltage. From the readings in the MTS screen and the multimeter, the potentiometers from the load cell signal conditioner were adjusted to obtain the cell constant of 0.02 mV/V.
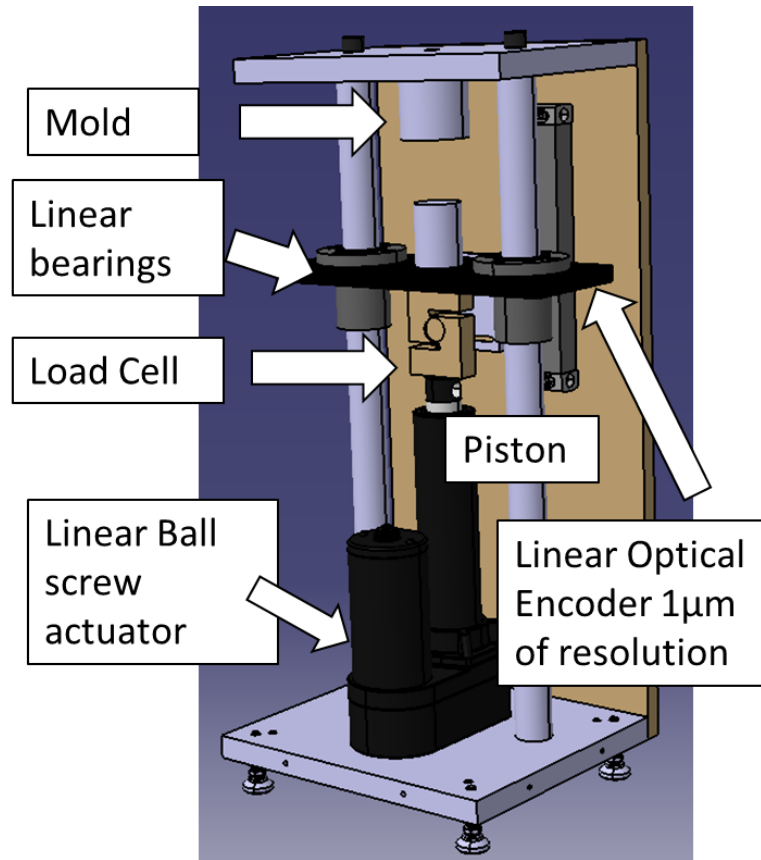
Figure 5.18: Second proposed mechatronic characterization device, Catia 3D Model
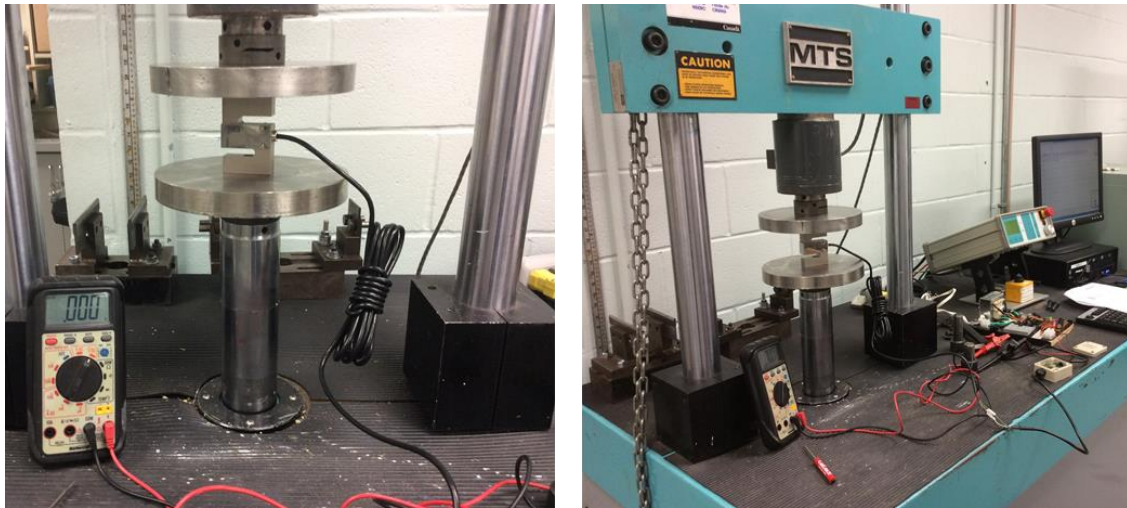
Figure 5.19: Load cell calibration setup

Table 5.3 shows the results from the load and unload test. As the results suggest the load cell was properly calibrated from factory and minimal tuning in the zero-drift potentiometer were required.

With this verification we were sure about the measure from the load cell and signal conditioner assembly.

Table 5.3: Load and unload calibration test

Force applied	kg	Volts measured	mV/V
462	47.10	0.94	0.02
1106	112.75	2.25	0.02
1800	183.50	3.67	0.02
386	39.35	0.78	0.02
860	87.67	1.75	0.02
1349	137.52	2.75	0.02
2385	243.14	4.86	0.02
3460	352.73	7.05	0.02
2712	276.48	5.52	0.02
1100	112.14	2.24	0.02
589	60.04	1.20	0.02

Figure 5.20 shows the compression spring used to test the linear actuator force. The spring has a compression constant of 207.3 N/mm. After applying 12 V to the motor an compressing the spring between 20 to 25 mm, we measure 4.23 kN and 5.29 kN, respectively. Therefore, the measured spring constant was 211.7 N/mm, close to the one specified in the catalog.

Figure 5.20: Compression spring

Figure 5.21 shows the prototyped mechatronic device. After successfully characterizing its force capabilities, we can be sure that the linear actuator can apply the required force of 2.58 kN listed in the list of requirements on Table 4.2.

Figure 5.21: Prototyped mechatronic device

5.2.4 Mechatronic device static and dynamic behavior

The next subject in the design iteration is related to the system time response. We proceeded to obtain the speed vs voltage behaviour. In this step we found several issues that will be described in detail.

After obtaining ambiguous measurements with the Atmel microcontroller, we considered the option of repeating all the test with a National Instruments NI-USB-6251 and the LabVIEW

platform for compare the quality of the collected data from the microcontroller. In that way, we test if the errors in the measurements were due to the lack of computing power as suggested in the QFD of the Figure 4.5.

Figure 5.22 shows the test setup derived from the product architecture and module identification from the Figure 4.18. The Switching Mode Power Supply (SMPS) convert the current from AC to DC. Then, a power MOSFET H-bridged receive the control signal to regulate the force, speed, position, etc.
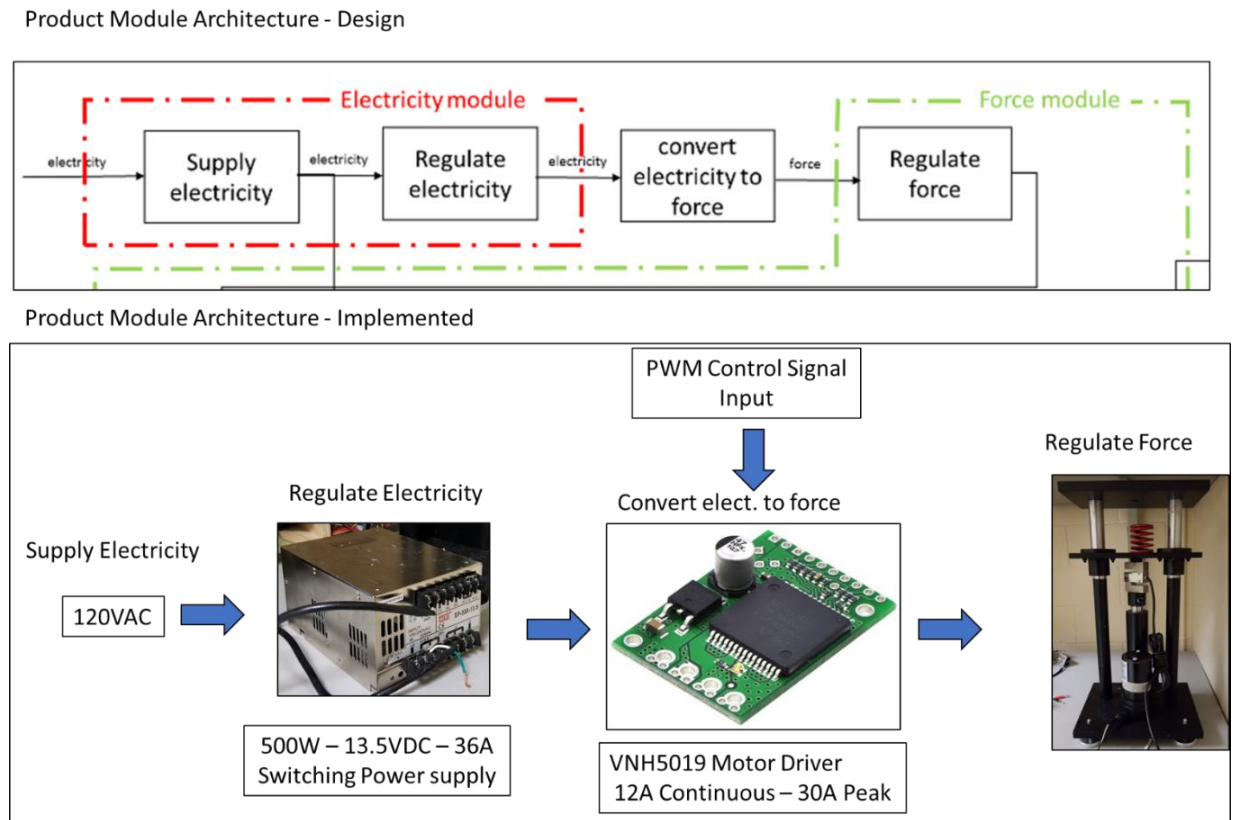
Figure 5.22: Linear actuator test setup

We test the linear actuator without load and measure the displacement with the embedded linear actuator position potentiometer. The raw data from the experiment present spikes of noise that makes impossible to obtain the position with the limited capabilities of the microcontroller. For that reason, we implemented a low pass filter to reduce the noise. Figure 5.23 shows the raw data before and after the low pass filter. When the motor is not running, from 0 – 40k Samples and 180k Samples to 300kSamples. Smaller peaks are present. This is due to the implementation of the SMPS power supply. These devices are smaller in size from their analog counter part, but the switching

induces noise to the signals. And next, form 40 k Samples to 180 k Samples, the SMPS powers the actuator and the noise increases dramatically. The signal to noise parameter is a major source of measuring error in all the analog signals. For that reason, optical encoders are preferred because provides immunity to the motor noise.
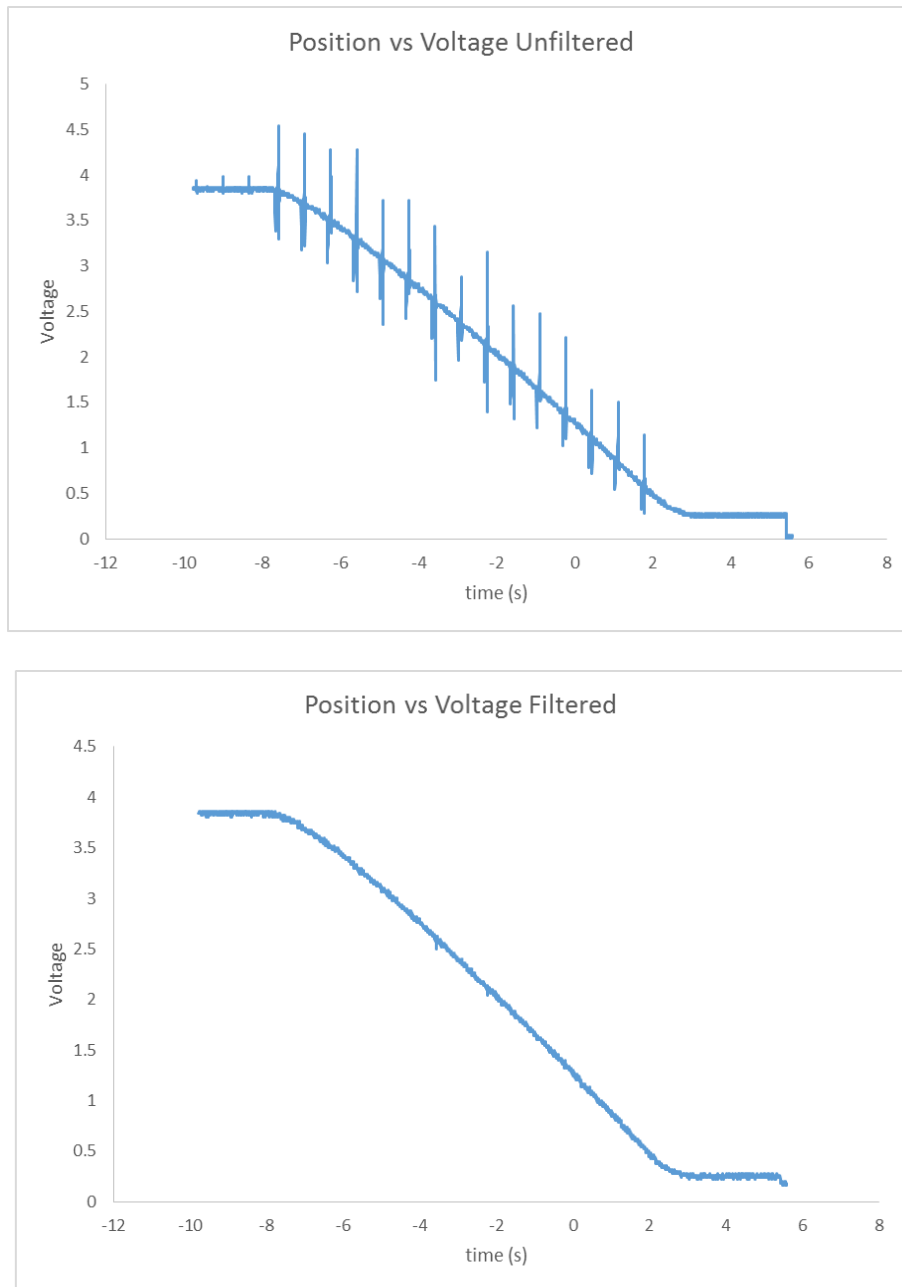
Figure 5.23: Noise in the analog position sensor

For the next test, a 150 LPI quadrature linear optical encoder was attached to the piston. Figure 5.24 and Figure 5.25 shows the good agreement between the data measured with an ATMEL Microcontroller and the NI-USB-6251 LabVIEW device.
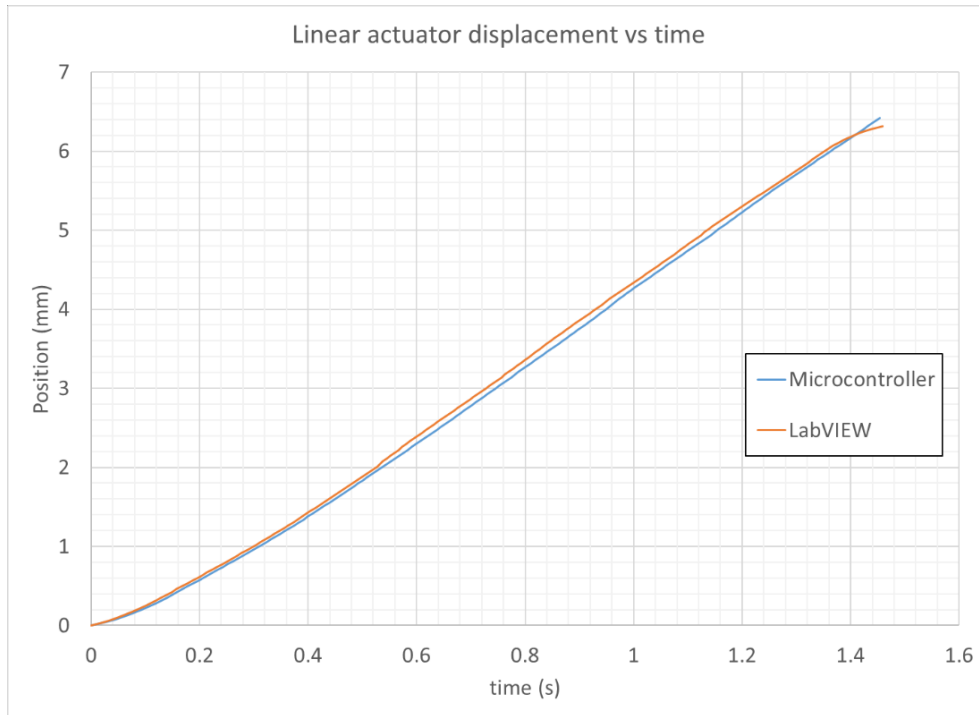
Figure 5.24: Microcontroller vs LabVIEW displacement measure
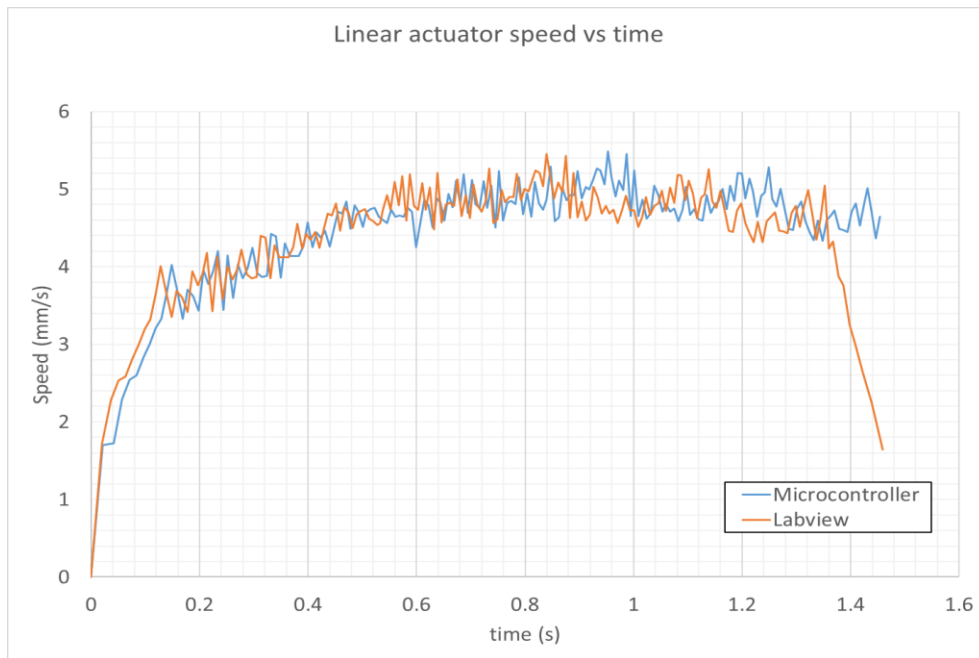
Figure 5.25: Microcontroller vs LabVIEW speed measure

We proceed to measure the linear actuator steady-state speed response from a set of step pulse experiments. As a result, the speed over voltage constant was found to be 1.47 mm/(s.V). In the Figure 5.26 the maximum measured speed was 17.7 mm/s which resembles the 17 mm/s provided by the specs sheet in Figure 5.13.

The chart shows speed (mm/s) versus Voltage with a linear fit: $y = 1.4751x$, $R^2 = 0.9879$.
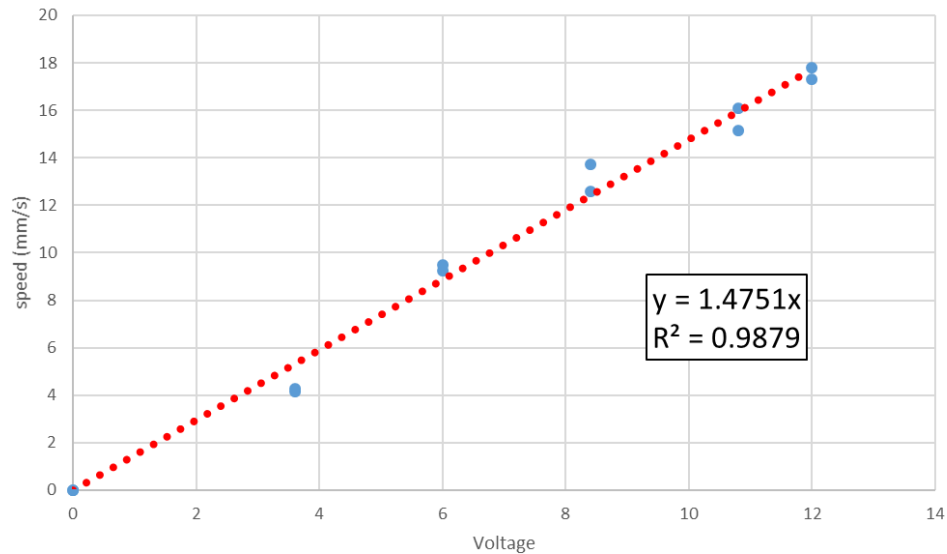
Figure 5.26: Linear actuator steady state speed response

In the final analysis, we present the normalized step response to PWM duty cycles of 40%, 80% and 100%. Figure 5.27 shows that the system displays a nonlinear response. In other words, the system dynamic time response changes with the voltage input. In this perspective the effects of the gears friction, backlash, lubrication, the interaction between the rolling balls and the nut of the ball-screw, etc. cannot be neglected and must be corrected physically or controlled. Considering that in speed the system presents a non-linear second-order time response, we conclude that the goal to achieve the required position for the mechatronic device is to control a servo linear actuator with a non-linear third-order position behaviour in the scale of sub-micrometers. The effort required to achieve that goal goes beyond the scope of this PhD project.
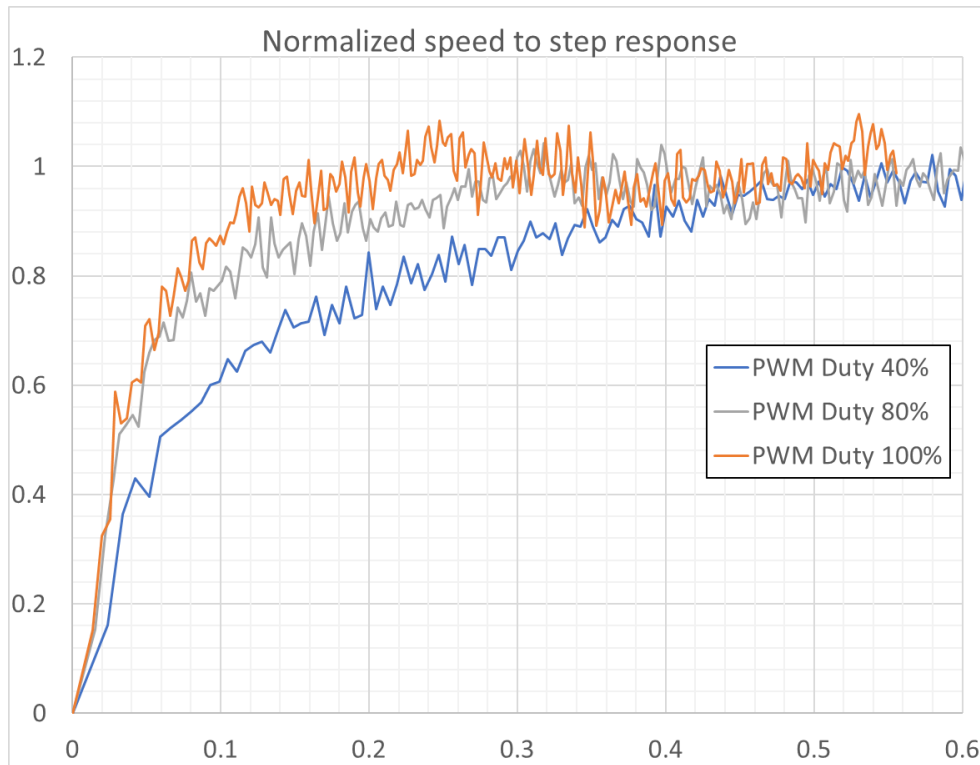
Figure 5.27: Linear actuator normalized speed response

5.2.5 Linear displacement, advancing in small steps

In this section we analyze the results of the QFD (Figure 4.5) regarding the linear displacement. Displacement resolution is the third most important scoring design parameter after the force and the computing power. In the QFD, negative relationships of this parameter are with the "High resolution and fast acquisition electronics", "Computing power and storage", "Design and engineering time" and "Machine production cost". In this context we will focus our resources to study the influence of the displacement resolution in the characterization device.

We experience the first three negative relationships when we attempt to increase the displacement resolution to 1 µm. For this purpose, we acquired the Chinese RLS100-1D-3M9N linear encoder presented in the Figure 5.28. At full speed the sensor gives a signal of 17.7 kHz using a single channel signal and 70.8 kHz using the full quadrature signal. As a consequence, the 8-bit microcontroller was short of resources to continue with the development.

Figure 5.28: Linear optical encoder with 1 µm of resolution

As the system grows, the required processing capacity increases. This is because the system must handle and process more signals (current, PWM, encoder, etc.). Figure 5.29 shows the current and future system iterations in terms of computing power. During the first iterations, we implemented Arduino, but to increase the PWM frequency from 490 Hz to an ultrasonic frequency of 20 kHz we had to code more efficient C libraries. Once upgraded, the motor run without audible noise from the control signal and we gain more control over the microcontroller peripherals with the custom routines. Then, LabVIEW validated the microcontroller software quality. And finally, with the arrival of the optical encoder and the full integration of all the signals, a 32-bit microcontroller was selected due to their power capabilities and cost-benefit over their 8-bit counterpart.
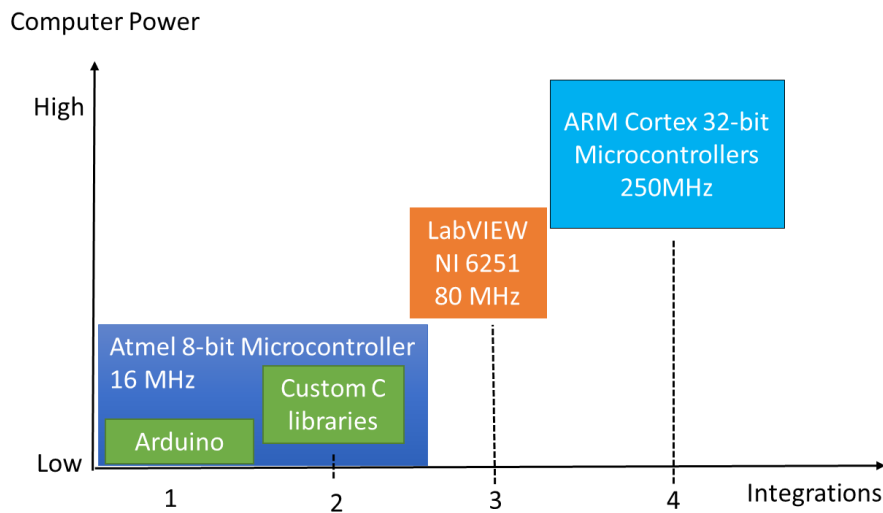
Figure 5.29: Increase in the computer power requirements by the system integrations

Unfortunately, 32-bit devices have a long learning curve and after four months of coding without much advances, we look for information about the average firmware development time for this type of projects. The markets study of 2017 from EE|Times [124] made a survey of 1 234 embedded firmware development companies. In 2017, the average project development time was 12.1 months for a team size average of 14.8 engineers, that covers hardware (39%) and software (61%). And

having only one software engineering available, we realize that was impossible to continue with the development of a proprietary framework as proposed in the requirement list on Table 4.4. Additionally, on each upgrade we could not recycle the code developed, for that reason a computer science firmware development strategy and coding standards must be implemented. Primarily because those strategies allows developing reusable firmware modules and user layers to upgrade to a more powerful microcontroller without affecting the implementation time [125]. The strategy tries to isolate the project code from the specific microcontroller hardware abstraction layers peripheral drivers, but that software development paradigm requires of additional strategic thinking that must be covered by the next team. For that purpose, Beningo *et al.* 2017 [125] describes how to create reusable firmware code for microcontrollers.

To continue with the analysis, we change the approach removing the "Machine production cost" criterion. Assuming no limitations in the price of the equipment, we analyse in a broad perspective the project requirements. The mechatronic characterization device requires of high resolution linear movements to test the material dynamic response. But, to what extent? Also, high-end electrical press has outstanding displacement resolution, Why, they cannot be used in the characterization of composite materials? Solving these questions will allow us to understand the requirements in terms of the piston linear displacement. Specifically, we will answer the next research question.

What is preventing researchers to use high-end commercial equipment that will allow the characterization of composite materials?

As we presented in the literature review, researchers used attachments to commercial characterization devices like the DMA and the Rheometer. We already stated that these devices lack the required force to test thick PMCMs. Naturally, the next candidates are the universal testing machines (UTM) because they can develop forces in the range of thousands of newtons and has optical displacement sensors that measures in the range of microns. With that in mind, let's examine the manufactures machine technical specifications.

Technical Specifications for the QM-5 UTM		
	QM - 5	QM-5-EXT
Capacity (kN)	5	5
Measuring accuracy (%)	±0.5	±0.5
Test force resolution	1/20000	1/20000
Total cross-head movement (mm)	400	400
Speed range (mm/min)	0.1 - 1000	0.1 -1000
Stroke resolution (mm)	0.0001	0.0001
Motor type	Servo Motor	Servo Motor

Figure 5.30: Qualitest UTM QM series specs. Adopted from [123]

MODEL	7602	7603
Load Capacity (kN)	2.5	5
Total cross-head movement (mm)	1,372	1,041
Speed range (mm/min)	0.1 - 1000	0.1 -1000
Stroke resolution (µm)	0.107	0.107
Motor type	Servo Motor	Servo Motor

Figure 5.31: ADMET eXpert 7600 UTM series specs. Adopted from [126]

For the machine specs on Figure 5.30 and Figure 5.31, we may say that the device can apply a force up to 5 kN with a resolutions $\leq$ 1 µm. In this perspective, the devices excel the test requirements. As a matter of fact, they deliberately omitted the most important parameter, the accuracy. This is due to the fact that the typical value ranges from ±3 µm to ±5 µm [127, 128]. Figure 5.32 shows the displacement sensor from the company FAGOR. Despite the manufacturer claims of resolutions as low as 0.01 µm, the accuracy remains between the typical interval range. Also, the value increases as the measured distance exceed one meter. To that respect, other UTM manufactures resolve to state values near the standard for displacement verification or ASTM E2309-16 [129]. Figure 5.33 shows a different way to describe the linear displacement, in this case the device has ±10 µm of minimal uncertain. Also, we could not find the displacement resolution for this product. We found surprisingly that in the Instron catalogs, one of the biggest companies in the field, the device displacement resolution and accuracy are not presented.

Alejandre *et al.* 2006 [130] studied the FAGOR SV device on Figure 5.32 and found that when the temperature increases from 20 °C to 55 °C the error increases 14 µm. In the same way, Lopez *et*

al. 2011 [131] showed that the accuracy of an optical encoder can change from ±5µm to ±10 µm due to mounting conditions and machine vibrations.

SVX	SVY	SVW	SVZ	SVP
Measurement	By means of a 20 µm-pitch graduated glass			
Glass thermal expansion coefficient	αtherm: 8 ppm/K aprox.			
Measuring resolution	1 µm	0,5 µm	0,1 µm	0,05 µm
Output signals	TTL differential	TTL differential	TTL differential	TTL differential
Incremental signal period	4 µm	2 µm	0,4 µm	0,2 µm
Limit frequency	500 KHz	1 MHz	1,5 MHz	500 KHz
Maximum speed	120 m/min	120 m/min	36 m/min	6 m/min (*)
Minimum distance between flanks	0,5 microseconds	0,25 microseconds	0,1 microseconds	0,3 microseconds
Accuracy	± 5 µm/m ± 3 µm/m	± 5 µm/m ± 3 µm/m	± 5 µm/m ± 3 µm/m	± 5 µm/m ± 3 µm/m
Operating temperature	0 ºC ... 50 ºC			
Storage temperature	-20 ºC ... 70 ºC			

Figure 5.32: Linear optical encoder series SV [128]

Test Frame Type and Name	Table-top Test Frame		
	AG-X Plus High-Speed	AG-X Plus Short-Column	AG-X Plus 10 kN
Test Frame Load Capacity	Max. 5 kN (1,100 lbs)	Max. 10 kN (2,200 lbs)	Max. 10 kN (2,200 lbs)
Crosshead Speed Range	0.001 to 3000 mm/min (0.00004 to 118 in/min)	0.005 to 1500 mm/min (0.00002 to 59 in/min)	0.005 to 1500 mm/min (0.00002 to 59 in/min)
Crosshead Speed Accuracy	Within ±0.1% of test speed		
Crosshead Positional Accuracy	±0.1% of indicated value or ±0.01mm, whichever is larger		
Effective Width	420 mm (16.5 in)		
Crosshead-Travel for Standard Height Models	Max. 1150 mm (45 in)	Max. 700 mm (28 in)	Max. 1150 mm (45 in)
Frame Rigidity	Min. 42 kN/mm (371 lbs/in)		

Figure 5.33: Shimadzu AG-X Plus Series UTM [132]

Figure 5.34 shows the ASTM E2309-16 device classification [129]. Class A minimal fixed error is 13 µm. This value is consistent with the values founded in the cited publications. In this perspective and using the manufacturer accuracy of ±3 with the mechatronic characterization device test displacement requirement of ±10 µm on Table 4.2, the uncertain in the measure is 30%. On the

other hand, if the test is made with a compliant a Class A device, the error in the measure is 130%, values not admissible for characterization scientific laboratory equipment.

| Classification | Resolution not to Exceed the Greater of: | |
	Fixed Error, mm [in.]	% of Reading
Class A	0.013 [0.0005]	±0.25
Class B	0.038 [0.0015]	±0.5
Class C	0.064 [0.0025]	±1.0
Class D	0.13 [0.005]	±1.5

Figure 5.34: Classification of displacement measuring systems [129]

Consequently, high-end machines have the dynamic force capabilities and linear displacement resolution. But they cannot meet the accuracy required for the characterization of composite materials.

In addition to the linear actuator non-linearity behavior, the sensor accuracy and the computing power, another factor that contributes to the displacement uncertainty is the machine stiffness. Figure 5.35 shows the simplified sketch of the implemented finite element structural analysis made in ABACUS. The purpose of this study is to observe the deflection of the simplified components to the required 2.5 kN force (Table 4.2). Also, the components are made of steel 304 under constant temperature and the only variable parameters are the piston rod length and the base reinforce thickness. Figure 5.36 presents the extreme case were the base is thin and flexible. In that case the piston imposes a deflection of 1 mm. On the other hand, when the base is reinforced with a thicker plate the piston compresses from the top (Figure 5.37). Table 5.4 shows the simulations results for a combination of base reinforcements and piston rod lengths. In the hypothetical case that the mechatronic machine deflection is not properly characterized or neglected, a 10.15 µm of error are added to the measured when the system is at maximum load.
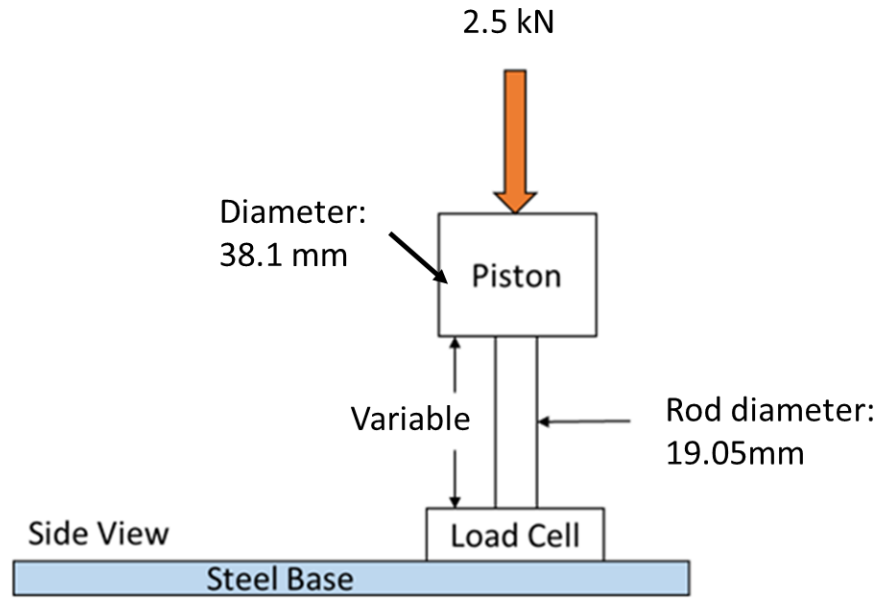
Figure 5.35: Simulation sketch of the base, load cell and piston assembly
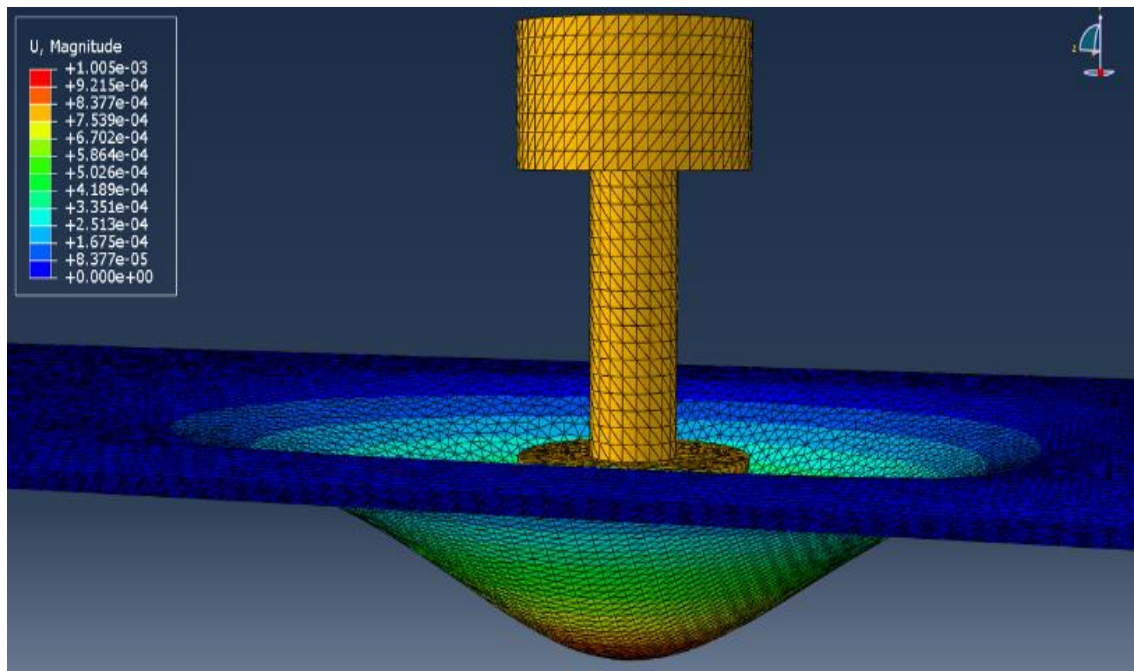
Figure 5.36: Machine base without reinforcement support
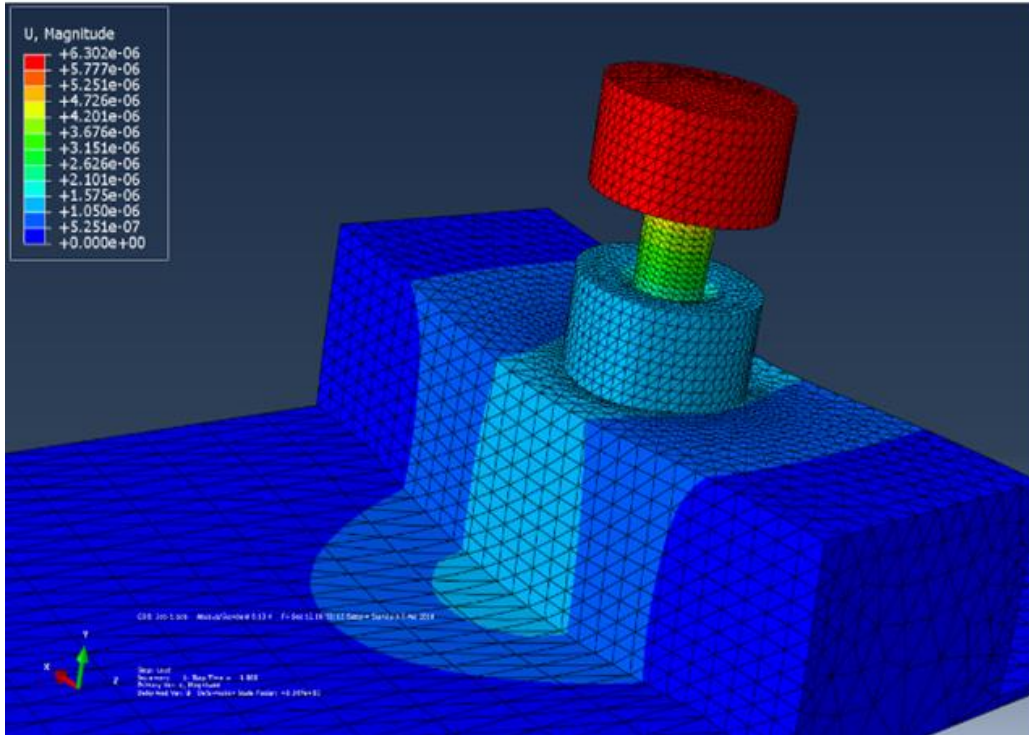
Figure 5.37: Machine with a 50.8 mm base reinforcement

Table 5.4: Structural analysis, piston and base deflection

Reinforcement Thickness (mm)	Piston rod Longitude (mm)	Base Deflection (µm)	Piston Compression (µm)	Deflection total (µm)
25.4	50.8	4.89	3.7	8.59
25.4	76.2	5.7	4.45	10.15
50.8	50.8	1.57	4.73	6.3
50.8	76.2	0.66	6.3	6.96

Until the uncertainty in the measure is not reduced to achieved ±0.25 % of the error in a displacement measured of ±10 µm, the characterization of composite materials will continue to be elusive. In connection with this PhD project we can be sure that the proposed mechatronic characterization device in the Figure 5.15 is in the right path. In other words, by separating the sample thickness selection (long displacement), from the test displacement (high accuracy), the device could reach the characterization test measuring conditions.

5.3 Discussion

Universal test machines are driven by ball screw actuators. Despite the servo drive state of the art capabilities, the uncertainty in the measurement of the optical linear encoders implemented in these devices induces an error between 30 to 130% when measuring ±10 µm. The increase of the temperature, the mechanical play, the components stiffness, the amount of load and the machine vibrations are among others the factors that increase the overall error and the machine uncertainty. To be able to characterize the PMCMs is required to improve the device accuracy. This is done with capacitive, laser, Eddy current, microminiature linear displacement transducers with small maximum measurement displacement (e.g. 0.5mm) and excellent resolution (≤0.025 µm). But the sensor accuracy is not the only factor to improve, it is also required to control the non-linear behavior of the motor, produce a well designed robust structure and develop high-quality electronics to improve the signal to error ratio. To this purpose, the proposed piezo-stack actuator could provide the dynamic mechanical movement using its linear behavior in a µm range of displacement. In the same way, by separating the measurement of the long displacement movement to open and close the mold from the precise test displacement, the characterization may reach acceptable conditions. But it will require of several design iterations to solve all the described situations. To answer the research question, we make the following statement:

To the best of our knowledge, to date, is still not possible to make a linear actuator with a force in the range of thousands of Newtons with a displacement in the range of mm and an accuracy ≤0.025 µm.

In a test with ±10 µm of strain that accuracy represents ±0.25% of error in the measure. Uncertain measurement required for E2309/E2309M verification compliance [129].

5.4 Conclusion

In order to identify the most critical machine components for design embodiment and reach the third objective (OB3). We followed the results presented in Chapter 4. In particular, the QFD presented in section 4.3.2. The weight matrix showed us that the most important design aspects for the mechatronic characterization device are the linear actuator, the computer processing power and the linear displacement resolution. We cover in detail these design specifications and conclude that the linear force and the linear displacement accuracy are the most critical components of the device,

without reaching these characteristics, any investment in other machine components will be futile. With that in mind, the third objective of identifying the most critical machine components was successfully achieved. In a broader context, we also identified that in order to reach the main research PhD objective of integrating multiple characterization laboratory equipment into a single device a new invention is required. Specifically, an actuator with a force capable of providing a force in the thousands of Newtons and a linear displacement accuracy ≤ 0.025 µm in a range of displacement of mm. This invention will provide the means to redefine the characterization of polymer matrix composite materials.

CHAPTER 6   CONCLUSION AND RECOMMENDATIONS

The characterization of PMCM relies on multiple characterization devices on which the variation on sample size from one device to the other induces uncertainty in the measurements. Moreover, the characterization of thick PMCM requires the sample to be representative of the internal structure of the composite structure, which in terms of sample size is too big for the current characterization laboratory equipment. The main objective of this PhD project was to integrate multiple characterization laboratory equipment into a single device for PMCMs. To reach this objective this thesis divided this task into three specific objectives.

The first objective identified the actual laboratory equipment limitations and the attempts made for researchers to obtain multiple PMCMs properties using a single experiment. The devices reviewed in the literature were properly classified in terms of their challenges and limitations. Then, to support the findings in the reviewed literature, laboratory experiments were performed to identify the manufacturing challenges. Following a through analysis, we identified the process challenges from the experiences using laboratory equipment, among others, the more important are prevent the resin to gel during the injection, clamp the injection tubes and mould ports, maintain an uniform temperature through the device, prevent resin leaks and unmold the part. These findings allowed us to formulate the mechatronics device requirements and properties. In connection with this first specific objective (OB1) we state that our first contribution is related to the characterization of PMCMs, we described in detail the properties development during a cure cycle and the typical laboratory equipment to measure them. In this respect, this work serves as a guideline on how to characterize the PMCM using typical laboratory equipment. Also, by finding the device limitations and manufacturing challenges, anybody interested in the manufacturing of this materials will know beforehand the problems and limitations of this type of process. Furthermore, if researchers decide to improve any of the reviewed devices, they could focus on the challenges summarized in the Table 2.1.

Our main contribution relates the second objective (OB2), we contribute with an integrated mechatronic design methodology that solves typical communication problems during the development of mechatronic devices. The V-shaped strategy describes the design steps, then the "wishes and demands" forms organize the project requirements on which the design team must concentrate its efforts. We found in the QFD a powerful design strategy that allowed us to identify

the critical part of the product. Moreover, the team realises where to put all the effort and energy. Finally, the functional diagram and product architecture allow us to define in detail the product capabilities and the device function tasks. We understand that there is no perfect design methodology, but any team that follows the proposed integrated methodology at early stages of the design task will increase chance of developing an integrated solution, as proactive design methodologies improve the final product. Also, upon implementation the production cost and engineering time will be greatly reduced. As the project grows, design strategies like the one proposed by Mohebbi *et al.* 2018 [12, 104] will speed up the design integration loops. Moreover, the forms, matrix and diagrams can be easily upgraded to the automated decision-making platform.

Finally, during the design embodiment we successfully identified the most critical machine component (OB3). At this stage all the information and experience gathered during this PhD converged to solve the next question:

What is preventing researchers to use high-end commercial equipment that will allow the characterization of composite materials in a single experiment?

The answer to that question is our third an final contribution. We required the information gathered during the first objective (OB1) to see the attempts made by researchers to solve it. As we observed that the identified team's efforts faded in 2015 and others simply change of strategy, we began to ask ourselves if the gap was related to lack of knowledge, budget or technology. The characterization of composite materials has been studied for decades which lead us to budget considerations. In this respect, we notice big companies such as TA Instrument and Boeing behind the reviewed works. In those cases, the budget was not a problem because they presented state of the art equipment in their publications. That leaves us with the technology subject. Upon implementation of the integrated methodology (OB2) we uncovered that the most significant aspect for the integration of multiple characterization devices into a single experiment was related to the device linear force and linear displacement resolution. To this respect, we put all our efforts into those two challenges during the design embodiment (OB3). As a result, we found out that the mechatronic device requires a high accuracy ≤ 0.025 µm to obtain $\pm 0.25\%$ of error in the measure. Otherwise, the measurements will be no-conforming with the E2309/E2309M verification standard [129]**.** In the case that the described actuator appears we recommend improving the linear ball screw actuator. Reduce the sources of non-linearities. At that point the amount of computer power

required will be greatly increased. To avoid spending years in software development, we recommend the implementation of a real time operating system (RTOS) and support the data acquisition with existing commercial devices. In the case contrary that the design team consider lower the system restrictions, we recommend begin by optimizing the sample size to reduce at maximum the applied force, them by updating the QFD in Figure 4.5 analyse the implications of that change. To put it differently, as the force increases, so does the machine error. This is because the structure, the actuator, the load cells and the ball screws deflect. Also, the error comes from the gears friction, damping and the backlash. Additionally, the effect of the temperature in the components will require a detailed analysis. During the presented design loops, we have not considered their effects. Finally, a laser interferometer will provide the means to successfully characterize the mechatronic device accuracy once prototyped. Reaching the grade of accuracy and force required for this characterization machine will be a breakthrough in the characterization of PMCMs.

6.1 Recommendations for future studies

We highly recommend continuing further with the design methodology and perform a new system integration with the results of this PhD project. Also, the future teams using this PhD work must update the requirements and system design tables and diagrams with the outcome of the that system integration. Maintaining good traceability of the project changes is crucial for the sanity of the project.

Future researchers must also focus their efforts on the development of the piezo stack proposed in section 5.2.2. That is in the case that the sample size and force requirements remain constant. Developing other system parts will be a waste of resources.

Finally, we do not intent to discourage the continuity of this research. On the contrary, acknowledging the system limitations will produce better products and the proposed methodology allows that flexibility. Figure 6.1 shows a possible product family for the characterization of PMCMs. We use the functional model and product architecture made in the section 4.5 to design it. In this scenario, less complex products will be developed. As modules are completed, they can be integrated in a superior product with better capabilities and maybe some day, the single mechatronic characterization device will see the light.
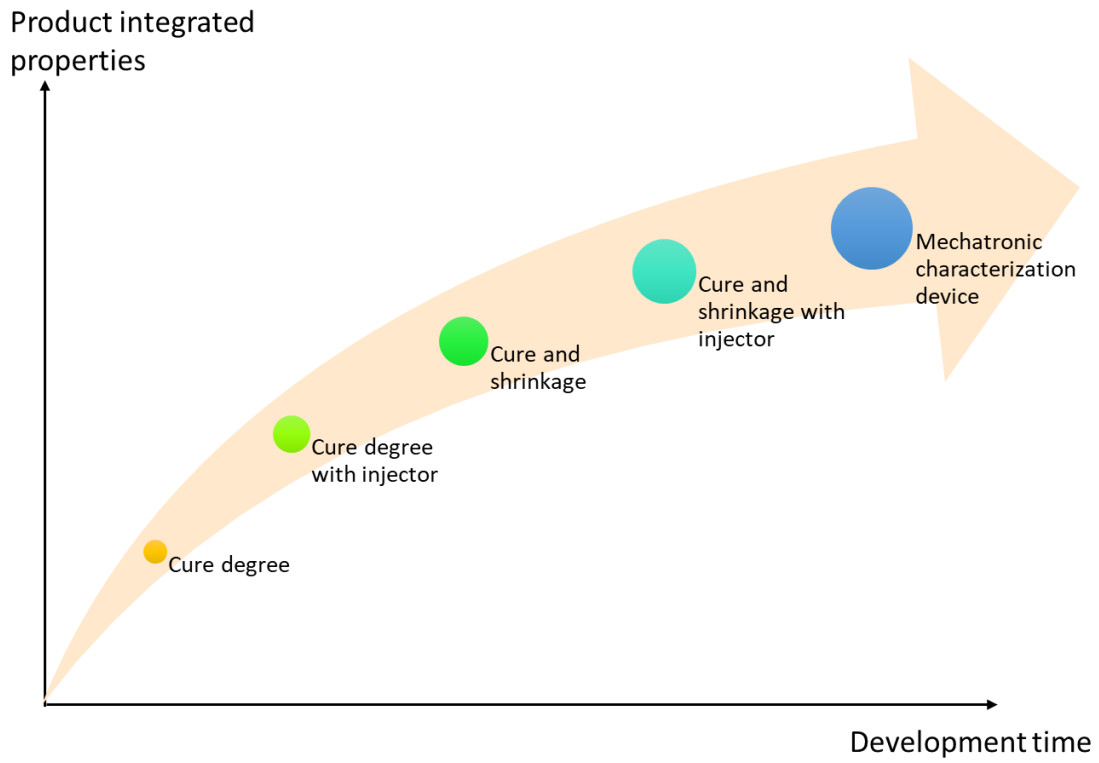
Figure 6.1: PMCMs characterization product family

BIBLIOGRAPHY

[1]   J. Mørkeberg Torry-Smith, A. Qamar, S. Achiche, J. Wikander, N. Henrik Mortensen, and C. During, "Challenges in Designing Mechatronic Systems," *Journal of Mechanical Design,* vol. 135, no. 1, pp. 011005-011005, 2012.

[2]   J. M. r. Torry-Smith, S. Achiche, N. H. Mortensen, A. Qamar, J. Wikander, and C. During, "Mechatronic Design - Still a Considerable Challenge," no. 54860, pp. 33-44, 2011.

[3]   J. M. Torry-Smith, N. H. Mortensen, and S. Achiche, "A proposal for a classification of product-related dependencies in development of mechatronic products," *Research in Engineering Design,* journal article vol. 25, no. 1, pp. 53-74, January 01 2014.

[4]   J. M. Torry-Smith, "Designing mechatronic products. Achieving integration by means of modelling dependencies," Dissertation, Technical University of Denmark, Copenhagen, 2013.

[5]   A. Mohebbi, L. Baron, S. Achiche, and L. Birglen, "Trends in concurrent, multi-criteria and optimal design of mechatronic systems: A review," in *Proceedings of the 2014 International Conference on Innovative Design and Manufacturing (ICIDM)*, 2014, pp. 88-93.

[6]   D. Malmquist, "A tool for holistic optimization of mechatronic design concepts," KTH Royal Institute of Technology, 2015.

[7]   R. B. Stone, K. L. Wood, and R. H. Crawford, "A heuristic method for identifying modules for product architectures," *Design Studies,* vol. 21, no. 1, pp. 5-31, 1// 2000.

[8]   B. Henriksen and C. Røstad, "Attacking the Critical Parts in Product Development," in *Advances in Production Management Systems. Sustainable Production and Service Supply Chains*, vol. 414, V. Prabhu, M. Taisch, and D. Kiritsis, Eds. (IFIP Advances in Information and Communication Technology: Springer Berlin Heidelberg, 2013, pp. 94-102.

[9]   J. B. Dahmus, J. P. Gonzalez-Zugasti, and K. N. Otto, "Modular product architecture," *Design Studies,* vol. 22, no. 5, pp. 409-424, 9// 2001.

[10]   K. Hölttä, E. S. Suh, and O. de Weck, "Tradeoff between modularity and performance for engineered systems and products," 2005.

[11] D. E. Whitney, "Physical limits to modularity," 2002.

[12] A. Mohebbi, S. Achiche, and L. Baron, "Mechatronic Multicriteria Profile (MMP) for Conceptual Design of a Robotic Visual Servoing System," no. 45851, p. V003T15A015, 2014.

[13] I. M. L. Ferreira and P. J. S. Gil, "Application and performance analysis of neural networks for decision support in conceptual design," *Expert Systems with Applications,* vol. 39, no. 9, pp. 7701-7708, 2012/07/01/ 2012.

[14] Z. Erden, A. Erden, and A. M. Erkmen, "A Petri net approach to behavioural simulation of design artefacts with application to mechatronic design," *Research in Engineering Design,* journal article vol. 14, no. 1, pp. 34-46, February 01 2003.

[15] J. Gausemeier and S. Moehringer, "New Guideline Vdi 2206-a Flexible Procedure Model for the Design of Mechatronic Systems," in *DS 31: Proceedings of ICED 03, the 14th International Conference on Engineering Design, Stockholm*, 2003.

[16] Boeing. (2018). *Boeing 787 dreamliner*. Available: http://www.boeing.com/commercial/787/

[17] Aiebus. (2017). *Composites: Airbus continues to shape the future*. Available: https://www.airbus.com/newsroom/news/en/2017/08/composites--airbus-continues-to-shape-the-future.html

[18] British_Airways. (2018). *Boeing 787-8*. Available: https://www.britishairways.com/en-ca/information/about-ba/fleet-facts/boeing787-8

[19] D. Gates. (2007). *Boeing finds 787 pieces aren't quite a perfect fit*. Available: http://seattletimes.com/html/businesstechnology/2003744076_787gaps12.html

[20] D. Gates. (2010). *Boeing calls two-week stop to 787 section deliveries to Everett*. Available: http://seattletimes.com/html/businesstechnology/2013256677_boeing26.html

[21] C. C. Sun, "Materials Science Tetrahedron—A Useful Tool for Pharmaceutical Research and Development," *Journal of Pharmaceutical Sciences,* vol. 98, no. 5, pp. 1671-1687, 2009/05/01/ 2009.

[22]   P. Wang *et al.*, "Practical aspects of structural and dynamic DNA nanotechnology," *MRS Bulletin,* vol. 42, no. 12, pp. 889-896, 2017.

[23]   W. D. Callister and D. G. Rethwisch, *Materials science and engineering: An Introduction*, 9E ed. John Wiley & Sons NY, 2014.

[24]   K. K. Chawla and M. Meyers, *Mechanical behavior of materials*. Prentice Hall Upper Saddle River, 1999.

[25]   M. Hartmann, M. Strebinger, and R. Hinterholzl, "An approach towards a basic material characterization for the simulation of process induced deformation," in *The 19 TH International Conference On Composite Materials*, Montreal, 2013.

[26]   P. P. Parlevliet, H. E. N. Bersee, and A. Beukers, "Residual stresses in thermoplastic composites—A study of the literature—Part II: Experimental techniques," *Composites Part A: Applied Science and Manufacturing,* vol. 38, no. 3, pp. 651-665, 3// 2007.

[27]   D. U. Shah and P. J. Schubel, "Evaluation of cure shrinkage measurement techniques for thermosetting resins," *Polymer Testing,* vol. 29, no. 6, pp. 629-639, 9// 2010.

[28]   Y. Nawab, S. Shahid, N. Boyard, and F. Jacquemin, "Chemical shrinkage characterization techniques for thermoset resins and associated composites," *Journal of Materials Science,* vol. 48, no. 16, pp. 5387-5409, 2013.

[29]   Y. Abou Msallem, F. Jacquemin, N. Boyard, A. Poitou, D. Delaunay, and S. Chatel, "Material characterization and residual stresses simulation during the manufacturing process of epoxy matrix composites," *Composites Part A: Applied Science and Manufacturing,* vol. 41, no. 1, pp. 108-115, 1// 2010.

[30]   L. Khoun, T. Centea, and P. Hubert, "Characterization Methodology of Thermoset Resins for the Processing of Composite Materials — Case Study: CYCOM 890RTM Epoxy Resin," *Journal of Composite Materials,* vol. 44, no. 11, pp. 1397-1415, June 1 2010.

[31]   P. J. Halley and M. E. Mackay, "Chemorheology of thermosets—an overview," *Polymer Engineering & Science,* vol. 36, no. 5, pp. 593-609, 1996.

[32] E. Ruiz and F. Trochu, "Thermomechanical properties during cure of glass-polyester RTM composites: elastic and viscoelastic modeling," *Journal of composite materials,* vol. 39, no. 10, pp. 881-916, 2005.

[33] N. Boyard, M. Vayer, C. Sinturel, R. Erre, and D. Delaunay, "Analysis and modeling of PVTX diagram of an unsaturated polyester resin, thermoplastic additive, and mineral fillers blend," *Journal of Applied Polymer Science,* vol. 88, no. 5, pp. 1258-1267, 2003.

[34] Y. Nawab, N. Boyard, V. Sobotka, P. Casari, and F. Jacquemin, "A device to measure the shrinkage and heat transfers during the curing cycle of thermoset composites," *Advanced Materials Research,* vol. 326, pp. 19-28, 2011.

[35] Y. Nawab, P. Casari, N. Boyard, and F. Jacquemin, "Characterization of the cure shrinkage, reaction kinetics, bulk modulus and thermal conductivity of thermoset resin from a single experiment," (in English), *Journal of Materials Science,* vol. 48, no. 6, pp. 2394-2403, 2013/03/01 2013.

[36] C. Billotte, F. M. Bernard, and E. Ruiz, "Chemical shrinkage and thermomechanical matched die characterization of an epoxy resin during cure by a novel in situ measurement method," *European Polymer Journal,* no. 0, 2013.

[37] M. Péron *et al.*, "PvT-HADDOC: A multi-axial strain analyzer and cure monitoring device for thermoset composites characterization during manufacturing," *Composites Part A: Applied Science and Manufacturing,* vol. 101, pp. 129-142, 2017.

[38] E. Ruiz, V. Achim, S. Soukane, F. Trochu, and J. Bréard, "Optimization of injection flow rate to minimize micro/macro-voids formation in resin transfer molded composites," *Composites Science and Technology,* vol. 66, no. 3–4, pp. 475-486, 3// 2006.

[39] L. Liu, B.-M. Zhang, D.-F. Wang, and Z.-J. Wu, "Effects of cure cycles on void content and mechanical properties of composite laminates," *Composite Structures,* vol. 73, no. 3, pp. 303-309, 6// 2006.

[40] P. Olivier, J. P. Cottu, and B. Ferret, "Effects of cure cycle pressure and voids on some mechanical properties of carbon/epoxy laminates," *Composites,* vol. 26, no. 7, pp. 509-515, 7// 1995.

[41] F. C. Campbell Jr, *Manufacturing processes for advanced composites*. Elsevier Science, 2003.

[42] H. Darcy, *Les fontaines publiques de la ville de Dijon: exposition et application*. Victor Dalmont, 1856.

[43] R. Etemadi, K. M. Pillai, P. K. Rohatgi, and S. A. Hamidi, "On Porosity Formation in Metal Matrix Composites Made with Dual-Scale Fiber Reinforcements Using Pressure Infiltration Process," *Metallurgical and Materials Transactions A,* journal article vol. 46, no. 5, pp. 2119-2133, May 01 2015.

[44] S. V. Hoa, *Principles of the manufacturing of composite materials*. DEStech Publications, Inc, 2009.

[45] *ASTM, D6289 − 13, Standard Test Method for Measuring Shrinkage from Mold Dimensions of Molded Thermosetting Plastics*, 2013.

[46] T. Garstka, N. Ersoy, K. D. Potter, and M. R. Wisnom, "In situ measurements of through-the-thickness strains during processing of AS4/8552 composite," *Composites Part A: Applied Science and Manufacturing,* vol. 38, no. 12, pp. 2517-2526, 12// 2007.

[47] E. Ruiz and F. Trochu, "Multi-criteria thermal optimization in liquid composite molding to reduce processing stresses and cycle time," *Composites Part A: Applied Science and Manufacturing,* vol. 37, no. 6, pp. 913-924, 6// 2006.

[48] A. C. Loos and G. S. Springer, "Curing of Epoxy Matrix Composites," *Journal of Composite Materials,* vol. 17, no. 2, pp. 135-169, March 1, 1983 1983.

[49] T. A. Bogetti and J. W. Gillespie Jr, "Process-induced stress and deformation in thick-section thermoset composite laminates," DTIC Document1990.

[50] A. A. Johnston, "An integrated model of the development of process-induced deformation in autoclave processing of composite structures," NQ27172 Ph.D., The University of British Columbia (Canada), Ann Arbor, 1998.

[51] G. G. Odian, *Principles of polymerization*. John Wiley & Sons, 2007.

[52] J. L. Kardos, M. P. Duduković, and R. Dave, "Void growth and resin transport during processing of thermosetting — Matrix composites," in *Epoxy Resins and Composites IV,*

vol. 80, K. Dušek, Ed. (Advances in Polymer Science: Springer Berlin Heidelberg, 1986, pp. 101-123.

[53]   R. S. Pierce, B. G. Falzon, and M. C. Thompson, "Permeability characterization of sheared carbon fiber textile preform," *Polymer Composites,* vol. 39, no. 7, pp. 2287-2298, 2018.

[54]   N. Vernet *et al.*, "Experimental determination of the permeability of engineering textiles: Benchmark II," *Composites Part A: Applied Science and Manufacturing,* vol. 61, pp. 172-184, 2014/06/01/ 2014.

[55]   J. M. Lawrence, J. Barr, R. Karmakar, and S. G. Advani, "Characterization of preform permeability in the presence of race tracking," *Composites Part A: Applied Science and Manufacturing,* vol. 35, no. 12, pp. 1393-1405, 12// 2004.

[56]   V. Antonucci, M. Giordano, A. Cusano, J. Nasser, and L. Nicolais, "Real time monitoring of cure and gelification of a thermoset matrix," *Composites Science and Technology,* vol. 66, no. 16, pp. 3273-3280, 12/18/ 2006.

[57]   A. M. T. Kosaka, T. Kajikawa, M. Koike, K. Kusukawa "Process monitoring of FRP laminates by embedded fiber optic sensors," in *The 19 TH International Conference On Composite Materials*, Montreal, 2013.

[58]   G. L. C. Sonnenfeld, F. Collombet, Y-H. Grunevald, B. Douchin, L. Crouzeix, M. Torres, T. Geernaert, S. Sulejmani, K. Chah, P. Mergo, H. Thienpont, F. Berghmans, "Cure cycle monitoring of laminated carbon fiber-reinforced plastic with Fiber Bragg Gratings in microstructured optical fiber," in *The 19 TH International Conference On Composite Materials*, Montreal, 2013.

[59]   M. Yeager, M. Todd, W. Gregory, and C. Key, "Assessment of embedded fiber Bragg gratings for structural health monitoring of composites," *Structural Health Monitoring,* vol. 16, no. 3, pp. 262-275, 2017.

[60]   *ASTM, D3171, Methods for Constituent Content of Composite Materials*, 2013.

[61]   Y. O. Kas and C. Kaynak, "Ultrasonic (C-scan) and microscopic evaluation of resin transfer molded epoxy composite plates," *Polymer Testing,* vol. 24, no. 1, pp. 114-120, 2// 2005.

[62] S. G. Advani and E. M. Sozer, *Process modeling in composites manufacturing*. CRC Press, 2002.

[63] S. Minakuchi, "Direct Measurement off Out-of-Plane and In-Plane Cure Shrinkage Strain in Composites by Embedded Fiber-Optic Sensors," in *The 19 TH International Conference On Composite Materials*, Montreal, 2013.

[64] D. Karalekas, J. Cugnoni, and J. Botsis, "Monitoring of process induced strains in a single fibre composite using FBG sensor: A methodological study," *Composites Part A: Applied Science and Manufacturing,* vol. 39, no. 7, pp. 1118-1127, 7// 2008.

[65] M. Giordano, A. Laudati, J. Nasser, L. Nicolais, A. Cusano, and A. Cutolo, "Monitoring by a single fiber Bragg grating of the process induced chemo-physical transformations of a model thermoset," *Sensors and Actuators A: Physical,* vol. 113, no. 2, pp. 166-173, 7/5/ 2004.

[66] A. Yousefi, P. G. Lafleur, and R. Gauvin, "Kinetic studies of thermoset cure reactions: A review," *Polymer Composites,* vol. 18, no. 2, pp. 157-168, 1997.

[67] P. Mallick, *Fiber-reinforced composites: materials, manufacturing, and design*. CRC press, 1993.

[68] J. D. Menczel and R. B. Prime, *Thermal analysis of polymers, fundamentals and applications*. Wiley. com, 2009.

[69] *ASTM, E1640 − 13, Standard Test Method for Assignment of the Glass Transition Temperature By Dynamic Mechanical Analysis*, 2013.

[70] G. Li, P. Lee-Sullivan, and R. Thring, "Determination of activation energy for glass transition of an epoxy adhesive using dynamic mechanical analysis," *Journal of thermal analysis and calorimetry,* vol. 60, no. 2, pp. 377-390, 2000.

[71] V. M. Karbhari and Q. Wang, "Multi-frequency dynamic mechanical thermal analysis of moisture uptake in E-glass/vinylester composites," *Composites Part B: Engineering,* vol. 35, no. 4, pp. 299-304, // 2004.

[72]   R. P. Chartoff, P. T. Weissman, and A. Sircar, "The Application of Dynamic Mechanical Methods to T~ g Determination in Polymers: An Overview," *ASTM SPECIAL TECHNICAL PUBLICATION,* vol. 1249, pp. 88-88, 1994.

[73]   M. Ivankovic, L. Incarnato, J. M. Kenny, and L. Nicolais, "Curing kinetics and chemorheology of epoxy/anhydride system," *Journal of Applied Polymer Science,* vol. 90, no. 11, pp. 3012-3019, 2003.

[74]   J. A. Ramos, N. Pagani, C. C. Riccardi, J. Borrajo, S. N. Goyanes, and I. Mondragon, "Cure kinetics and shrinkage model for epoxy-amine systems," *Polymer,* vol. 46, no. 10, pp. 3323-3328, 4/25/ 2005.

[75]   K. C. Cole, J. J. Hechler, and D. Noel, "A new approach to modeling the cure kinetics of epoxy/amine thermosetting resins. 2. Application to a typical system based on bis[4-(diglycidylamino)phenyl]methane and bis(4-aminophenyl) sulfone," *Macromolecules,* vol. 24, no. 11, pp. 3098-3110, 1991/05/01 1991.

[76]   *ASTM, D4473 - 08, Standard Test Method for Plastics: Dynamic Mechanical Properties: Cure Behavior*, 2008.

[77]   J. B. Enns and J. K. Gillham, "Time–temperature–transformation (TTT) cure diagram: Modeling the cure behavior of thermosets," *Journal of Applied Polymer Science,* vol. 28, no. 8, pp. 2567-2591, 1983.

[78]   J. Castro and C. Macosko, "Studies of mold filling and curing in the reaction injection molding process," *AIChE Journal,* vol. 28, no. 2, pp. 250-260, 1982.

[79]   P. Hubert, "Aspects of flow and compaction of laminated composite shapes during cure," University of British Columbia, 1996.

[80]   M. Haider, P. Hubert, and L. Lessard, "Cure shrinkage characterization and modeling of a polyester resin containing low profile additives," *Composites Part A: Applied Science and Manufacturing,* vol. 38, no. 3, pp. 994-1009, 3// 2007.

[81]   L. Khoun and P. Hubert, "Cure shrinkage characterization of an epoxy resin system by two in situ measurement methods," *Polymer Composites,* vol. 31, no. 9, pp. 1603-1610, 2010.

[82]   K. F. Schoch Jr, P. A. Panackal, and P. P. Frank, "Real-time measurement of resin shrinkage during cure," *Thermochimica Acta,* vol. 417, no. 1, pp. 115-118, 7/9/ 2004.

[83]   N. Boyard, M. Vayer, C. Sinturel, R. Erre, and D. Delaunay, "Modeling PVTX diagrams: Application to various blends based on unsaturated polyester—Influence of thermoplastic additive, fillers, and reinforcements," *Journal of Applied Polymer Science,* vol. 92, no. 5, pp. 2976-2988, 2004.

[84]   Y. K. Kim and I. M. Daniel, "Cure Cycle Effect on Composite Structures Manufactured by Resin Transfer Molding," *Journal of Composite Materials,* vol. 36, no. 14, pp. 1725-1743, July 1, 2002 2002.

[85]   C. Billotte, F. M. Bernard, E. Ruiz, F. Cara, and H. Baurier, "Chemical shrinkage and thermomechanical characterization of an epoxy resin during cure by a novel in situ measurement method," in *2nd Joint US-Canada Conference on Composites - American Society for Composites, 26th Annual Technical Conference: Canadian Association for Composite Structures and Materials, September 26, 2011 - September 28, 2011*, Montreal, QC, Canada, 2011: DEStech Publications Inc.

[86]   C. Billote and E. Ruiz, "Thermo flux Project description meetings," A. Ramirez, Ed., ed, 2013.

[87]   G. Van Assche, H. Miltner, C. Block, B. Van Mele, V. Janssens, and P. Van Puyvelde, "Rheo-DSC: a hybrid technique for simultaneous rheological and calorimetric measurements," in *Proceedings of the 35th Annual Conference of the North American Thermal Analysis Society*, 2007, pp. 2 pages on CD-ROM.

[88]   S. Kiewiet, V. Janssens, H. E. Miltner, G. Van Assche, P. Van Puyvelde, and B. Van Mele, "RheoDSC: A hyphenated technique for the simultaneous measurement of calorimetric and rheological evolutions," *Review of Scientific Instruments,* vol. 79, no. 2, pp. -, 2008.

[89]   V. Janssens, C. Block, G. Assche, B. Mele, and P. Puyvelde, "RheoDSC: design and validation of a new hybrid measurement technique," (in English), *Journal of Thermal Analysis and Calorimetry,* vol. 98, no. 3, pp. 675-681, 2009/12/01 2009.

[90]   C. Block, A. K. Ghosh, B. Van Mele, and G. Van Assche, "RheoDSC: Design optimisation by heat transfer modelling," *Thermochimica Acta,* vol. 547, no. 0, pp. 130-140, 11/10/ 2012.

[91] C. Block, B. Van Mele, P. Van Puyvelde, and G. Van Assche, "Time–temperature-transformation (TTT) and temperature–conversion-transformation (TxT) cure diagrams by RheoDSC: Combined rheometry and calorimetry on an epoxy-amine thermoset," *Reactive and Functional Polymers,* vol. 73, no. 2, pp. 332-339, 2// 2013.

[92] NETZSCH. (2014). *Dielectric Cure Monitoring*. Available: http://www.netzsch-thermal-analysis.com/us/home/

[93] A. Chaloupka, T. Pflock, R. Horny, N. Rudolph, and S. R. Horn, "Dielectric and rheological study of the molecular dynamics during the cure of an epoxy resin," *Journal of Polymer Science Part B: Polymer Physics,* vol. 56, no. 12, pp. 907-913, 2018.

[94] F. Lionetto and A. Maffezzoli, "Monitoring the Cure State of Thermosetting Resins by Ultrasound," *Materials,* vol. 6, no. 9, pp. 3783-3804, 2013.

[95] F. Lionetto and A. Maffezzoli, "Polymer characterization by ultrasonic wave propagation," *Advances in Polymer Technology,* vol. 27, no. 2, pp. 63-73, 2008.

[96] F. Lionetto, A. Tarzia, M. Coluccia, and A. Maffezzoli, "Air-Coupled Ultrasonic Cure Monitoring of Unsaturated Polyester Resins," *Macromolecular Symposia,* vol. 247, no. 1, pp. 50-58, 2007.

[97] F. Lionetto, R. Rizzo, V. A. M. Luprano, and A. Maffezzoli, "Phase transformations during the cure of unsaturated polyester resins," *Materials Science and Engineering: A,* vol. 370, no. 1–2, pp. 284-287, 4/15/ 2004.

[98] J. McHugh, *Ultrasound technique for the dynamic mechanical analysis (DMA) of polymers*. Bundesanstalt für Materialforschung und-prüfung (BAM), 2008.

[99] S. Goyanes, W. Salgueiro, A. Somoza, J. A. Ramos, and I. Mondragon, "Direct relationships between volume variations at macro and nanoscale in epoxy systems. PALS/PVT measurements," *Polymer,* vol. 45, no. 19, pp. 6691-6697, 2004/09/03/ 2004.

[100] J. Wang, "PVT properties of polymers for injection molding," in *Some Critical Issues for Injection Molding*: InTech, 2012.

[101] D. Walsh and P. Zoller, *Standard pressure volume temperature data for polymers*. CRC Press, 1995.

[102] C. Pupin, A. Ross, C. Dubois, J.-C. Rietsch, N. Vernet, and E. Ruiz, "Formation and suppression of volatile-induced porosities in an RTM epoxy resin," *Composites Part A: Applied Science and Manufacturing,* vol. 94, pp. 146-157, 2017/03/01/ 2017.

[103] DOW_Plastics. (2013). *Epoxy Novolac Resins*. Available: http://msdssearch.dow.com/PublishedLiteratureDOWCOM/dh_0030/0901b8038003042d.pdf?filepath=/296-00279.pdf&fromPage=GetDoc

[104] A. Mohebbi, S. Achiche, and L. Baron, "Multi-criteria fuzzy decision support for conceptual evaluation in design of mechatronic systems: a quadrotor design case study," *Research in Engineering Design,* journal article vol. 29, no. 3, pp. 329-349, July 01 2018.

[105] G. Pahl, W. Beitz, J. Feldhusen, and K. H. Grote, *Engineering design: a systematic approach*. Springer London, 2007.

[106] J. Terninko, *Step-by-step QFD: customer-driven product design*. Crc Press, 1997.

[107] J. Buur, *A theoretical approach to mechatronics design*. Institute for Engineering Design, Technical University of Denmark Denmark, 1990.

[108] L.-K. Chan and M.-L. Wu, "Quality function deployment: A literature review," *European journal of operational research,* vol. 143, no. 3, pp. 463-497, 2002.

[109] L.-K. Chan and M.-L. Wu, "Quality Function Deployment: A Comprehensive Review of Its Concepts and Methods," *Quality Engineering,* vol. 15, no. 1, pp. 23-35, 2002/09/24 2002.

[110] N. K. Naik, M. Sirisha, and A. Inani, "Permeability characterization of polymer matrix composites by RTM/VARTM," *Progress in Aerospace Sciences,* vol. 65, pp. 22-40, 2014/02/01/ 2014.

[111] Air_Academy_Associates. (2018). *Free QFD templates*. Available: http://www.qfdonline.com/templates/

[112] T. Weilkiens, "Systems Engineering with SysML/UML - Modeling, Analysis, Design," ed: Elsevier.

[113] S. Friedenthal, A. Moore, and R. Steiner, *A Practical Guide to SysML : The Systems Modeling Language*. San Francisco, UNITED STATES: Elsevier Science & Technology, 2014.

[114] DMR_Seals. (2018). *Piston seals*. Available: http://www.dmrseals.co.uk/Piston.htm

[115] METRAVIB, "Stage de formation: DMA Rappels sur la Viscoélasticité et la DMA," 2016.

[116] Vibration_Research, "Electrodynamic Shaker VR5800," 2018.

[117] J.-J. Tzen, S.-L. Jeng, and W.-H. Chieng, "Modeling of piezoelectric actuator for compensation and controller design," *Precision Engineering,* vol. 27, no. 1, pp. 70-86, 1// 2003.

[118] K. Tran, H. Phan, H. Lee, Y. Kim, and H. Park, "Blocking force of a piezoelectric stack actuator made of single crystal layers (PMN-29PT)," *Smart Materials and Structures,* vol. 25, no. 9, p. 095038, 2016.

[119] PiezoDrive. (2018). *SA Series 150V Piezo stack actuators*. Available: https://www.piezodrive.com/actuators/150v-piezo-stack-actuators/

[120] Physik_Instruments, "PICA Power Piezo Actuators," P. M. positioning, Ed., ed, 2018.

[121] AZO_Materials. (2018). *Materials Testing - Testing Procedures That can Be Performed Using a Universal Testing Machine*. Available: https://www.azom.com/article.aspx?ArticleID=4426

[122] Nook_Industries. (2018). *Commercial series ND8 DC actuator features*. Available: http://www.nookindustries.com

[123] OMEGA. (2018). *1-Piece Mica Insulated band heater*. Available: https://www.omega.ca/pptst_eng/MB-1_HEATER.html

[124] ASPENCORE, "2017 Ebbedded Markets Study," Available: https://m.eet.com/media/1246048/2017-embedded-market-study.pdf

[125] J. Beningo, J. Beningo, and Anglin, *Reusable Firmware Development*. Springer, 2017.

[126] ADMET. (2018). *eXpert 7600 brochure*. Available: https://www.admet.com/products/universal-testing-machines/expert-7600/

[127] I. Alejandre and M. Artés, "Method for the evaluation of optical encoders performance under vibration," *Precision Engineering,* vol. 31, no. 2, pp. 114-121, 2007/04/01/ 2007.

[128] FAGOR_AUTOMATION, "Linear and angular encoders for CNC machines and High Accuracy Applications," ed, 2018.

[129] *ASTM, E2309/E2309M-16, Standard Practices for Verification of Displacement Measuring Systems and Devices Used in Material Testing Machine*, 2016.

[130] I. Alejandre and M. Artes, "Thermal non-linear behaviour in optical linear encoders," *International Journal of Machine Tools and Manufacture,* vol. 46, no. 12, pp. 1319-1325, 2006/10/01/ 2006.

[131] J. López, M. Artés, and I. Alejandre, "Analysis of optical linear encoders' errors under vibration at different mounting conditions," *Measurement,* vol. 44, no. 8, pp. 1367-1380, 2011/10/01/ 2011.

[132] SHIMADZU. (2018). *AG-X Plus Series Universal Electromechanical Test Frames*. Available: https://www.ssi.shimadzu.com/products/universal-tensile-testing/ag-x-plus-specifications.html

[133] V. Achim and E. Ruiz, "Guiding selection for reduced process development time in RTM," *International journal of material forming,* vol. 3, no. 2, pp. 1277-1286, 2010.

[134] J. Rösler, H. Harders, and M. Bäker, *Mechanical behaviour of engineering materials: metals, ceramics, polymers, and composites*. Springer, 2007.

[135] S. L. Agius, K. J. C. Magniez, and B. L. Fox, "Cure behaviour and void development within rapidly cured out-of-autoclave composites," *Composites Part B: Engineering,* vol. 47, no. 0, pp. 230-237, 4// 2013.

[136] C. Dong, "Modeling the Dimensional Variations of Composites Using Effective Coefficients of Thermal Expansion," *Journal of Composite Materials,* vol. 43, no. 22, pp. 2639-2652, October 1, 2009 2009.

[137] P. P. Parlevliet, H. E. N. Bersee, and A. Beukers, "Residual stresses in thermoplastic composites – a study of the literature. Part III: Effects of thermal residual stresses,"

Composites Part A: Applied Science and Manufacturing, vol. 38, no. 6, pp. 1581-1596, 6// 2007.

[138] J. Kardos, R. Dave, and M. Dudukovic, "Voids in composites," in *Manufacturing international conference proceedings: ASTM*, 1988, vol. 4, pp. 41-48.

[139] S. T. Peters, "Handbook of composites," 2012.

[140] Hondaunning. (2014). *Carbon Tech*. Available: http://www.hondatuningmagazine.com/tech/htup_0710_carbon_tech/photo_20.html

[141] ZOLTEK. (2014). *Panex prepreg tapes*. Available: http://www.zoltek.com/products/panex-35/prepreg/

[142] csmres.co.uk. (2014). *Robot and software for fiber placement*. Available: http://csmres.co.uk/cs.public.upd/article-images/coriolis241110-0070HD.jpg

[143] PCM_INNOVATION. (2014). *Aeronautic*. Available: http://www.pcminnovation.com/en/marches-cibles/aerospatial/

APPENDIX A – POLYMER MATRIX COMPOSITES

A composite material joins two or more materials to improve a specific set of properties that materials in a separate state do not possess. The bonding can be done in scales as tiny as nanometers but the definition states clearly that the constituent materials do not dissolve each other like alloys, instead, they retain their chemical, physical and mechanical identities.

The polymer matrix composites are made of two main constituents, the fiber reinforcement and the polymer matrix (see Figure A.1). Fiber reinforcements can be continuous or discontinuous and their main role is to support the mechanical load applied to the composite part. The most widely used reinforcements are made of Glass, Aramid, Carbon or organic fibers. On the other hand, -the role of the polymer matrix is to transfer the loads to the fibers, to maintain the fibers aligned, to give shape to the part and provide protection against the environment.
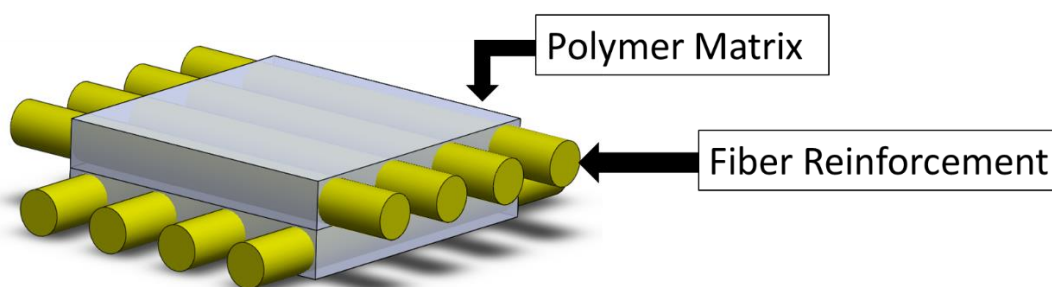
Figure A.1: Polymer matrix composite model

There are two types of polymer resins used in the manufacturing of composite materials, thermoset and thermoplastic polymers, but the molding process for each polymer are significantly different. In thermoplastics polymers, the polymerization reaction is made by the plastics manufacturer. The part manufacturer takes the polymer and applies heat to melt the thermoplastic. Then, pressure is applied to give the desired shape to the part. Generally, the thermoplastic melts into a high viscous resin[1], for this reason, the fiber impregnation and molding process for thermoplastics composites required of especial techniques that are out of the scope of this research.

---

[1] At processing temperature, the thermoplastics is a thick-flow with a viscosity between 105-109 cP; while the thermosets is liquid with a viscosity between 50 – 500 cP[62]

Contrary to thermoplastics, the thermoset polymer begins as a low molecular weight and low viscous unreacted resin. During manufacturing, the manufacturer is responsible for conducting the chemical process of polymerization to solidify the resin, this is called curing. The kinetics of the curing reaction is one of the most studied phenomena that explain the morphological changes of the structure of the material during processing. During curing, the thermosetting resin undergoes a transformation from a liquid to rubbery and finally to a solid material. This transformation is irreversible and exothermic[2] as the chemical reaction form crosslinks. The chemical reaction can be accelerated or decelerated by controlling the temperature of the process. That is why, a good understanding of the curing mechanisms and the influence of process parameters on the reaction allows the optimization of the manufacturing process of composites [47, 133].

The curing stages are well studied and defined; in the Figure A.2 those phases are presented. First, the thermoset are in form of a monomer or an unreacted resin, then to allows the resin to cure the monomer can be mixed with a cross-linking (curing) agent, an initiator, an inhibitors and a catalyst; the resultant properties of the polymer depends of the curing agent used[41, 44]; In the Figure A.2.a the resin is ready to cure, in this stage the chemical reaction can be formulated to begin at room or higher temperatures. Catalyzed resins could contain inhibitors to prolong the storage time prior to manufacturing. Small amount of diluents (3-5%)[41] are often added, this reduce viscosity, reduce the chemical shrinkage and lower the exothermal. The latter is a main concern in thicker parts because the cross-linking is the result of chemical reactions driven by the supplied heat and/or the exothermic heat generated by the reaction itself; this means that the heat generated in the core of the thick part is not pulled away so easily because some polymers do not conduct heat causing the degradation of the matrix material [44]. Prior to cure, to improve fiber wettability, resins are heated to reduce their viscosity.

When the curing initiates, the size of the molecules begin to increase (Figure A.2.b), some resins polymerizes too slow, for this reason catalyst are added; the catalyst just activates the process but not take part in the chemical reaction[41]. When the reaction accelerates, more cross-links are formed resulting in a viscosity increase because the available volume within thin molecular arrangement decreases, in this stage the resin turns into a rubber like state called gelation (Figure

---

[2] In chemistry, any reaction that releases energy is referred as an exothermic reaction.

A.2.c). When the resin gels it can not possible to be re-melted because further heating completes cross-linking. This additional heating characterizes the thermosets with a long processing time until the resin is fully cured (Figure A.2.d).
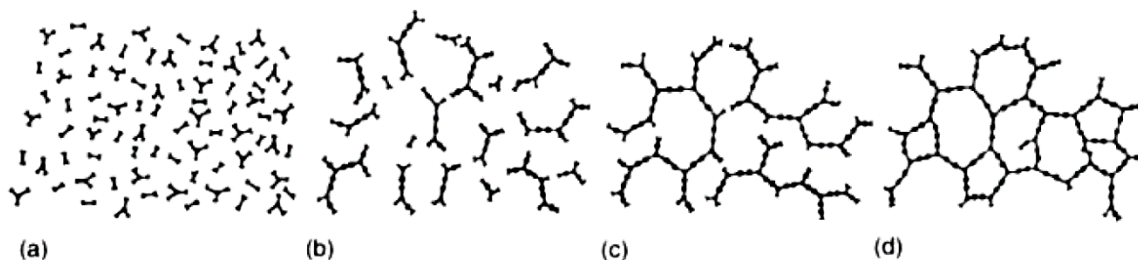

Figure A.2: Thermoset resin phases[41]

The cure of a thermoset needs an optimum temperature; the rate of cure can be increase by raising the temperature but temperatures above the optimum makes the cure so rapidly that over reactions causes the material to degrade and temperatures below the optimum the curing is too slow causing long curing cycles[67].

The cross-linking density and the shorter polymer chain lengths between cross-links produce a chemical shrinkage in the polymer, also have a direct impact in the increment of stiffness and thermal resistance in the material but with the outcome of a brittle, low strain to failure and poor impact properties structure[41]. The properties that are related to the molecular structure of the thermosets are the glass transition temperature, modulus, toughness, strength, elongation and moisture absorption. To alter these properties, the chemical structure of the monomer can be modified changing his formulation by the type of curing agent or the hardener used during the curing process.

There is a broad selection of thermosets resins for composites with different chemical structures and properties in which the Polyester, Epoxy, Bismaleimide, Cyanate Ester, Polyimide and Phenolic resins are generally used.

APPENDIX B – MANUFACTURING PROCESS

In the manufacturing of composite materials, the part takes shape and the material properties are developed. Consequently, the quality of the part depends on the manufacturing process, in which the polymeric matrix and the reinforcing fiber are combined and consolidated to form the composite.

An optimal part has a high fiber content[1] uniformly distributed and aligned within the matrix [41, 44, 62]. The manufacturing process should ensure complete curing of the resin, while minimizing the number of voids and defects [38, 135]. Finally, the process must generate the geometry while maintaining good dimensional control on the part by minimizing the residual stresses in the manufacturing part [136, 137].

To produce thermoset composites there are several types of manufacturing processes, in which the following steps can be highlight:

Table B.1 : Manufacturing of composites, general steps

Step	Description
a	Mold Setup.
b	Fiber Placement.
c	Resin Impregnation + plies consolidation.
d	Part cure.
e	Cooling to temperature ambient + de-mold.

In the first step (a) the mold is prepared with release agents or layers of non-stick material. This is because the resin adheres during curing. A good surface finish in the part depends on a good surface finish of the mold and a mold release agent.

In the step (b), the fiber fabrics are cut and aligned according to the desired properties and shape of the composite part. Advanced composites are made of continuous fibers, aligned, woven or stitched as shown in the Figure B.1.

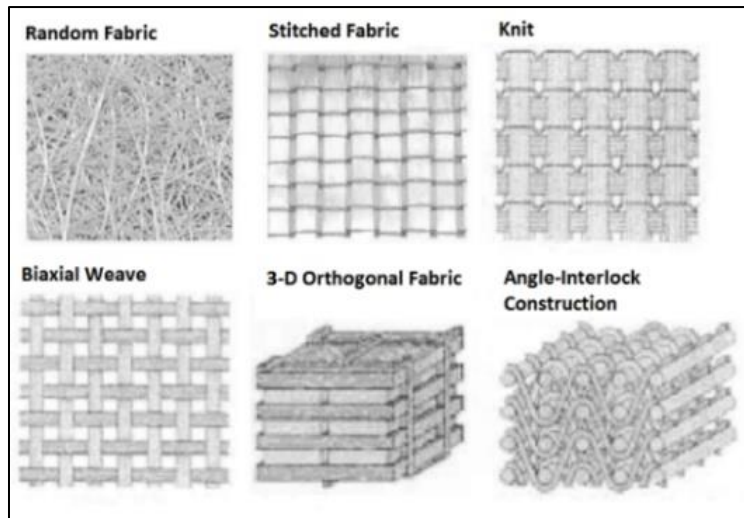[1] The aerospace industry has the highest fiber content, about 60% [134].

Figure B.1 :Architectures of reinforcing fiber preforms[62]

Usually the fiber fabrics are stacked in the direction of the load applied to the part, but in other applications it is necessary to balance the charge capacity of the part, in this manner the composite presents quasi-isotropic properties. These two types of structures are shown in Figure B.2.
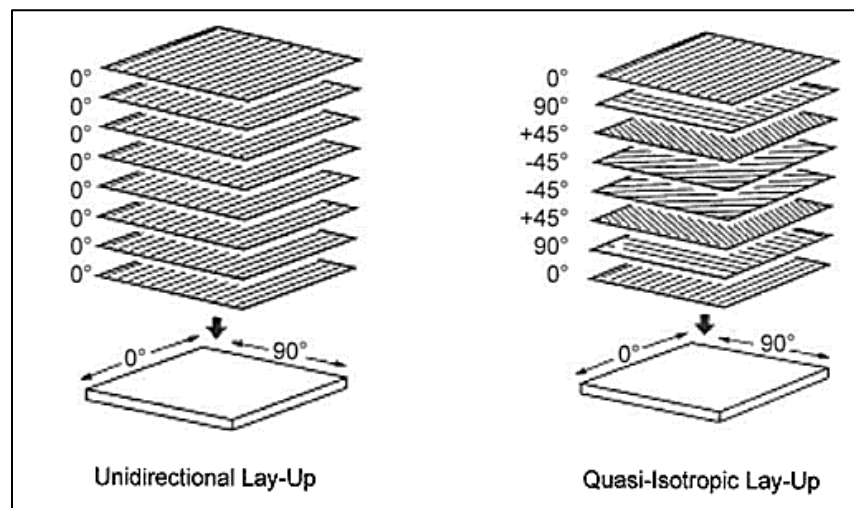

Figure B.2: Typical stacked sequences[41]

Once the plies are defined, the lay-up or preform placement is made. In open mold process the fibers are generally covered with a flexible bag which is the sealed under vacuum. On the other hand, in close mold process, the mold needs to be completely sealed to prevent the resin leaks. The Figure B.3 shows the similarity between the preform and the final product.
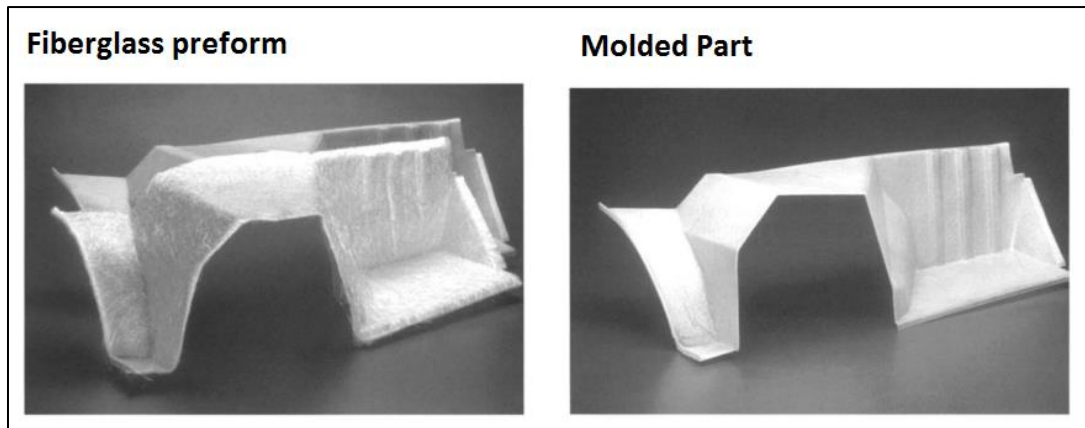
Figure B.3: Preform and molded part example[41]

To allow the flow of resin during the impregnation of step (c), the resin may be heated previously. This step should be completed as soon possible because with the degree of cure of the resin, the viscosity rises until it reaches a gel state or even solidify. After the impregnation and maintaining a low viscosity state, consolidation pressure can be applied. Consolidation pressure improves adhesion between layers and prevents the formation of porosities [40, 52, 138].

Next, the part is cured in the step (d). In this step the resin is already catalyzed[2] which means that the chemical cure reaction has been started even before the impregnation step. To speed up the cure the temperature is raised until the resin reaches a high degree of cure and has solidified.

In the final stage (e), the resin has fully developed the mechanical properties (solid state) and can be removed from the mold. Some process de-mold the part and continue applying high temperature in a hoven to fully cure the part; this saves cycle time because several parts can continue curing in the post-cure oven and the mold can be prepared to the next cycle.

B.1 Wet lay-up process

This process requires a lot of manual labor but produce good results at a low production. Curing can be at room temperature and the process does not require high tech equipment. This process is used for example in the manufacturing of surf boards.

---

[2]Catalyzer is also known as initiator. The catalyzer decomposes and add free radicals that reacts with the resin in a copolymerization reaction. At elevate temperatures the decomposition rate is accelerated [139].
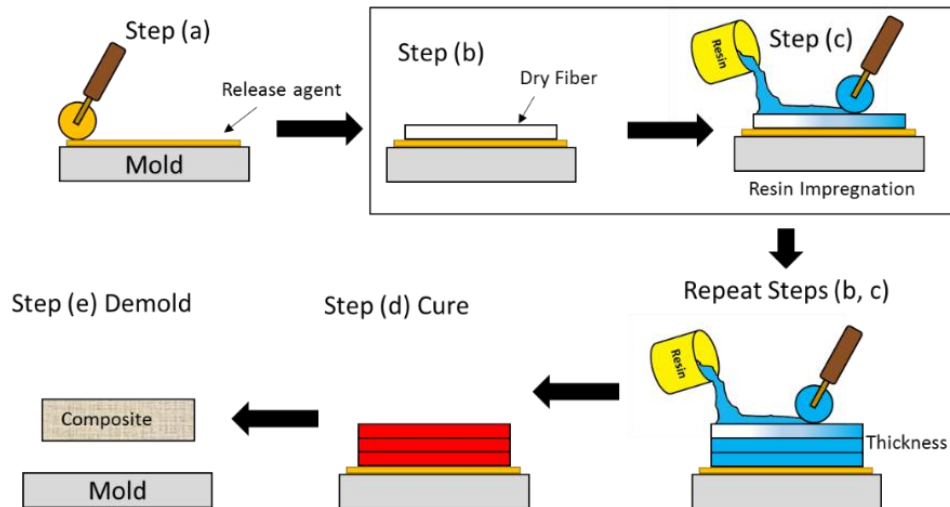
Figure B.4: Wet Lay-Up Process

B.2 Pre-impregnated resin fabric

To speed up the manufacturing of composites steps (b) and (c) are joined into a resin impregnation process. A dry fiber is woven and then immersed in a bath of resin in which is impregnated. The resin is partially cured to maintain the configuration of the fibers[3]. Finally, the sheet is covered with baking paper before being rolled up and sold. This configuration is known as "Prepreg" and the process is presented in the Figure B.5.
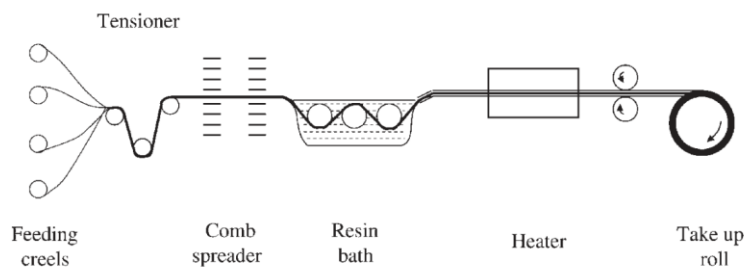
Figure B.5: Prepreg process[44]

---

3 The pre-preg undergoes 30% of degree of cure to allow the resin to develop the mechanical properties to maintain the sheet shape and hold the fibers together [44].

The prepreg are flexible and sticky with a thickness around 150 mm. The resin is catalyzed and ready to cure, which is why inhibitors[4] are added. To increase their shelf life, prepreg must be transported and stored in fridges around -5 °C. Prepreg sheets are cut and Lay-up in the mold either manually or in an automated way (stages a, b). Then, the process generally ends with steps (d) and (e).

Figure B.6: Prepreg sheet, roll and lay-up [140-143]

B.3 Autoclave

The autoclave is the most used process in the aerospace industry. This is because large parts with great complexity can be made. This process spends a lot of time in the lay-up of the prepreg into the mold. An autoclave is a big oven where hot gas flows and apply pressure to the part. Because the prepreg containing 42% excess of resin [41], the part is subjected to vacuum and pressure to move the resin into a material called bleeder and consolidate the plies. This process produces parts having good dimensional stability and low void content since the resin has two opportunities to impregnate the resin; first, when the prepreg is manufactured and second, when the layers are consolidated inside the autoclave. The Figure B.7 shows an outline of the autoclave process.

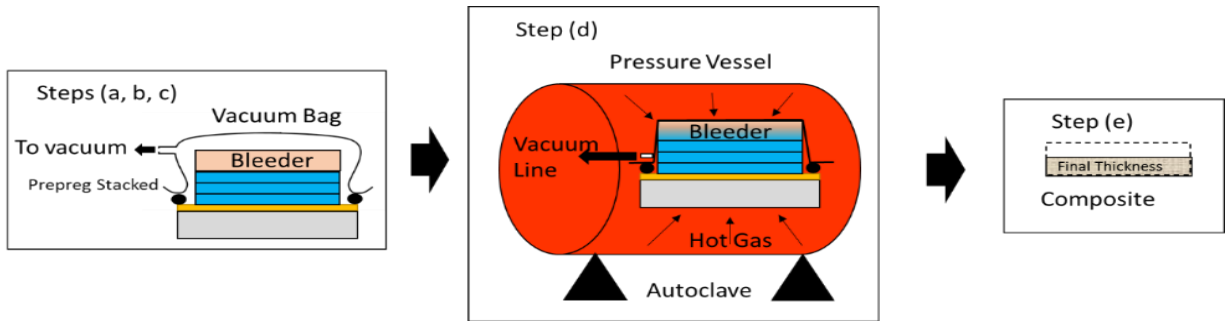[4] An inhibitor is a chemical compound that absorbs free radicals[44].

Figure B.7: Autoclave process

B.4 Liquid Composite Molding

Liquid composite molding (LCM) produces three-dimensional parts with a high degree of complexity allowing the reduction in the number of parts required for large assemblies. Other advantages are the inclusion of metal inserts, composites with multiple cores, high reproducibility and lower production cycles.

The resin transfer molding (RTM) is the most widely used in LCM. In this process, resin is injected under pressure into a closed mold. The resin impregnates the fibers displacing air trapped within the preform. The process is shown in the Figure B.8.
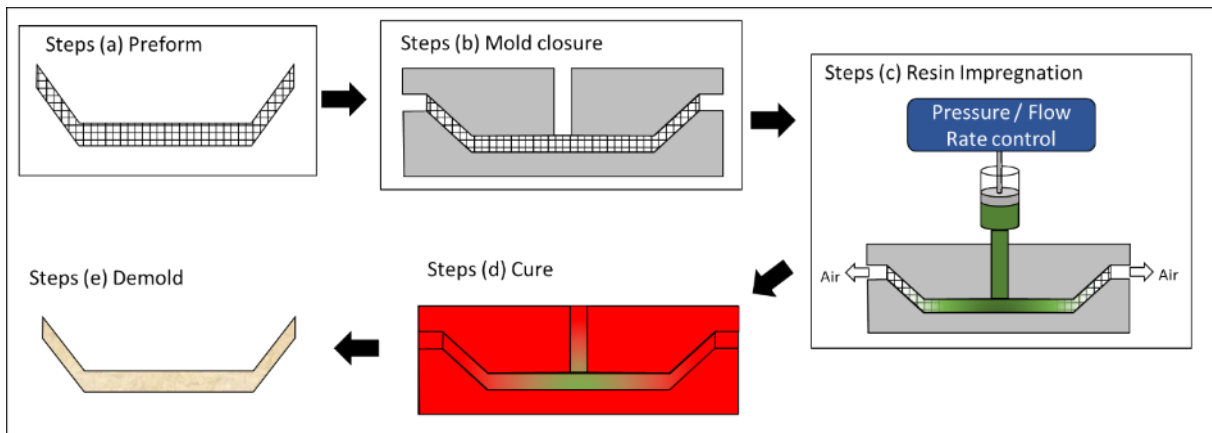
Figure B.8: RTM process

Other variations in LCM that includes a single-sided mold are presented in the Figure B.9. Vacuum-assisted resin transfer molding (VARTM) in which the part is molded with a one side rigid face and a flexible bag. The resin is sucked by the vacuum pump while the fibers are impregnated, and the bag consolidates the part pushing towards the rigid face of the mold. Seaman

composite resin infusion molding process (SCRIMP), in this process the resin is applied using distribution channels so when the vacuum is applied the fluid impregnates the fibers though the part thickness. Resin film infusion molding (RFIM) melts the resin layers placed in between the dry fibers. Then, the vacuum pressure infuses and consolidate the part.
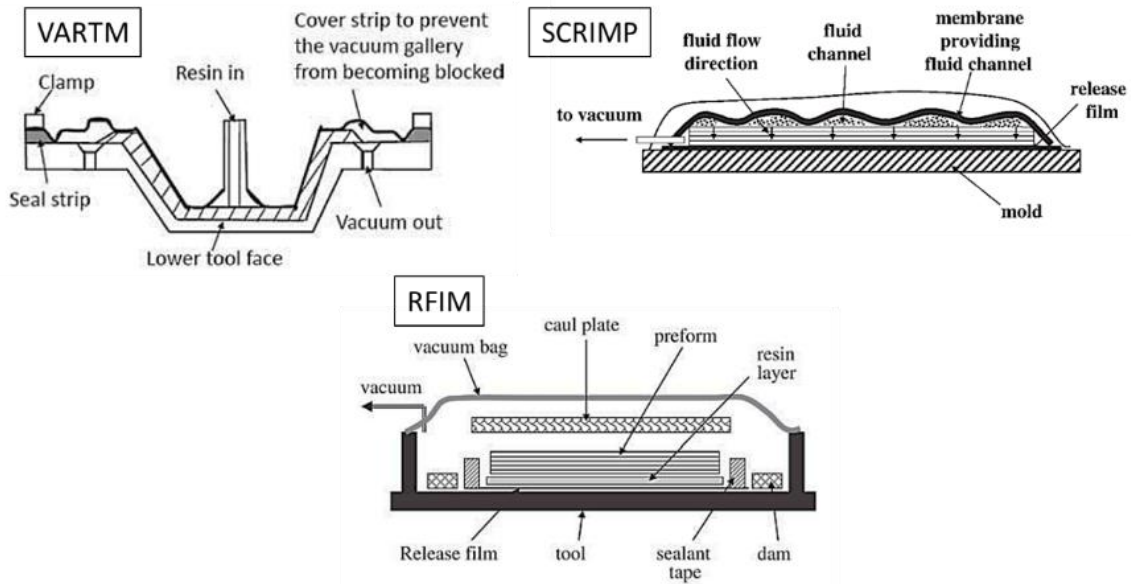

Figure B.9: LCM variations[44]

APPENDIX C – DESIGN ITERATIONS

During the implementation of the proposed mechatronic design methodology many product integrations were made. In those meetings, the designers present their ideas and test results, if the product or ideas shown benefits for the project, it remains in the design table. Often, through the analysis of the proposed solutions, the design teams realize that the requirements need to be adjusted, in that way, the project can maintain its progress.

In this annex, we describe a series of proposed solutions and the experience gather during those project design iterations. Some of the proposed solutions intended to solve problems in the device that to date remains unknown. One example of this is the injection system.

C.1. Linear force actuators

The core of the mechatronic characterization devices is in the linear actuator force. We test and analyze two options before choosing a ball screw linear actuator. Figure C.1 shows the Chinese HB-DJ805 linear actuator from the HongBa company. It is a permanent DC motor powering a lead screw with a gear ration of 30:1, 8.5 mm/s of linear speed and a load capacity of 11 kN. This device is a low-cost actuator that includes a resistive linear displacement sensor.

Figure C.1: Chinese lead screw linear actuator

The actuator showed promising results but as the tests progressed, the flaws appeared. We found it very noisy, also the linear speed was very slow. But the major problem was the backlash. We perceive it by hearing a noise that the gearbox and the nut make during a change of direction. It appeared that the backlash increased with every cycle (piston up and down). We let the actuator to perform up and down cycles about four hours, after that time we begin to see the small delay that

the piston presented when changing the direction. At that point we realize that the nut – screw friction was a major trade off for this type of actuator.

Figure C.2 shows the screw-jack alternative. Screw jacks are devices capable to easily lift loads in the range of tons, but as shown in the picture they are very bulky, due to their worm gearbox. Despite the capability to attach a commercial servomotor with a high-resolution encoder, we found it useless because it is required to measure the linear displacement directly. Also, the worm gearbox requires of constant lubrication to maintain their performance, which raises some concerns about it. At the end, when the team saw the 3D model we found it too bulky and heavy, which could greatly increase the final structure.
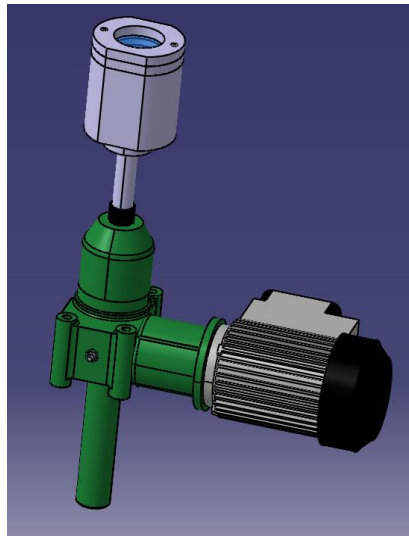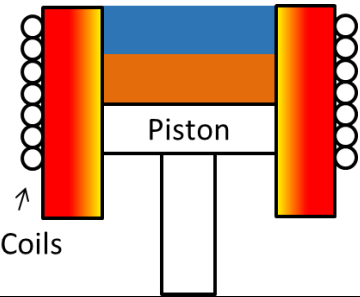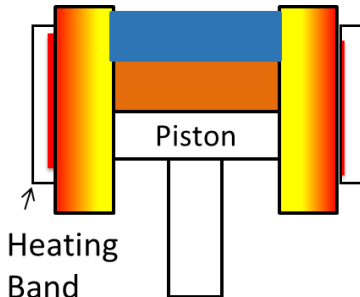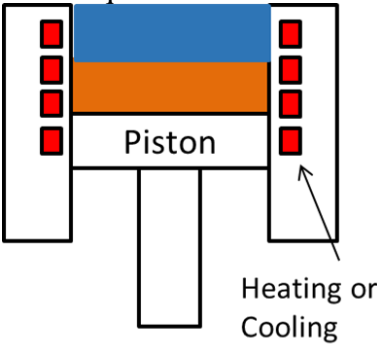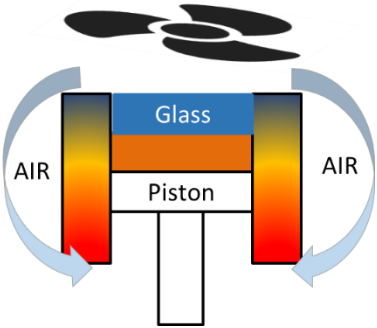

Figure C.2: Screw jack alternative

C.2. The heating and cooling system

To heat the mold, we decided to implement electrical heaters, that is because they are easy to setup. But we acknowledge that reaching high temperatures and heating rates becomes difficult if the mold requires of thick walls. For that reason, other alternatives were reviewed.

Table C.1 presents the reviewed heating and cooling solutions. It could be difficult to cool down the mold, the cooling liquid in hot press molds is usually water, that requires the disposal or cooling and recirculation of the hot water. Also, consider that the cooling liquid will have a big thermal shock at the beginning of the cooling cycle, this is because the liquid changes from room temperature to about 200 ºC. On the other hand, forced air is too slow and a noise solution.

Table C.1: Heating and cooling solutions

Alternative	Pros	Cons
Induction Coils	Fast Heating. Low power. Smaller and easy to control.	Can affect the sensors by the induced magnetic field. Complex electronics.
Conduction Heating Band	Medium Heating speed. Easy to control. Easy to setup. Many commercial options available.	High power requirement Electronics required good power dissipation and high current switching transistors.
Liquid Conduction Heating or Cooling fluid	Slow Heating. Difficult to control. The system can cool down.	Requires pumping system.
Forced air cooling 	Easy to setup. Commercial solutions.	Non-uniform cooling. Slow cooling in thick wall. High noise.

C.3. Injection ports

One important aspect of the mechatronic characterization device is that the sample thickness can be selected in a range of 1 mm to 20 mm. If we consider that the device will have an injection system, the injection port requires of careful thinking.

Figure C.3 shows a preliminary design of the injection port location. We thought that the best location is near the glass window and the remaining question is about the port size. It could be possible that this parameter determines the minimum sample thickness. Also, it could be possible that the port's position has an influence over the fiber impregnation due to the race tracking phenomena that occurs near the contact between the fiber and the mold walls. In this case the phenomenon could appear in the glass window.
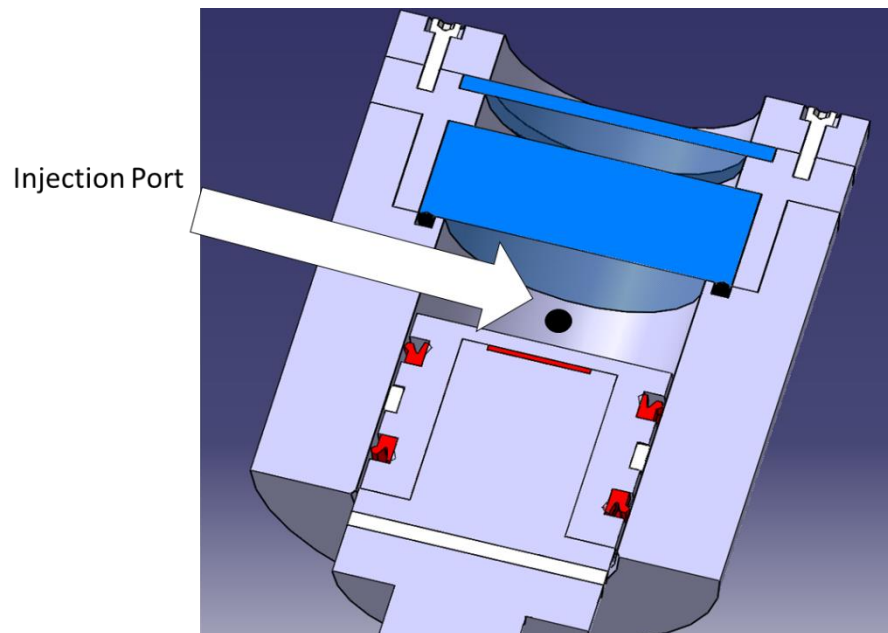
Figure C.3: Injection port location

C.4. Displacement sensor temperature effects

Two phenomena have influence over the accuracy of the displacement sensor. The first one is the mold temperature, for that reason it is highly recommended to have the sensor as far as possible from the heat source. For that reason, measure the piston displacement using the piston rod becomes a good alternative, the problem with that approach is that will require to know exactly how much compression the piston will suffer to the applied force. That measure or calibration could

be a big challenge. Figure C.4 shows a possible solution to this problem. A quartz rod located as close as possible to the sample could provide the means to reduce the impact of the temperature by isolating the sensor with a low coefficient of thermal expansion material. Considering that the sensor will measure directly the sample thickness removing the necessity to characterize the piston volumetric changes.
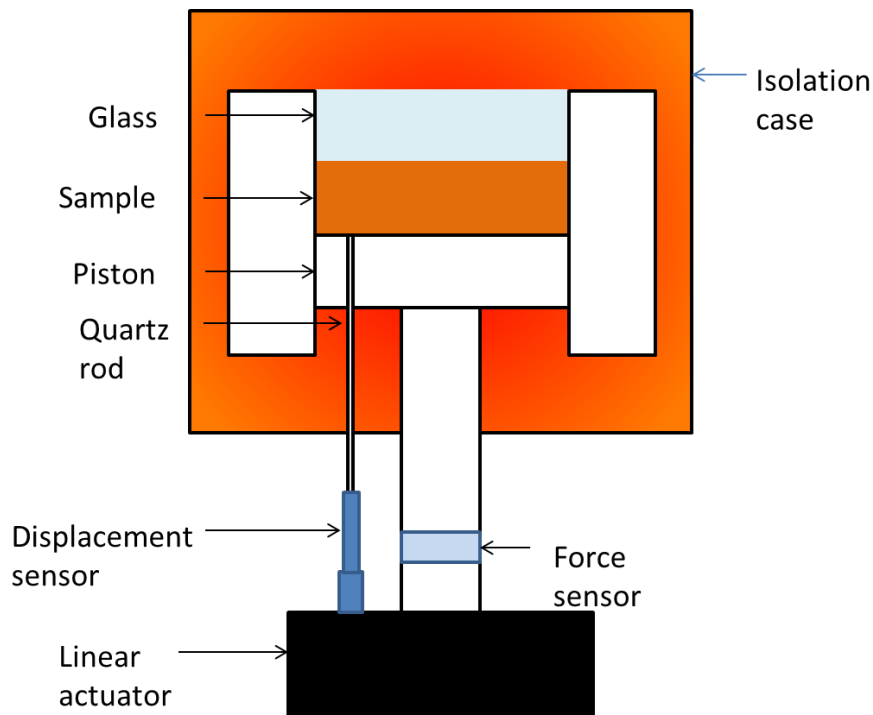

Figure C.4: Displacement sensor alternative fixture

C.5. The injection system

The injection system represents one of the many challenges in this special device. During this research we found that a rechargeable cartridge could reduce the setup time by reducing the cleaning and loading time. Also, could provide a safety layer for the user and the machine.

Figure C.5 shows the injection system proposed design. It has a motorized linear actuator, a displacement sensor to measure the piston displacement can obtain the flow rate. A rechargeable cartridge a cap with the injection port and the degassing port. The challenge in this design is how to measure the applied force or the injection pressure. This is because anything in contact with the resin should be cleaned with a solvent or replaced. An alternative could be a type of double piston or monitoring the motor current.
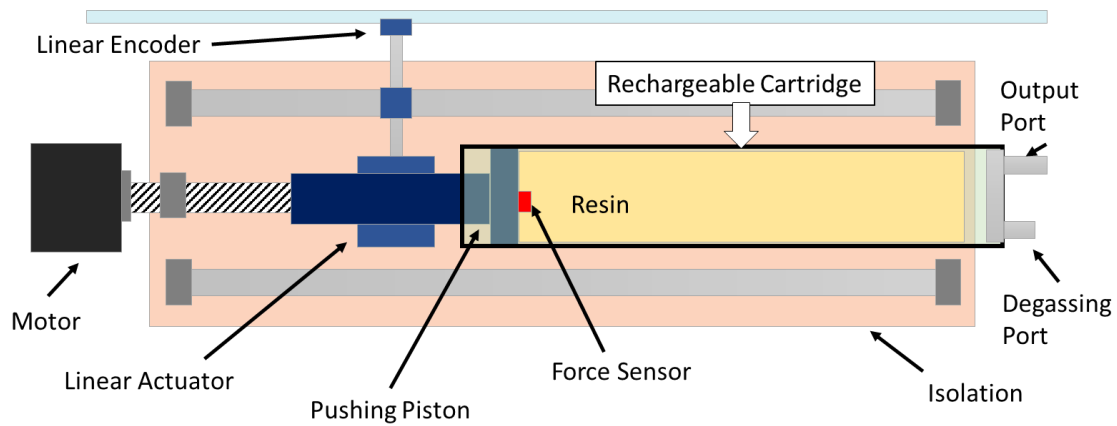
Figure C.5: Rechargeable injection system

C.6. Modifications made to the linear actuator

Finally, we present the modifications made to the selected linear actuator. In the Figure C.6 we can see the included potentiometer that intends to measure the piston displacement. It has a white wear that rotates the blue potentiometer. We found that the measure is not accurate, the gears that turn the potentiometer slips and the measuring voltage range changes when the piston moves up and down several times, a zero switch is required. Also, the output voltage begins from a value different from zero and end in a value far from the reference value. As a result, the analog to digital full resolution is not used affecting the converter resolution. At the end, it is recommended to measure the piston displacement directly and to reduce the actuator size, we remove the sensor and its support saving a few centimeters on the final prototype.
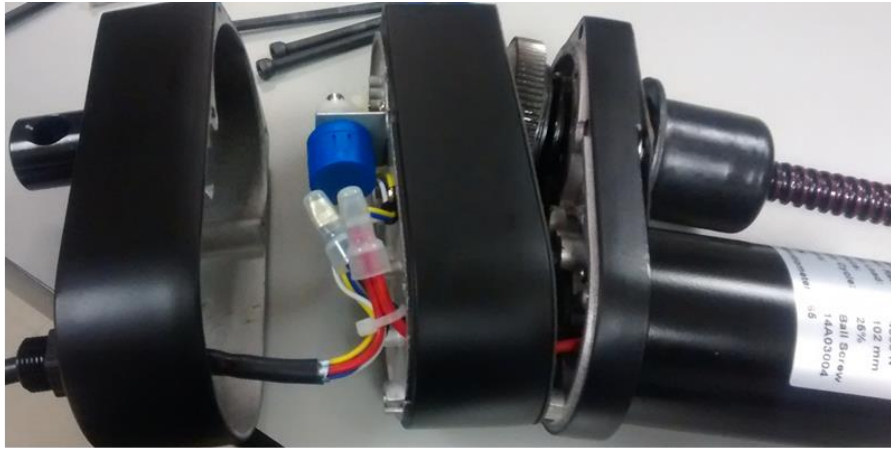
Potentiometer
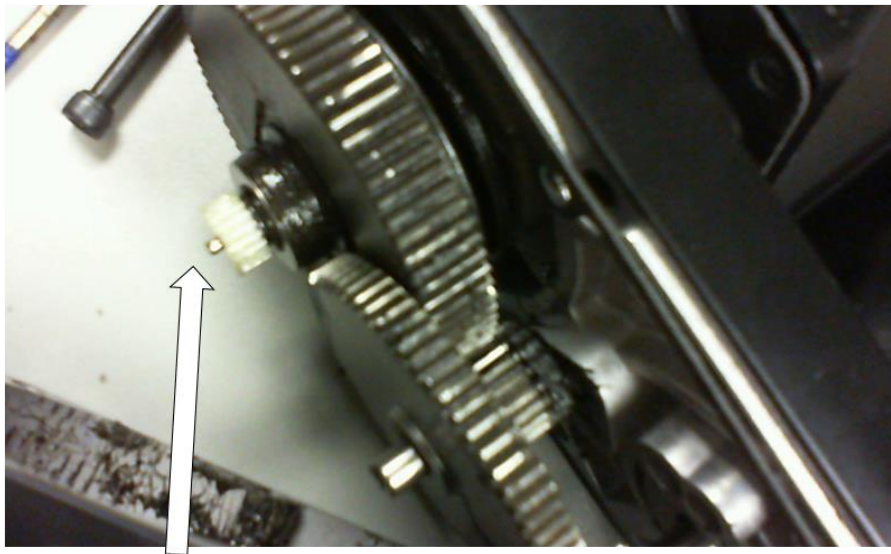
Gear to move the potentiometer

Figure C.6: Potentiometer sensor inside the actuator